CHANGES IN THE SOUTHERN HEMISPHERE SUBTROPICAL JET STREAM OVER THE TWENTY FIRST CENTURY

MUHAMMAD YUNUS BIN AHMAD MAZUKI

INSTITUTE OF GRADUATE STUDIES
UNIVERSITY OF MALAYA
KUALA LUMPUR

2016

University of Malaya

CHANGES IN THE SOUTHERN HEMISPHERE SUBTROPICAL JET STREAM OVER THE TWENTY FIRST CENTURY

MUHAMMAD YUNUS BIN AHMAD MAZUKI

DISSERTATION SUBMITTED IN FULFILMENT OF THE REQUIREMENTS FOR THE DEGREE OF MASTER OF PHILOSOPHY

INSTITUTE OF GRADUATE STUDIES
UNIVERSITY OF MALAYA
KUALA LUMPUR

2016

University of Malaya

UNIVERSITY OF MALAYA

ORIGINAL LITERARY WORK DECLARATION

Name of Candidate: Muhammad Yunus Bin Ahmad Mazuki

Matric No: HGA120014

Name of Degree: Master of Philosophy

Title of Project Paper/Research Report/Dissertation/Thesis ("this Work"):

Changes in the Southern Hemisphere Subtropical Jet Stream over the Twenty First Century

Field of Study: Earth Science

I do solemnly and sincerely declare that:

(1) I am the sole author/writer of this Work;
(2) This Work is original;
(3) Any use of any work in which copyright exists was done by way of fair dealing and for permitted purposes and any excerpt or extract from, or reference to or reproduction of any copyright work has been disclosed expressly and sufficiently and the title of the Work and its authorship have been acknowledged in this Work;
(4) I do not have any actual knowledge nor do I ought reasonably to know that the making of this work constitutes an infringement of any copyright work;
(5) I hereby assign all and every rights in the copyright to this Work to the University of Malaya ("UM"), who henceforth shall be owner of the copyright in this Work and that any reproduction or use in any form or by any means whatsoever is prohibited without the written consent of UM having been first had and obtained;
(6) I am fully aware that if in the course of making this Work I have infringed any copyright whether intentionally or otherwise, I may be subject to legal action or any other action as may be determined by UM.

Candidate's Signature Date:

Subscribed and solemnly declared before,

Witness's Signature Date:

Name:

Designation:

University of Malaya

ABSTRACT

This study focuses on the historical and projected changes in the strength and meridional location of the Southern Hemisphere Subtropical Jet (STJ) using the output of Coupled Model Intercomparison Project Phase 5 (CMIP5) models. CMIP5 model output forms the basis of the Intergovermental Panel on Climate Change (IPCC) Fifth Assessment Reports (AR5). The study consists of three parts. The first part is to assess the ability of the selected CMIP5 models in simulating the historical variability of STJ. The second part is to investigate how the CMIP5 models simulate the impacts of El Niño-Southern Oscillation (ENSO) on STJ. The third part is to examine the projected changes in the strength and meridional location of STJ in 21st Century.

In the first part, ERA-Interim reanalysis data is used to evaluate the historical simulation of STJ by 18 selected CMIP5 models for the period 1979 – 2012. Based on the climatology of the STJ from ERA-Interim, the area of study was selected as 70 °E to 290°E, 20°S to 40°S, and between the heights at 300 hPa and 100 hPa which is over the Indian and Southern Pacific Oceans. Southern Hemispheric winter period (June, July, August) was selected for the study since STJ is strongest and well-defined during the period. Analysis based on ERA-Interim shows that STJ weakens at the rate of 0.176 $ms^{-1}decade^{-1}$ and shifts polewards at 0.10 $°decade^{-1}$, however both trends are not significant. Historical simulations of STJ by the CMIP5 models show a wide range of trends in strength and meridional location of STJ, with a multi-model mean of 0.42 $ms^{-1}decade^{-1}$ strengthening and 0.04$°decade^{-1}$ equatorward shift respectively. In contrast to the ERA-Interim analysis, 94% of the CMIP5 models show a strengthening of STJ in the historical simulation. Variability of the jet strength in each individual CMIP5 model is significantly ($p \leq 0.05$) linked to the sea surface temperature changes over the eastern tropical Pacific.

University of Malaya

Second part of the study involved the assessment of the ability of the CMIP5 models in simulating ENSO effects on STJ. Results show that 47% of the CMIP5 models used in this study were able to simulate ENSO impacts realistically in terms of observed pattern. However, the models perform poorly in reproducing the observed changes in the intensity of STJ.

Last part of the study consists of CMIP5 model projections with Representative Concentration Pathways (RCP) 4.5 and 8.5 to analyse the changes of the STJ for the period 2011 – 2099. The multi-model mean trend of the 18 CMIP5 models project a statistically significant ($p \leq 0.05$) increase in STJ strength at the rate of 0.29 $ms^{-1}decade^{-1}$ and 0.60 $ms^{-1}decade^{-1}$ by 2099 for respective RCP 4.5 and RCP 8.5 scenarios. Also, the mean meridional location of STJ is projected to shift poleward by 0.006°$decade^{-1}$ and 0.042°$decade^{-1}$ by 2099 for respective RCP 4.5 and RCP 8.5 scenarios. However, this trend is significant ($p \leq 0.05$) only in RCP 8.5 scenario.

University of Malaya

ABSTRAK

Fokus kajian ini adalah terhadap sejarah dan unjuran perubahan arus udara jet Hemisfera Selatan (STJ) dengan menggunakan hasil keluaran model *Coupled Model Intercomparison Project Phase 5* (CMIP5). Hasil keluaran model CMIP5 membentuk asas *Fifth Assessment Reports* (AR5) oleh *Intergovermental Panel on Climate Change* (IPCC). Kajian ini terbahagi kepada tiga bahagian. Bahagian pertama menilai kebolehan model CMIP5 terpilih dalam mensimulasi kepelbagaian sejarah STJ. Bahagian kedua menyiasat bagaimana model CMIP5 mensimulasi kesan *El Niño-Southern Oscillation* (ENSO) terhadap STJ. Bahagian ketiga mengkaji unjuran perubahan kekuatan dan kedudukan meridian STJ di abad ke-21.

Di bahagian pertama, *reanalysis* ERA-Interim digunakan sebagai asas perbandingan untuk menilai simulasi sejarah STJ oleh 18 model CMIP5 terpilih untuk tempoh 1979-2012. Bedasarkan klimatologi STJ daripada ERA-Interim, kawasan kajian yang dipilih adalah 70°E hingga 290°E, 20°S hingga 40°S, dan di antara aras ketinggian 300 hPa hingga 100 hPa yang terletak di Laut India dan Laut Pasifik Selatan. Tempoh musim sejuk Hemisfera Selatan (Jun, Julai, Ogos) dipilih untuk kajian memandangkan STJ adalah paling kuat dan sangat stabil semasa tempoh tersebut. Kajian bedasarkan ERA-Interim menunjukkan bahawa STJ melemah pada kadar 0.176 $ms^{-1}dekad^{-1}$ dan anjakan ke arah kutub pada kadar 0.10°$dekad^{-1}$, bagaimanapun kedua anjakan tersebut adalah tidak bererti. Simulasi sejarah STJ oleh model CMIP5 menunjukkan julat arah aliran yang luas didalam kekuatan dan kedudukan meridan STJ, dengan nilai min bagi purata model himpunan menunjukkan STJ menguat dengan kadar 0.42 $ms^{-1}dekad^{-1}$ dan menganjak ke arah khatulistiwa dengan 0.04°$dekad^{-1}$. Berlawanan dengan *renalysis* ERA-Interim, 94% model CMIP5 menujukkan penguatan STJ didalam simulasi sejarahnya. Kepelbagian kekuatan jet di dalam setiap model CMIP5 dapat dikaitkan

University of Malaya

dengan perubahan suhu permukaan laut di bahagian Pasifik khatulistiwa timur pada tahap keertian $p \leq 0.05$.

Di bahagian kedua kajian, penilaian kebolehan model CMIP5 dalam mensimulasi kesan ENSO terhadap STJ telah dijalankan. Keputusan menunjukkan 47% model CMIP5 yang digunakan didalam kejian ini dapat mensimulasi kesan ENSO secara praktikal dari segi corak tercerap. Walau bagaimanapun, model tersebut berprestasi lemah didalam menghasil semula perubahan tercerap keamatan STJ.

Bahagian terakhir kajian terdiri daripada unjuran model CMIP5 menggunakan *Representative Concentration Pathways* (RCP) 4.5 dan 8.5 untuk megkaji perubahan STJ untuk tempoh 2011-2099. Min purata model himpunan menujukkan peningkatan secara keertian ($p \leq 0.05$) kekuatan STJ menjelang 2099 pada kadar 0.29 $ms^{-1}dekad^{-1}$ bagi senario RCP 4.5 dan 0.60 $ms^{-1}dekad^{-1}$ bagi senario RCP 8.5. Selain itu, kedudukan meridan STJ diunjurkan beranjak kearah kutub pada kadar 0.006°$dekad^{-1}$ bagi senario RCP 4.5 dan 0.042°$dekad^{-1}$ bagi senario RCP 8.5. Walau bagaimanapun, hanya kes senario RCP 8.5 sahaja pergerakan arah aliran ini signifikan ($p \leq 0.05$).

University of Malaya

ACKNOWLEDGEMENTS

I would like to thank my supervisors, Dr. Sheeba Nettukandy Chenoli and Yang Berbahagia Profesor Dato' Dr. Azizan bin Hj Abu Samah for all the guidance given to me, for all the time taken in teaching me and perseverance in dealing with me. I express my gratitude to Mr. Ooi See Hai for all the help given in statistical analysis, scripting and proofreading written material. I also would like to thank Professor John Turner (British Antarctic Survey) for the ideas and discussions poured into this study.

This research was supported by Universiti Malaya through the grant (UMRG176-12SUS) and Ministry of Science Technology and Innovation (Malaysia) Grant Flag Ship (GA007-2014FL). I would like to thank my colleagues from National Antarctic Research Centre who provided insight and expertise that greatly assisted this research.

And finally, I would like to thank my wife and family for their support and encouragement throughout this study.

University of Malaya

TABLE OF CONTENTS

University of Malaya

University of Malaya

University of Malaya

LIST OF FIGURES

University of Malaya

University of Malaya

University of Malaya

LIST OF TABLES

University of Malaya

LIST OF SYMBOLS AND ABBREVIATIONS

CC	:	Central canal
DAB	:	3,3'-diaminobenzidine
HRP	:	Horseradish peroxidase
MS222	:	Tricaine methanesulfonate asdfkj hasjkldfh askjldfh asjkdfh askjdfh klasjdh fklajsdfh sklajdh f
AOGCM	:	Atmosphere-Ocean Coupled General Circulation Models
ACC	:	Anomaly Correlation Coefficient
AR4	:	Fourth Assessment Report of the Intergovernmental Panel on Climate Change
AR5	:	Fifth Assessment Report of the Intergovernmental Panel on Climate Change
CMIP	:	Coupled Model Intercomparison Project
CMIP3	:	Coupled Model Intercomparison Project Third Phase
CMIP5	:	Coupled Model Intercomparison Project Fifth Phase
COADS	:	Comprehensive Ocean-Atmosphere Data Set
DJF	:	December January February
ENSO	:	El Niño-Southern Oscillation
ECMWF	:	European Centre for Medium Range Weather Forecasting
GCM	:	General Circulation Model
GTS	:	Global Telecommunication System
HadISST	:	Hadley Centre Sea Ice and Sea Surface Temperature
HC	:	Hadley Circulation
IPCC	:	Intergovernmental Panel on Climate Change
JJA	:	June July August

University of Malaya

MAM	:	March April May
MARS	:	Meteorological Archival and Retrieval System
MDB	:	Met Office Marine Data Bank
NH	:	Northern Hemisphere
OSTIA	:	Operational Sea Surface Temperature and Sea-Ice Analysis
PFJ	:	Polar Front Jet Stream
RCP	:	Representative Concentration Pathway
SAM	:	Southern Annular Mode
SH	:	Southern Hemisphere
SON	:	September October November
SST	:	Sea Surface Temperature
STJ	:	Subtropical Jet Stream
UNEP	:	United Nations Environment Programme
WCRP	:	World Climate Research Programme
WGCM	:	Working Group on Coupled Modelling
WMO	:	World Meteorological Organisation

University of Malaya

LIST OF APPENDICES

University of Malaya

CHAPTER 1: INTRODUCTION

1.1 Introduction

Jet stream refers to bands of narrow high speed air current flowing in one direction, hundreds of kilometres long, less than several kilometres wide, typically less than 1.6 kilometres thick. In the central core of a jet stream, wind speed often exceeds 50 ms^{-1} and at times reaches 100 ms^{-1} (Holton, 1992). Jet stream is commonly found near the tropopause at elevation between 10 km to 14 km (Holton, 1992) in the middle and higher latitudes. The World Meteorological Organization (WMO) defines jet stream as air currents with quasi horizontal axes which are thousands of kilometres long, hundreds of kilometres wide, and several kilometres deep. Wind speed in the core of a jet stream should exceed 30 ms^{-1}, with vertical gradient on the order of 5 ms^{-1} km^{-1} and horizontal gradient on the order of 5 ms^{-1} 100 km^{-1}.

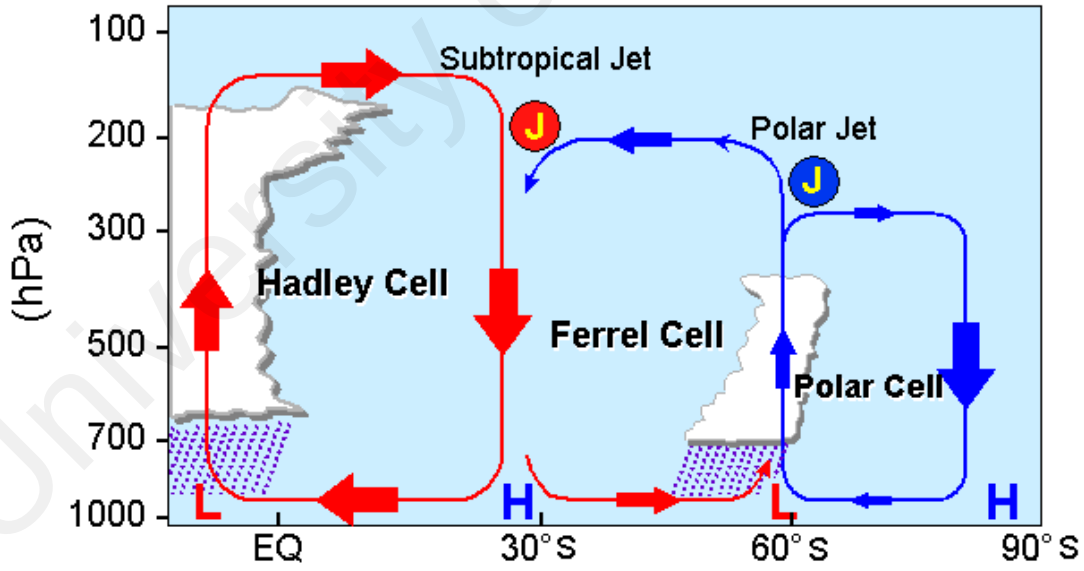

Figure 1.1 Cross section of atmosphere circulation detailing the locations of major jet streams. Modified from (http://ljp.gcess.cn/dct/page/65607, accessed at 01 Jan 2016)

In both Northern Hemisphere (NH) and Southern Hemisphere (SH), there are two main jet streams, namely subtropical jet stream and polar front jet stream (PFJ). Both jet streams flow from the west to the east all year around. At times subtropical jet stream and

University of Malaya

polar front jet stream merge together, creating a wide area of fast flowing wind (Barnes & Hartmann, 2011). Jet streams are formed by a combination of a planet's rotation on its axis and atmospheric heating by solar radiation. They form near boundaries of adjacent air masses with significant differences in temperature, such as the boundary of cold polar region and the warmer air towards the equator. Thus STJ is located in the tropopause level between Hadley and Ferrel cells at the poleward edge of Hadley Cell (HC) as shown in the Figure 1.1 (Gallego et al., 2005). Consequently, STJ is used as an indicator of the poleward edge of HC (Held & Hou, 1980). Since these hot and cold air boundaries are most pronounced in winter, jet streams are the strongest at this time in both hemispheres.

Jet stream plays an important role in the earth's climate and weather system. Position and intensity of jet stream have been used for weather prediction and long term climate planning. Synoptic scale disturbances tend to form in the entry and exit regions of maximum jet stream wind speed and propagate eastward along tracks following the jet axis (Holton, 1992). Therefore, the change in position of jet stream affects storm tracks, global weather patterns, temperature and precipitation. Jet streams also play a major role in the global transfer of heat (Holton, 1992) and dispersion of pollutants and volcanic ashes.

One of the major events in the 20th century is the global warming. The earth's average surface temperature has risen by 0.74 °C ± 0.18 °C over the years 1906 – 2005 (IPCC, 2007). This is also accompanied by decrease in snow cover over the Northern Hemisphere, decrease in sea ice extent in the Arctic, warming of the oceans, rising sea level, increase in tropospheric water vapour, warming of the troposphere and cooling of the stratosphere as reported in the Intergovernmental Panel on Climate Change (IPCC) Fourth Assessment Report (AR4). This report has also envisaged the poleward shift of jet stream under global warming.

University of Malaya

1.2 General Circulation Models

In order to study and analyse the poleward shift of jet stream under global warming, it is needed to understand the earth's climate through a mathematical model that is able to simulate the earth's climate. However, given the complexity of earth's climate, there is a limit on what a model can resolve. Model relies on simplifying assumptions and parameterisations. Physical processes that are too small-scale and complex to be physically represented in the model such as cloud microphysics are replaced by simplified parameters within the climate system for feasible computation. Such model is called the General Circulation Model (GCM).

Owing to the limitation in assumptions and parameterisations, biases are introduced at varying magnitudes. Therefore, the model outputs are generally compared and evaluated against observations.

1.3 Intergovernmental Panel on Climate Change (IPCC)

In recognition of the problem of global warming, the IPCC, an international intergovernmental scientific body which provides authoritative statement of prevailing understandings of climate change was established in 1988 by the World Meteorological Organization (WMO) and the United Nations Environment Programme (UNEP) for the purpose of assessing and disseminating "the authoritative scientific, technical and socioeconomic information relevant for the understanding of the risk of human-induced climate change". IPCC produces comprehensive assessments of current climate scientific findings every five to seven years, the latest publication being the Fifth Assessment Report (AR5). AR5 was produced based on the analysis of Coupled Model Intercomparison Project Phase 5 (CMIP5). The assessments include inputs from global climate experts, published and peer reviewed scientific literatures, from over 190 countries. The draft reports of IPCC undergo more scrutiny than any other documents

University of Malaya

in the history of science (Edwards, 2010), however IPCC does not carry out research work on its own.

1.4 Coupled Model Intercomparison Project

Coupled Model Intercomparison Project (CMIP) was established by the Working Group on Coupled Modelling (WGCM) under the World Climate Research Programme (WCRP) of WMO as a standard experimental protocol for studying the output of coupled atmosphere-ocean general circulation models (AOGCMs). CMIP provides a community-based infrastructure in support of climate model diagnosis, validation, intercomparison, documentation and data access. This framework enables a diverse community of scientists to analyse GCMs in a systematic fashion - a process that serves to facilitate model improvement. Virtually the entire international climate modelling community has participated in this project since its inception in 1995. The current fifth phase of CMIP, or CMIP5 focuses on cloud and carbon cycle experimentation. Its activities include i) assessing the mechanisms responsible for model differences in poorly understood feedbacks associated with the carbon cycle and clouds, ii) examining climate 'predictability' and exploring the ability of models to predict climate on decadal time series, iii) determining why similarly forced models produce a range of responses, iv) evaluate how realistic the model are in simulating the recent past to provide projections of future climate change on two time scales, i.e. near term (out to 2035) and long term (out to 2100 and beyond), and v) understanding some of the factors responsible for differences in model projections, including quantifying some key feedbacks such as those involving clouds and carbon cycles.

CMIP5 experiments are divided into two types, long-term integrations (in time scale of century) and near term integrations (in time scale of 10 – 30 years) which are also known as decadal prediction experiments (Meehl et al., 2009). The long-term integration

University of Malaya

result is used in this study. It starts from multi-century preindustrial control (quasi equilibrium) integrations and are integrated using atmosphere-ocean global climate models, which were the standard in the previous CMIP phases. The long-term integration contains both historical and future projection experiments.

1.5 Problem Statement

Jet stream plays an active and important role in the earth's climate. In particular Southern Hemisphere Subtropical Jet Stream has a major role in influencing the equatorial climate of the SH. In the future changes under the global warming scenario, it is critical to study and review the STJ with updated information from the current global climate perspectives and technological advances.

1.6 Objectives of the Study

The objectives of this study are:

1. To assess how the historical runs of the selected CMIP5 models represent the strength, position and variability of the Southern Hemisphere Subtropical Jet Stream.
2. To investigate the role of the broad scale climate phenomenon El Niño-Southern Oscillation (ENSO) on the variability of the Southern Hemisphere Subtropical Jet Stream.
3. To examine the future trends in strength, position, and variability of the Southern Hemisphere Subtropical Jet Stream based on future predictions from CMIP5 models under two greenhouse gases emission scenarios:
    a) Intermediate energy usage scenario
    b) High energy-intensive scenario

University of Malaya

1.7 Research Question and Challenge

The first part of this study will focuses on the trend in the strength and location of STJ and also assess the historical simulation of CMIP5 models to investigate how the CMIP5 models simulate the trend in the strength and location of STJ compared to observation. A future poleward shift of the STJ will be quantified based on future predictions from CMIP5 models under two greenhouse gases emission scenarios. As the climate processes are not fully resolved in the models, simulation of STJ may differs from the observation. A systematic approach that reduces biases as much as possible is needed when dealing with a large number of model outputs.

A very pertinent research question that will be addressed in this thesis is the impacts of El Niño-Southern Oscillation on the variability of STJ based on observation as well as CMIP5 data. Historical CMIP5 runs are forced by projected greenhouse gas concentrations, ozone amounts, aerosols etc. and no observational data are assimilated in the simulations. As ENSO events are natural climate variability and individual ENSO events in the various CMIP5 models used in the study will not occur at the same time as those in the 'real' world, CMIP5 models are not able to simulate ENSO events accurately as it occurred in the real world. This could pose a challenge in assessing the impacts of ENSO on STJ appropriately.

1.8 Research Importance

Changes in the strength and poleward shift of the jet stream affect the surface temperature, extent of sea ice (Thompson & Solomon, 2002), variations in frequencies and intensity of storms (Yin, 2005), location of arid regions (Lu, Vecchi, & Reichler, 2007), strength of wind-driven oceanic circulations (Russell, Dixon, Gnanadesikan, Stouffer, & Toggweiler, 2006), and exchange of CO_2 and heat between atmosphere and

University of Malaya

ocean (Mignone, Gnanadesikan, Sarmiento, & Slater, 2006). As such, this study is of great research importance.

In addition, recently available CMIP5 model output provides an opportunity to update our understanding on the variability of jet stream. Findings from this study will be of valuable feedback to the major climate modelling centres so as to assess their models development in greater detail.

1.9 Thesis Structure

Chapter 1 gives the general description of the jet stream. Chapter 2 reviews recent literatures on STJ. Data, models, and methodologies used to investigate the variability of STJ are elaborated in Chapter 3. Chapter 4 and Chapter 5 discuss the results. Chapter 6 summarises and highlights the major findings of the study with indication of possible future work.

University of Malaya

CHAPTER 2: LITERATURE REVIEW

2.1 Introduction

There are many recent studies on STJ because of its significant role in the climate and mesoscales features of Southern Hemisphere (Lu et al., 2007; Thompson & Solomon, 2002; Yin, 2005). The intensification and poleward shift of STJ in response to climate change have been reported in AR4 as well as in AR5 (G. Chen & Held, 2007; Kidston & Vallis, 2011; Lorenz & Deweaver, 2007). Thus, it is important to understand how STJ changes in the past and future in response to climate change. Section 2.2 starts with the understanding of the variability of STJ in terms of its spatial and temporal distributions. Section 2.3 details the historical review in the trends of jet stream. Section 2.4 looks into climate variability linked to STJ. Section 2.5 examines the projected changes in the STJ. Section 2.6 deals with the advancement of CMIP5 from CMIP3 regarding STJ and ENSO. Section 2.7 concludes the chapter.

2.2 Variability in Southern Hemisphere Subtropical Jet Stream

Nakamura & Shimpo (2004) and Gallego et al. (2005) show that strength of STJ varies seasonally. Their study highlights that STJ intensifies and starts to form across South Pacific Ocean through early austral autumn (March, April, and May (MAM)), and extends to the Indian Ocean. As mid-latitude baroclinicity increases through austral winter (June, July, and August (JJA)) STJ exhibits intense formation and widest zonal extent. STJ gradually weakens throughout austral spring (September, October, and November (SON)) and continues to weaken during austral summer (December, January, and February (DJF)). The maximum intensity of STJ during winter is located at approximately 30 °S, and between 110 °E and 200 °E, across Australia and the western south Pacific Ocean with mean maximum zonal wind speed around 50 ms^{-1} – 55 ms^{-1} (H Nakamura & Shimpo, 2004). S Lee & Kim (2003), Hisashi Nakamura, Sampe, Tanimoto, & Shimpo (2004), Koch, Wernli, & Davies (2006), Archer & Caldeira (2008) and Pena-ortiz,

University of Malaya

Gallego, Ribera, Ordonez, & Alvarez-castro (2013) state that the strongest wind speed associated with STJ is in winter when the STJ rings most of the hemisphere. The meridional location of STJ also varies seasonally. According to Gallego et al. (2005), the location of STJ can shift abruptly from 42 °S to 30 °S during transition from austral summer to austral fall. During late austral fall (May) to late austral spring (November) STJ is located within 30 °S to 35 °S. As concluded by Pena-ortiz, Gallego, Ribera, Ordonez, & Alvarez-castro (2013), jet stream is so diverse in structure (spatially) and changes so fast (temporally) that its climatic characterisation is very difficult.

B. Chen, Smith, & Bromwich (1996) describes the structure of jet streams in the SH as a concentric structure, with a persistent branch as PFJ around Antarctica and a seasonally varying branch as STJ at about 30 °S. Archer & Caldeira (2008), and Koch, Wernli, & Davies (2006) describe STJ as seasonal varying ring at about 30°S, with Gallego et al. (2005) adding that there is a clear distinction to PFJ in all seasons except austral summer. Koch, Wernli, & Davies (2006) and Bordi, Fraedrich, Lunkeit, & Sutera (2007), on the other hand, describe jet stream in SH as double jet structure of STJ and PFJ, with STJ transitioning into PFJ. Archer & Caldeira (2008) stated that SH STJ have a more symmetrical distribution compared to jet stream in NH because of the greater ocean extent in the SH. Furthermore, James (2006) added that during winter, Antarctica is surrounded by sea ice, thereby increasing the temperature gradient between equator and pole which shapes the distribution of STJ in SH. Bals-Elsholz et al. (2001) highlight the splitting of STJ into two jets across New Zealand which is a characteristic feature of the SH STJ. The equatorward branch of STJ is located between 20 °S and 25 °S while the poleward branch of STJ is located between 25 °S and 40 °S. As pointed out by Koch, Wernli, & Davies (2006) and Archer & Caldeira (2008) STJ is not a permanent continuous structure, rather it is fragmented, meandering with notable wind speed and varying heights, especially during the transitional months, where the distinction between

University of Malaya

STJ and PFJ becomes ambiguous. Thus, clear and precise identification of jet stream is difficult.

2.3 Historical Trend in the STJ

There have been several studies that focused on the change and trend in strength and meridional location of STJ over the past decades. Gallego et al. (2005) stated that STJ weakens at 0.5 ms^{-1} $decade^{-1}$ rate for the period 1958 – 2002 based on NCEP/NCAR reanalysis. Archer & Caldeira (2008) reports that STJ weakens at the rate of 0.365 ms^{-1} $decade^{-1}$ for the period 1979 – 2011 based on ERA-40 however strengthen at the rate of 0.422 ms^{-1} $decade^{-1}$ for the period 1979-2011 based on NCEP/NCAR. Pena-ortiz, Gallego, Ribera, Ordonez, & Alvarez-castro (2013) study shows that STJ weakens at the rate of 0.48 ms^{-1} $decade^{-1}$ for the period 1958 – 2008 but strengthen at the rate of 0.60 ms^{-1} $decade^{-1}$ for the a different period 1979 – 2008 based on NCEP reanalysis. The same study, using 20^{th} Century reanalysis shows that STJ strengthen at the rate of 1.00 ms^{-1} $decade^{-1}$ for the period 1958 – 2008 and also strengthen at the rate of 0.67 ms^{-1} $decade^{-1}$ for a different period 1979 – 2008. Pena-ortiz, Gallego, Ribera, Ordonez, & Alvarez-castro (2013) argued that the inconsistencies and lack of agreement in the trend of the strength of STJ are due to the difficulty in constructing the climatology of STJ, because of the spatial and temporal diversity in structure of STJ.

Most of the observational studies agree that STJ in both hemispheres is shifting poleward. However, there is disagreement in the rate at which the jet streams shift towards the poles. Gallego et al. (2005) stated that STJ has shift poleward significantly during 1979 – 2002. Fu, Johanson, Wallace, & Reichler (2006) reported that over the period 1979 – 2005 STJ has shifted polewards by 1 degree from observation of change in atmospheric temperature based on NCEP/NCAR reanalysis data. Archer & Caldeira (2008) reported that STJ shifts poleward by 0.063 ° $decade^{-1}$ for the period 1979 – 2011

University of Malaya

based on ERA-40, and 0.111 ° decade^{-1} for the period 1979 – 2011 based on NCEP/NCAR. The study by Pena-ortiz, Gallego, Ribera, Ordonez, & Alvarez-castro (2013) shows that STJ shifts polewards by 0.02 ° decade^{-1} for the period 1958-2008 based on NCEP however using 20th Century Reanalysis STJ shifts equatorwards by 0.10 ° decade^{-1}. The same study shows STJ shifts poleward at the rate of 0.33 ° decade^{-1} and 0.11 ° decade^{-1} for a different period of 1979 – 2008 based on NCEP and 20th Century Reanalysis respectively. Similar to the disagreement in the change of strength of STJ, Pena-ortiz, Gallego, Ribera, Ordonez, & Alvarez-castro (2013) argued that the lack of agreement in the magnitude of poleward shift of STJ is due to the difficulty in constructing the climatology of STJ.

2.4 Climate Variability Linked to the Jet Stream

Nakamura & Shimpo (2004) studied the association between storm tracks, jet streams and midlatitude oceanic fronts. They concluded that seasonal evolution of a subtropical jet stream influence storm track activity over South Pacific. Hisashi Nakamura et al. (2004) stated that the intensification of STJ during winter traps most of the upper-level eddy activity, which causes main storm track to form along STJ, with suppressed baroclinicity eddy growth. When STJ weakens, main storm track forms over surface baroclinic zone (stippled at ~45 degree latitude), anchored by a subpolar frontal zone.

According to Diaz & Bradley (2004) Hadley Circulation is fundamentally important to understand the climate system and its changes have important impacts on global climate including subtropical jet stream. Hu & Fu (2007) described Hadley Circulation as a thermally driven meridional circulation, where warmer tropical air rises due to the release of latent heat and flows polewards in both hemispheres. They noted that the meridional location of subtropical jet stream marks the poleward limit of Hadley Circulation, while Held & Hou (1980) and Lindzen & Hou (1988) associated the strength

University of Malaya

of HC to the strength of STJ during austral winter. E. A. Barnes & Polvani (2013) established that while mid-latitude jet stream and HC can mutually influence each other, the mechanisms and the causal relations behind such interactions may be quite diverse.

2.4.1 Impacts of ENSO on the STJ

Zhang, Wallace, & Battisti (1997), Trenberth (1997) and Wang, Wu, Fu, & Al (2000) describe ENSO as a global climate phenomenon originating in tropical Pacific region with inter-annual to decadal time scales. Wang, Wu, Fu, & Al (2000) observed the periodicity of ENSO is 2 to 10 years and it consists of two phases, El Niño and La Niña. According to B. Chen et al. (1996), Dore (2005), Gallego et al. (2005) ENSO affects precipitation, Asian climate, wind fields, sea level pressure, and more importantly the meridional location and strength of STJ. B. Chen et al. (1996) and Sinclair (1996) stated that the influence of ENSO on the SH upper-level winds, especially on the variability of the wind strengths has been recognized for some time. Gallego et al. (2005) added that during El Niño phase the strength of STJ is 50% stronger than that during La Niña phase over the Pacific region. An accurate ENSO simulation in the climate models poses a difficult task since it involves complex interactions of various oceanic and atmospheric processes. Turner (2004) pointed that more work is needed in understanding ENSO and its relation to jet streams, as well as the mechanism whereby the ENSO signals are transmitted southwards.

2.5 Projected Changes in STJ

There have been studies that tried to quantify how STJ is going to change in the future based on CMIP3 and CMIP5 model output. Studies by Lorenz & Deweaver (2007), Son et al. (2010), Son et al. (2008) and Thompson & Solomon (2002) indicated that in CMIP3 projection, STJ shifts polewards in response to increase in greenhouse gas and global warming. According to Yin (2005), Delcambre, Lorenz, Vimont, & Martin (2013) and

University of Malaya

Harvey, Shaffrey, & Woollings (2014), majority of climate simulations by latest and advanced coupled modes predict poleward shift of jet streams, with disagreement in the magnitude of the jet response. Ceppi, Zelinka, & Hartmann (2014) find that the poleward shift of jet stream in CMIP5 strongly correlates with the meridional gradient of absorbed shortwave radiation. Wilcox, Gray, & Charlton-Perez, (2012) show that for the summer season, STJ shifts poleward by up to 3 degrees, and the shift is linked to changes in the meridional temperature gradient in upper troposphere.

2.6 Advancement of CMIP5 from CMIP3 regarding STJ and ENSO

Earlier studies by Guilyardi (2006), Achuta Rao & Sperber (2006) and Leloup, Lengaigne, & Boulanger (2008) have shown that there is a large variation in the spatial pattern and magnitude of SST in the equatorial Pacific during ENSO as simulated by the CMIP3 models when compared to the observations. Leloup, Lengaigne, & Boulanger (2008), Bellenger, Guilyardi, Leloup, Lengaigne, & Vialard (2014) and Watterson 2015) confirmed that the ability of climate models to simulate ENSO has improved over the recent few years. The CMIP3 models do not systematically simulate their maximum ENSO amplitude in the same area as observed and the spatial patterns extend further into the western Pacific. Yeh, Ham, & Lee (2012) noted that the patterns of tropical warming over the second half of the twentieth century has changed from La Niña like structure in CMIP3 to El Niño like structure in CMIP5. As noted by Bellenger, Guilyardi, Leloup, Lengaigne, & Vialard (2014), even though there is no significant improvement in the CMIP5 models performance in simulating ENSO when compared to the CMIP3, certain features and processes of ENSO life cycle, such as the location of surface temperature anomalies and seasonal phase locking, have been improved slightly.

Karpechko, Gillett, Marshall, & Scaife (2008) added that in CMIP5, some models with top elevation layer above 1 hPa are available, whereas most CMIP3 models did not have

University of Malaya

a well-resolved stratosphere to accurately simulate upper troposphere jet stream. In addition, Maloney & Chelton (2006) pointed out that there are 12 models in CMIP5 with latitudinal resolution less than 1.5 °. Guemas & Codron (2011) and Hourdin et al. (2013) link high resolution in some CMIP5 models (compared to CMIP3 models) to the reductions in the meridional position biases of jet stream. These advancement and improvement in CMIP5 models make the CMIP5 more suitable than those of earlier generations for assessing the response of the Southern Hemisphere subtropical jet stream for future climate projections.

Kidston & Gerber (2010) and Barnes & Hartmann (2011) found that the magnitude of the poleward jet shift in CMIP3 models are correlated with biases in the initial position of the jet in 20th century simulations. This has been improved in CMIP5 models as pointed out by Wilcox et al. (2012) that in austral summer, the magnitude of the jet shift is independent of the initial latitude of the jet. Miller, Schmidt, & Shindell (2006), Son et al. (2010), Arblaster, Meehl, & Karoly (2011) and Polvani, Waugh, Correa, & Son (2011) found that in austral summer the response of jet stream to GHG increases may be largely cancelled out by the response to ozone recovery during the first half of the 21st century in CMIP5. This is due to the standardised inclusion of the representation of stratospheric ozone changes, which was missing in some of the CMIP3 models.

2.7 Conclusions

As mentioned in the earlier part of this chapter, the literatures show that STJ is most stable and clearly defined in JJA, making JJA period more suitable for this study.

Previous studies have differing results on the rate and magnitude of changes in the strength of STJ. They also have differing opinion on the magnitude of change in the meridional location of STJ. However they agree that STJ is shifting polewards. The difficulty of constructing the climatology of STJ was attributed by Pena-ortiz, Gallego,

University of Malaya

Ribera, Ordonez, & Alvarez-castro (2013) as the reason for inconsistencies and lack of agreement in the change of the strength of STJ and its meridional location.

Studies also show that ENSO influences the strength and location of STJ. However, more work is needed to understand the relation and mechanism between STJ and ENSO. Hence, this study will also look into how the CMIP5 models simulate the impacts of ENSO on STJ.

The realistic projections of meridional location, trend of the STJ, and the understanding of the mechanism behind it, are very important. CMIP5 is currently the most suitable ensemble of models in carrying out future projection studies of STJ.

University of Malaya

CHAPTER 3: DATA AND METHODOLOGY

3.1 Introduction

This chapter provides the description of data and methods employed in this study. Data used are model generated reanalysis data sets in place of observation. For simulation of historical and future projections, output of CMIP5 models are utilised. In order to reduce the altitude related biases, three-dimensional analysis are performed, instead of the conventionally used two dimensional analysis.

3.2 Reanalysis Data

Reanalysis is a systematic model approach to produce gridded data sets for climate monitoring and research. Observational data available only at observation stations are assimilated into a model with an unchanging data assimilation scheme to produce gridded data set on a global scale, including areas where there are no observations. This unchanging framework provides a dynamically consistent estimate of the climate state at each time step. The only component of the framework that varies is the sources of the raw observational input data. This is unavoidable due to the ever changing observational network which includes, radiosonde, satellite, buoy, aircraft and ship reports. Various reanalysis products have proven to be quite useful when used with appropriate care (Dee et al., 2011).

There are several reanalysis data such as the first generation, e.g. NCEP-NCAR and NCEP-DOE, the second generation, e.g. ERA-40 and JRA25 and the current generation, e.g. ERA-Interim. Each generation of the data were improved by using more sophisticated data assimilation approaches. For this study, ERA-Interim reanalysis field is used as the 'truth' to assess the model simulations.

University of Malaya

3.2.1 ERA-Interim Reanalysis Data

ERA-Interim is the latest global atmospheric reanalysis dataset produced by European Centre for Medium-Range Weather Forecasts (ECMWF) by assimilation of observational data which includes ground stations, radiosonde, and satellite data and forecast model. ERA-Interim covers the period 1 January 1979 until current observations. Data prior to 1979 were not available due to the lack of satellite sounder data for use in the data assimilation process (Dee et al., 2011). It uses T255 spectral harmonic representation for basic dynamical fields and a reduced Gaussian grid N218 with approximately uniform horizontal spacing of 79 km (Dee et al., 2011). ERA-Interim assimilates four analyses per day at 00, 06, 12 and 18 UTC. A variety of data in uniform latitude/longitude grids (0.125 ° × 0.125 °, 0.5 ° × 0.5 °, 0.75 ° × 0.75 °, 1 ° × 1 °, 1.5 ° × 1.5 °, 2 ° × 2 °, 2.5 ° × 2.5 °, and 3 ° × 3 °) with 37 vertical heights is provided through the Meteorological Archival and Retrieval System (MARS) hosted by ECMWF. ERA-Interim is regarded as the most realistic of the various reanalysis dataset (Bracegirdle & Marshall, 2012; Bromwich, Nicolas, & Monaghan, 2011; Simmons et al., 2014). Therefore, ERA-Interim is used as the benchmark in assessing the performance of CMIP5 models in simulating STJ.

3.2.2 Hadley Centre Sea Ice and Sea Surface Temperature (HadISST)

ERA-Interim does have sea surface temperature (SST) data, but the data was derived from several sources over several different periods (Dee et al., 2011). Prior to 2002, the SST data were derived from optimum interpolation from NCEP-2D-Var and NCEP OISST V2. During 2002-2009, the SST was derived from NCEP RTG. Beyond 2009, the SST data used Operational Sea Surface Temperature and Sea-Ice Analysis (OSTIA). The assimilation technique used was also not well documented. Therefore, in this study we use SST data from Hadley Centre Sea Ice and Sea Surface Temperature (HadISST) (Rayner et al., 2003). HadISST contains SST data on 1 ° × 1 ° resolution from 1871 to current. HadISST sources data from the Met Office Marine Data Bank (MDB), Global

University of Malaya

Telecommunication System (GTS) and Comprehensive Ocean-Atmosphere Data Set (COADS), digitized sea ice charts, passive microwave retrievals and many others. HadISST has better SST representation through the assimilation technique used and thus has less inherent assimilation biases (Rayner et al., 2003).

3.2.3 CMIP5 Models

The main model data used in this thesis is the selected ensembles of climate models that participated in CMIP5 (Taylor, Stouffer, & Meehl, 2012). Among the 56 available CMIP5 models outputs (as of May 2016), 18 were used for a computationally affordable and in-depth analysis. The models were selected in such a way that all the necessary parameters are available for historical and future projections of RCP 4.5 and RCP 8.5 scenario. Historical (all forcings) output were used for historical simulation covering the period 1979 – 2012. For future projections covering the period 2011 – 2099, output from RCP 4.5 and RCP 8.5 scenarios are used. RCP 4.5 is a scenario of increase in global mean radiative forcing relative to the year 1750 by 4.5 W m^{-2} with carbon emission peaking in 2040 and stabilised by 2100. RCP 4.5 is an intermediate energy usage scenario, taking into account the intervention of government and international bodies in reducing the pollutants and greenhouse gases in the atmosphere. RCP 8.5 is a high energy-intensive scenario which is the result of high population growth and lower rate of technology development (van Vuuren et al., 2011). As RCP 8.5 scenario has higher intensity of warming than RCP 4.5 scenario, RCP 8.5 can validate the trends and changes occurred in RCP 4.5 scenario.

University of Malaya

Table 3.1 Namelist of CMIP 5 models used in this study, with the institutions/modelling centres and the countries of origin

Nu.	Model	Country	Institution/Modelling Centre
1	BCC-CSM1.1	China	Beijing Climate Center, China Meteorological Administration
2	CanESM2	Canada	Canadian Centre for Climate Modelling and Analysis
3	CCSM4	USA	National Center for Atmospheric Research
4	CNRM-CM5	France	Centre National de Recherches Meteorologiques / Centre Europeen de Recherche et Formation Avancees en Calcul Scientifique
5	CSIRO-Mk3.6.0	Australia	Commonwealth Scientific and Industrial Research Organisation in collaboration with the Queensland Climate Change Centre of Excellence
6	GFDL-CM3	USA	Geophysical Fluid Dynamics Laboratory
7	GISS-E2-R	USA	NASA Goddard Institute for Space Studies
8	HadCM3	UK	Met Office Hadley Centre (additional HadGEM2-ES realizations contributed by Instituto Nacional de Pesquisas Espaciais)
9	HadGEM2-CC		
10	HadGEM2-ES		
11	INM-CM4	Russia	Institute for Numerical Mathematics
12	IPSL-CM5A-LR	France	Institut Pierre-Simon Laplace
13	IPSL-CM5A-MR		
14	MIROC5	Japan	Atmosphere and Ocean Research Institute (The University of Tokyo), National Institute for Environmental Studies, and Japan Agency for Marine-Earth Science and Technology
15	MIROC-ESM		
16	MIROC-ESM-CHEM		
17	MPI-ESM-LR	Germany	Max Planck Institute for Meteorology (MPI-M)
18	NorESM1-M	Norway	Norwegian Climate Centre

The models and its participating institution and the details of resolution of the models are listed in Table 3.1 and Table 3.2. Resolutions of the SST parameter from the models are not listed as they have varying longitude and latitude resolution for each model. For models that have more than one ensemble, an unweighted average was calculated for all the ensembles beforehand and then used as the representative of the model. In order to represent the average of the CMIP5 models for analysis, unweighted multi-model mean approach is adopted by averaging all the individual model analysis results.

University of Malaya

Table 3.2 Resolutions of CMIP5 models used in this study

Nu.	Model Name	Total Level	Grid Size:		Number of Ensembles
			Longitude (°)	Latitude (°)	
1	BCC-CSM1.1	17	2.8125	2.767	1
2	CanESM2	22	2.8125	2.767	5
3	CCSM4	17	1.25	0.9424	6
4	CNRM-CM5	17	1.40625	1.40626	5
5	CSIRO-Mk3.6.0	18	2.875	1.849	10
6	GFDL-CM3	25	2.0	2.5	1
7	GISS-E2-R	17	2.5	2.0	3
8	HadCM3	17	3.75	2.5	10
9	HadGEM2-CC	23	1.875	1.25	3
10	HadGEM2-ES	17	1.875	1.25	4
11	INM-CM4	17	2.0	1.5	1
12	IPSL-CM5A-LR	17	3.75	3.7895	4
13	IPSL-CM5A-MR	17	2.5	1.2676	1
14	MIROC5	17	1.40625	1.389	3
15	MIROC-ESM	35	2.8125	2.767	1
16	MIROC-ESM-CHEM	35	2.8125	2.767	1
17	MPI-ESM-LR	25	1.875	2.767	3
18	NorESM1-M	17	2.5	1.89745	1

3.3 Selection of the Study Area

The study area is selected based on the climatology of STJ obtained from the zonal wind between 300 hPa and 100 hPa analysis of ERA-Interim. The monthly and seasonal mean zonal wind components, and the annual cycle of wind speed as well as the locations of the jet stream were analysed to determine the best area to work on. Here we examine the year-to-year features of the STJ during winters in order to distinguish it from the PFJ. Analysis of the variations in the strength of the STJ and its meridional position shows that the spatial location of the jet core is always confined to the area 20 °S to 40 °S, 70 °E to 290 °E (Figure 3.1) during winters. Thus, the study area selected shows a clearly defined jet stream. In addition, it facilitates the separation of the core of the STJ from the PFJ so as to avoid the Atlantic sector where the STJ often merges with the PFJ. In fact, several

University of Malaya

earlier studies (Liu, Yuan, Rind, Martinson, & Nin, 2002; Rind, Chandler, Lerner, Martinson, & Yuan, 2001; Yuan, 2004) showed that the ENSO-related changes in the strength of the STJ are mainly located in this area. Furthermore, strongest teleconnections are commonly observed in winter when the mean meridional temperature gradient is large (Strong & Davis, 2008). Hence, this study has selected the area defined above as our study area (Figure 3.1) which covers parts of the Indian Ocean and the South Pacific Ocean.

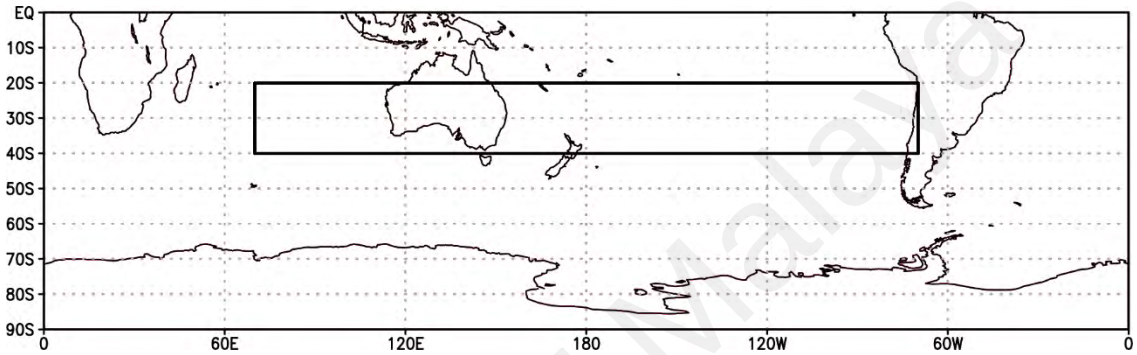

Figure 3.1 Selected area of study (70 °E to 290 °E, 20 °S to 40 °S)

3.4 Three Dimensional Analysis to Identify the Jet Core

There are several past studies that used reanalysis data to identify the location, strength and to quantify the trend in the location and strength of STJ. Discrepancies in the assessment of the strength and the meridional location of STJ have been attributed to deficiencies in methodology, data, and oversimplification using averages (Pena-ortiz et al., 2013). Many previous studies used reduced two-dimensional analysis such as selecting a static pressure level i.e. 200 hPa (Athanasiadis, Wallace, & Wettstein, 2010), average wind displayed in latitude-height cross-section (Athanasiadis et al., 2010), average wind at some predefined level near the tropopause (Blackmon, Wallace, Lau, & Mullen, 1977; Kidson, 1999), and temporal averages of any flow variable (Strong & Davis, 2008). These methods are good in describing basic characteristics of zonal circulation. However, instantaneous distributions of jet stream are much more complex and thus several jet properties are lost from averaging (Koch et al., 2006; Limbach,

University of Malaya

Schömer, & Wernli, 2012). Such two-dimensional method introduces biases related to the simplified axis such as altitude location of the jet core, and degradation of information from averaging. A precise characterization of jet stream trends is not really attainable with zonally averaged values (Pena-ortiz et al., 2013). In addition, the preliminary work carried out in this study also shows that the jet core is not always at a static pressure level in the ERA-Interim and CMIP5 models output. Therefore, by not taking into account the altitude of STJ can give rise to wrong estimations (Strong & Davis, 2008).

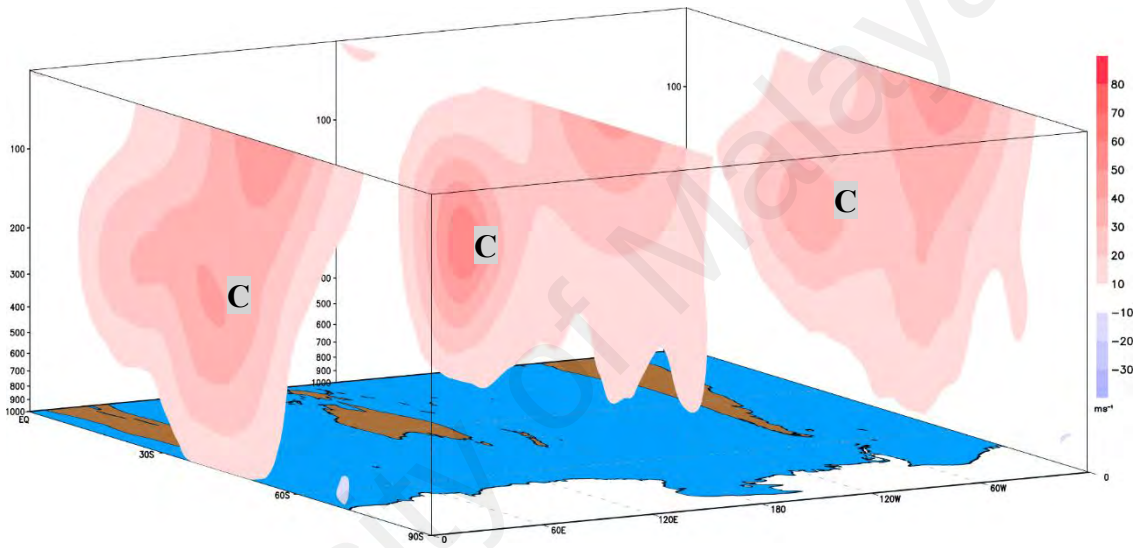

Figure 3.2 Three latitude-altitude cross section of zonal wind at 0 °E, 180 °E, and 320 °E for July 1990. Colour bar denotes wind speed in ms^{-1}

In view of the above, this study adopts a three-dimensional analysis based on (Pena-ortiz et al., 2013) instead of the reduced two-dimensional analysis. The three dimensional analysis lowers biases and information loss (Manney et al., 2011; Strong & Davis, 2008). It can capture short-term temporal and spatial variations of jet stream's altitude (Pena-ortiz et al., 2013), detect even the less frequent or weaker jet branches which otherwise could have been hidden behind temporal or spatial wind velocity averages. It also reflect both the steady and transient variabilities of the jet (Strong & Davis, 2008).

University of Malaya

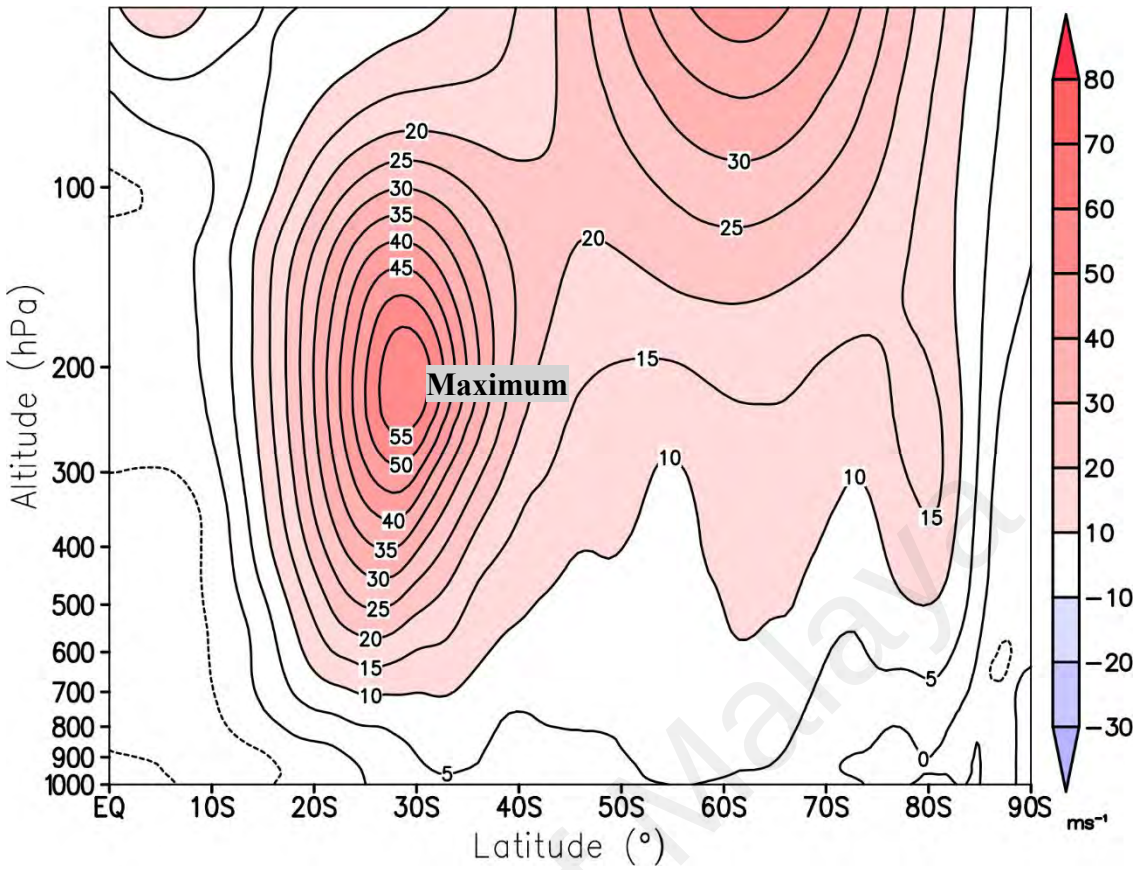

Figure 3.3 A Single latitude-altitude cross section of zonal wind along 180 °E for July 1990. Colour bar denotes wind speed (ms^{-1})

In order to identify the jet core, monthly mean zonal winds are analysed to locate the zonal wind maximum in the vertical between 300 hPa and 100 hPa, from 20 °S to 40 °S at each longitudinal slice between 70 °E – 290 °E. The description is visualised in Figure 3.2, showing mean zonal wind from 300 hPa to 100 hPa, 20 °S to 40 °S between the longitudes 70 °E – 290 °E for July 1990. The letter C shows the core of the STJ at different longitudes during the period. Figure 3.3 shows a single latitude-altitude cross section of zonal wind in July 1990 along 180 °E. No minimum speed threshold was used in selecting the wind maximum. Instead, the wind maxima must satisfy the condition of being greater than the surrounding points. The magnitude of wind maxima is taken as the jet core strength and the latitude of this wind maximum is taken as the meridional location of the jet core. The resulted data is then visually checked to filter any jet core/wind maximum that is not continuous in strength and meridional location for that particular month. To

University of Malaya

obtain the mean strength and location of STJ for the particular month, the jet core values and their corresponding latitudes from all the longitudinal slices are averaged. The procedure is repeated for winter month (JJA) in the Southern Hemisphere for the historical period 1979 – 2012 and for future projection period 2011 – 2099 for all the selected CMIP5 models.

The calculated values of the winter months (June, July, and August) for each selected years (1979 to 2012 for historical and 2011 to 2099 for future projection) were then used to find the long term average, the trends in the strength of STJ and the meridional location of STJ. The significance of the trend at ($p \leq 0.05$) (significant level of 95% confidence level) is calculated through two-tailed t-test with reduced degree of freedom (Bretherton, Widmann, Dymnikov, Wallace, & Bladé, 1999).

University of Malaya

CHAPTER 4: REPRESENTATION OF THE STJ AND THE IMPACTS OF ENSO ON THE STRENGTH AND MERIDIONAL LOCATION OF STJ BASED ON THE HISTORICAL RUNS OF THE CMIP5 MODELS

4.1 Introduction

This chapter focuses on the historical simulation of STJ by 18 selected CMIP5 models for the period 1979 – 2012 and also covers the assessment of the ability of the CMIP5 models in simulating ENSO effects on the STJ.

Section 4.2 is deals with the climatology of the STJ using ERA Interim reanalysis. Section 4.3 examines how CMIP5 models simulate the impacts of ENSO on STJ. Section 4.4 consists of evaluation of historical simulation of STJ by CMIP5 models and its comparison with the reanalysis field to investigate how the CMIP5 models carried out historical simulations of STJ and identify the differences between the observation and the simulations.

4.2 Climatology of Jet Stream

A climatology of STJ is constructed using zonal wind averaged between 300 – 100 hPa levels from the ERA-Interim reanalysis datasets. This will enable the detection of the annual and seasonal variability in the strength as well as the meridional location of STJ.

4.2.1 Annual and Seasonal Cycle of STJ

Monthly and seasonal variations in the strength of STJ were obtained from the long-term monthly averages of zonal wind between the altitudes of 300 – 100 hPa levels for the period of January 1979 to December 2012.

University of Malaya

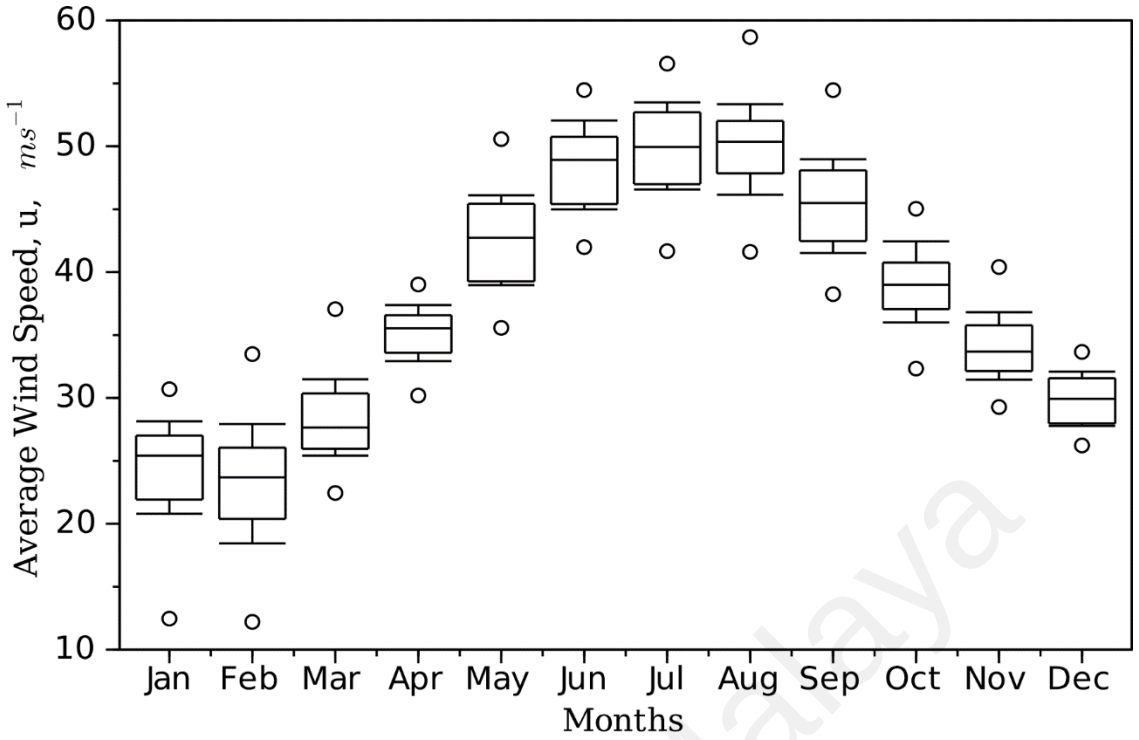

Figure 4.1 Wind maxima from monthly mean of zonal wind averaged between 300 – 100 hPa from ERA-Interim for the period 1979 – 2012 in the study area (refer Figure 3.1). The whiskers indicate one standard deviation and the circles indicate the range of the values

Boxplot in Figure 4.1 illustrates the average of wind maxima from monthly mean of zonal wind within the study area. The whiskers indicate one standard deviation while the circles the range of the values. The spread of standard deviation from June to August is the smallest, followed by December to February, indicating the stability of STJ in these seasons. For March to May and September to November, the spread of standard deviation are large, due to the strengthening and weakening of STJ during these transitional months. This indicates that the STJ strengthens rapidly during MAM and weaken slowly during SON.

University of Malaya

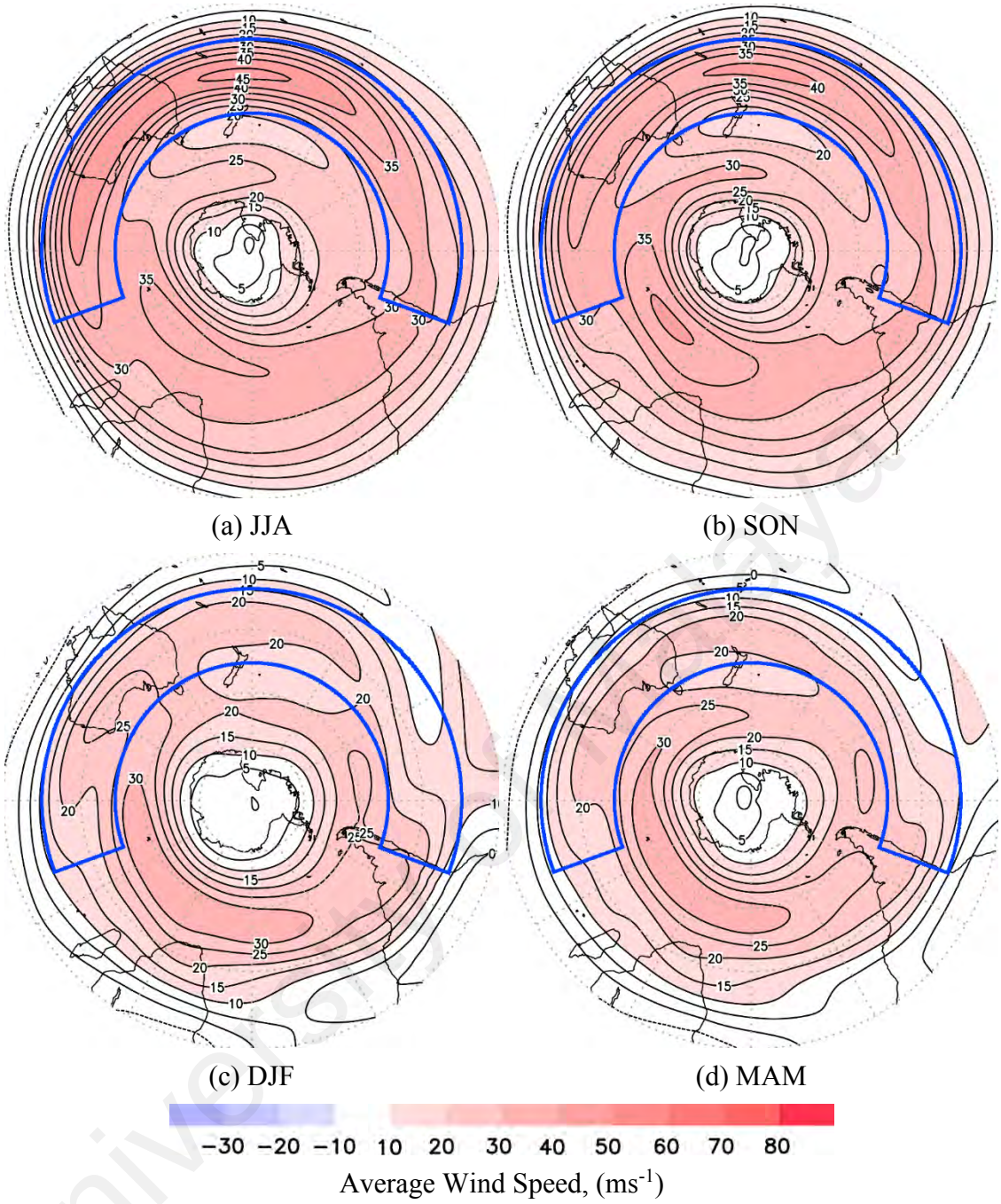

Figure 4.2 Seasonal average of zonal wind averaged between 300 – 100 hPa for the period 1979-2012. Contour marks zonal wind speed every 5 ms^{-1}. Colour bar denotes scales of zonal wind speed in ms^{-1}. Blue box highlights the study area

Figure 4.2 shows the seasonal averages of zonal wind averaged between 300 – 100 hPa levels for the period 1979 – 2012. In the study area of Indian Ocean and Southern Pacific Ocean (refer Figure 3.1), STJ is strongest and clearly defined in JJA. This is followed by its lower strength in SON. In DJF and MAM, STJ are not well defined.

It can be depicted from the Figure 4.1 and Figure 4.2 that STJ is strongest during austral winter and weakest during the austral summer. STJ strengthens rapidly during MAM, peaks in JJA, weakens gradually during SON and dips in DJF. In addition, the low standard deviation and range of zonal wind during winter in Figure 4.1 shows that STJ is most stable during austral winter. The average zonal wind speeds of STJ in austral winter and austral summer are 49.43 ms^{-1} and 25.87 ms^{-1} respectively. In austral spring, the strength of STJ gradually weakens with a wind speed of 45 ms^{-1} in September to 34 ms^{-1} in November. In austral autumn, the strength of STJ gradually strengthens from wind speed of 32 ms^{-1} in March to 42 ms^{-1} in May. Based on the monthly average and seasonal average of zonal wind, it can be seen clearly that the strength of STJ is highest during austral winter and varies significantly over the seasons with a large interannual variability in strength.

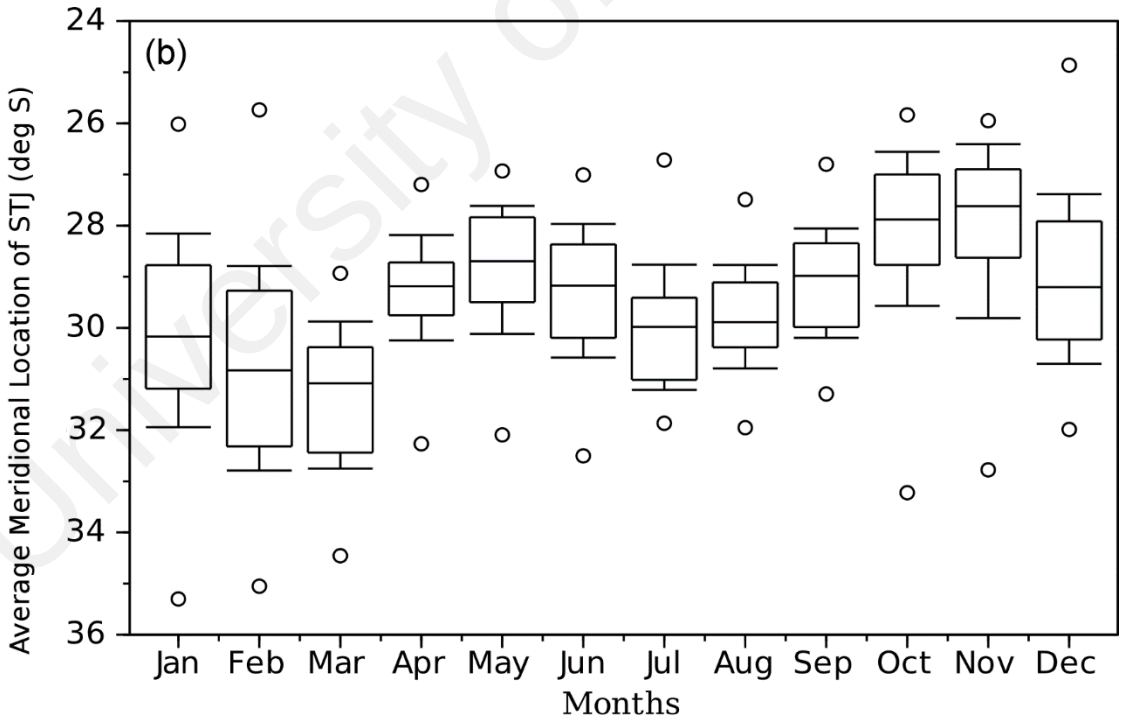

Figure 4.3 Monthly mean of meridional location of zonal wind maxima averaged between 300 – 100 hPa from ERA-Interim for the period 1979 – 2012 in the study area (refer Figure 3.1). The whiskers indicate one standard deviation and the circles indicate the range of the values

University of Malaya

Figure 4.3 shows the seasonal variation in the mean meridional location of STJ. The STJ during summer displays a maximum poleward location at 31 °S and shifts equatorwards during autumn and spring. During winter, the meridional location of STJ is most stable at around 30 °S. During JJA the core of STJ is located at 30 °S between the longitudes 70 °E to 240 °E. Therefore, in this study, average location of STJ is determined to be confined to the area 70 °E to 290 °E and latitude from 20 °S to 40 °S.

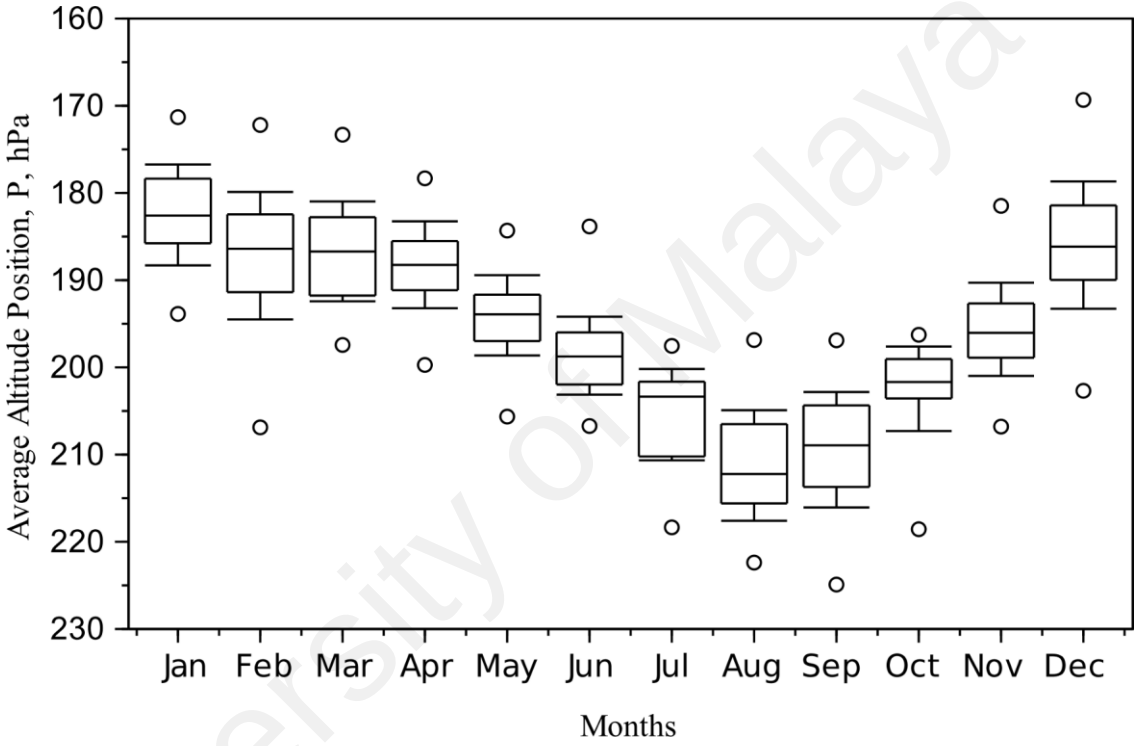

Figure 4.4 Long term monthly mean of altitude location of zonal wind maxima from ERA-Interim for the period 1979 – 2012 in the study area (refer Figure 3.1). The whiskers indicate one standard deviation and the circles indicate the range of the values

Figure 4.4 and Figure 3.1 show that the core of STJ is not confined to 200 hPa level. Instead, STJ altitude varies from 225 hPa to 175 hPa. In addition, CMIP5 models may simulate STJ differently as from observation. Therefore, in this study, the altitude and the area selected is 300 hPa to 100 hPa, 20 °S to 40 °S, and 70 °E to 290 °E respectively.

University of Malaya

4.3 Impacts of El Niño-Southern Oscillation on STJ

ENSO is the dominant factor of global climate variability (Trenberth, 1997; Y. Zhang et al., 1997). The strength of STJ is strongly affected by the state of the sea surface temperatures (SST) across the tropical ocean in response to the changes in phase of the ENSO (Sampe, Nakamura, Goto, & Ohfuchi, 2010). The ENSO influence is noticeable more in the Pacific sector than the other parts of the SH (Gallego et al., 2005; Turner, 2004). The effect of the ENSO cycle on the jet stream is noticeable in the meridional location of the STJ and in particular on its strength. During El Niño phase, the strength of the STJ over the Pacific area is 25 – 50% greater than that during the La Niña phase (Gallego et al., 2005). In contrast, the STJ speed over the Atlantic and Indian Oceans shows a decrease of 10 – 20% during the El Niño phase (Gallego et al., 2005). Furthermore, the location of the STJ over the Pacific area is found to be displaced equatorwards compared to the mean location.

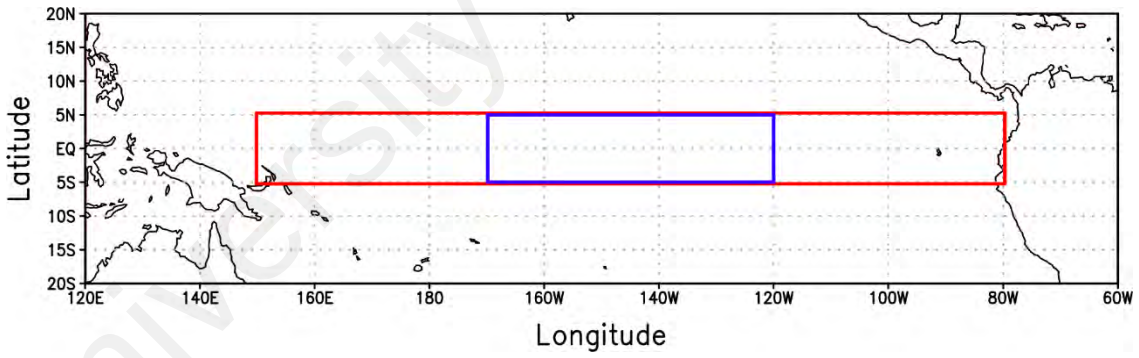

Figure 4.5 Red box highlight the equatorial pacific area used in the identification of ENSO events. Blue box highlights the traditionally used Niño 3.4 region. Red box highlight region of equatorial Pacific

Conventionally, ENSO severities are evaluated based on Oceanic Niño Index developed by National Oceanic and Atmospheric Administration, U.S. Department of Commerce. To identify El Niño and La Niña events in the tropical Pacific, 3-month running mean of SST anomaly for the Niño 3.4 region (5 °N – 5 °S, 190 °E – 240 °E, indicated in Figure 4.5 by the blue box) were calculated. ENSO events are defined if the

University of Malaya

average SST from Niño 3.4 region of consecutive overlapping 3-month periods at or above the +0.5 °C anomaly for El Niño events and at or below the -0.5 °C anomaly for La Niña events.

The conventional method however cannot be applied for analysis of ENSO in CMIP5 models. CMIP5 historical runs do not include any real observations in the model assimilation. Therefore, the ENSO events in CMIP5 models will not occur at the same time as ENSO events in the real world. Thus an expanded method based on the conventional method by Leloup et al. (2008) is adapted for both CMIP5 models and ERA-Interim for comparison.

In order to identify El Niño and La Niña events in the CMIP5 models and ERA-Interim, we use SST anomaly along the equatorial Pacific as defined by Leloup et al. (2008). SST is averaged over the region 5 °N – 5 °S, 150 °E – 280 °E (indicated in Figure 4.5 by the red box) for each month from January 1979 to December 2012. Monthly SST anomaly from each CMIP5 models used for this study were calculated and SST anomaly were then smoothed using a 3 month running mean. In this approach, El Niño (La Niña) events are defined as events with at least six consecutive months with SST anomaly greater (lower) than half a standard deviation of the SST anomalies (Leloup et al., 2008) for each model. All of the El Niño and La Niña events identified within 1979 to 2012 were used to study the impact of ENSO on STJ.

University of Malaya

Table 4.1 ENSO events defined using equatorial SST anomaly during the period 1979 – 2012 based on HadISST

El Niño Events	La Niña Events
1982	1984
1983	1985
1987	1988
1991	1989
1997	1998
2002	1999
2009	2000
	2007
	2010

Table 4.2 Number of ENSO events identified in CMIP5 models during the period 1979 – 2012

Model	Number of El Niño events	Number of La Niña events
BCC-CSM1.1	11	8
CanESM2	11	6
CCSM4	8	7
CNRM-CM5	5	8
CSIRO-Mk3.6.0	11	8
GFDL-CM3	11	7
GISS-E2-R	13	8
HadCM3	11	8
HadGEM2-CC	9	8
HadGEM2-ES	9	9
INM-CM4	8	10
IPSL-CM5A-LR	11	7
IPSL-CM5A-MR	11	7
MIROC5	8	13
MIROC-ESM	7	5
MIROC-ESM-CHEM	8	8
MPI-ESM-LR	9	7
NorESM1-M	8	9
*ERA-Interim	7	9

University of Malaya

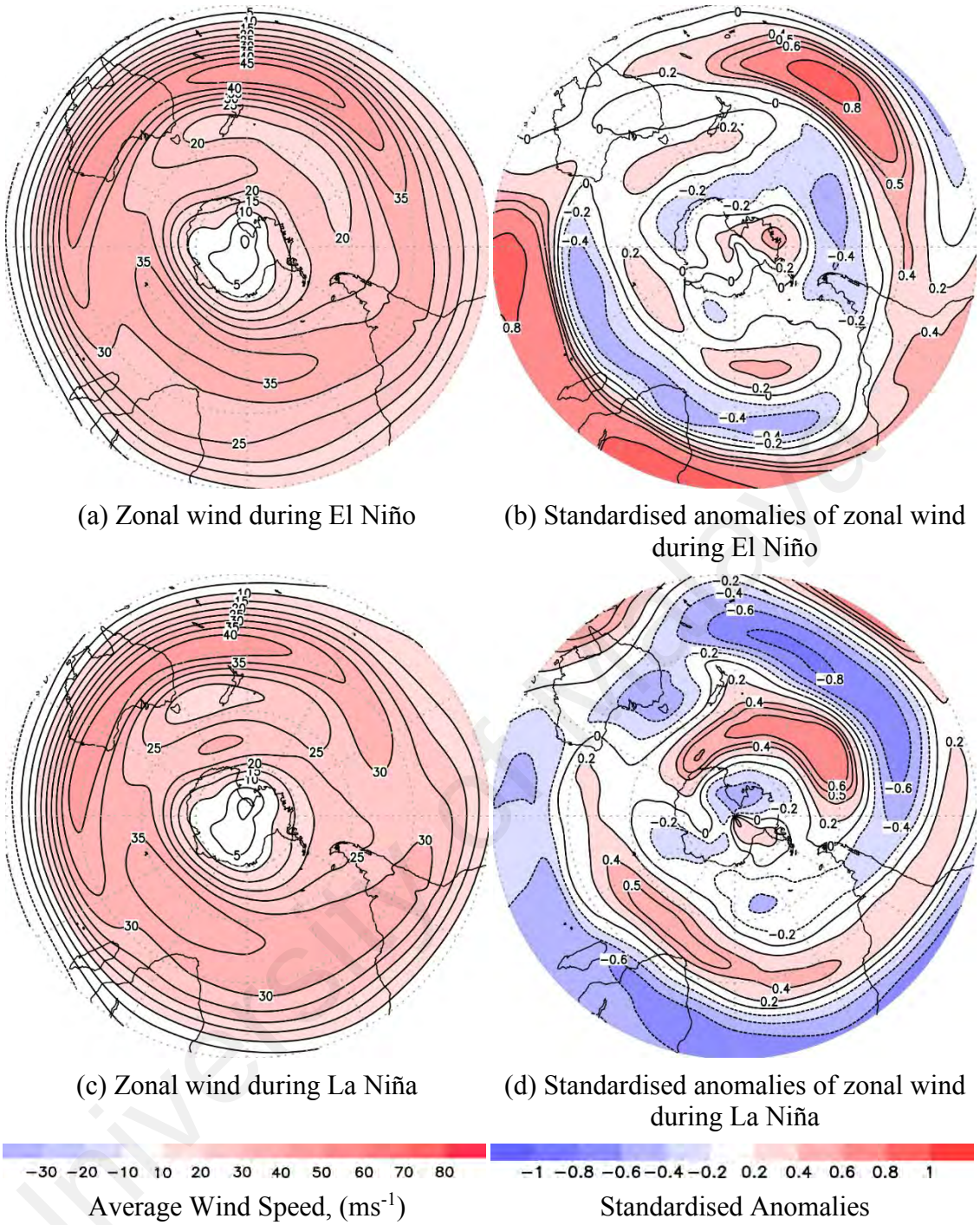

(a) Zonal wind during El Niño

(b) Standardised anomalies of zonal wind during El Niño

(c) Zonal wind during La Niña

(d) Standardised anomalies of zonal wind during La Niña

Figure 4.6 Composite of zonal wind averaged between 300 – 100 hPa for (a) El Niño phase and (c) La Niña phase and its standardised anomalies for (b) El Niño phase and (d) La Niña phase based on ERA-Interim for the period 1979 – 2012

Table 4.1 lists the ENSO events from ERA-Interim based on the method by Leloup et al. (2008). Table 4.2 list the number of ENSO events in CMIP5 models. 84.2% of the models simulated more El Niño events compared to the El Niño events from ERA-Interim., 5.3 % of the model simulated the same number of events as in

ERA-Interim and 5.3% of the models simulated fewer events of El Niño compared to ERA-Interim. In contrast, 73.7% of the models simulated fewer La Niña events, 10.5% of the models simulated the same number of events and 10.5% of the models simulated more La Niña events compared to ERA-Interim.

The impacts of ENSO on STJ are quantified through standardised anomaly of zonal wind during the ENSO events. Figure 4.6 shows the composite zonal wind averaged between 300 – 100 hPa for (a) El Niño phase and (c) for La Niña phase and its standardised anomalies for (b) El Niño phase and (d) for La Niña phase based on ERA-Interim for the period 1979 – 2012. From Figure 4.6 it can be noted that there is a strong positive standardised anomaly of zonal wind over the southern Pacific Ocean centred at 210 °E and 25 °S with magnitude reaching 0.9, and negative standardised anomaly (<-0.5) over the Atlantic Ocean and south of Africa and Indian Ocean around 30°S. It can be also noted that STJ is stronger and shifts eastwards in the Pacific Ocean during the El Niño phase. Bals-Elsholz et al. (2001) suggested that a baroclinic zone across Australia develops during the austral winter as a result of the cooling of the continent in contrast to the western Pacific warm pool during El Niño. Hence, this modulates the strength and position of the STJ (Seager, Harnik, Kushnir, Robinson, & Miller, 2003). Liu et al. (2002) suggest increased convection associated with El Niño events alters the mean meridional atmospheric circulation of the subtropical jet position and strength. During La Niña, there is a strong negative standardised anomaly of zonal wind over the Southern Pacific Ocean centred at 210 °E and 25 °E and a band of positive standardised anomaly (>0.5) south of Africa centred at 30 °E and 42 °S.

University of Malaya

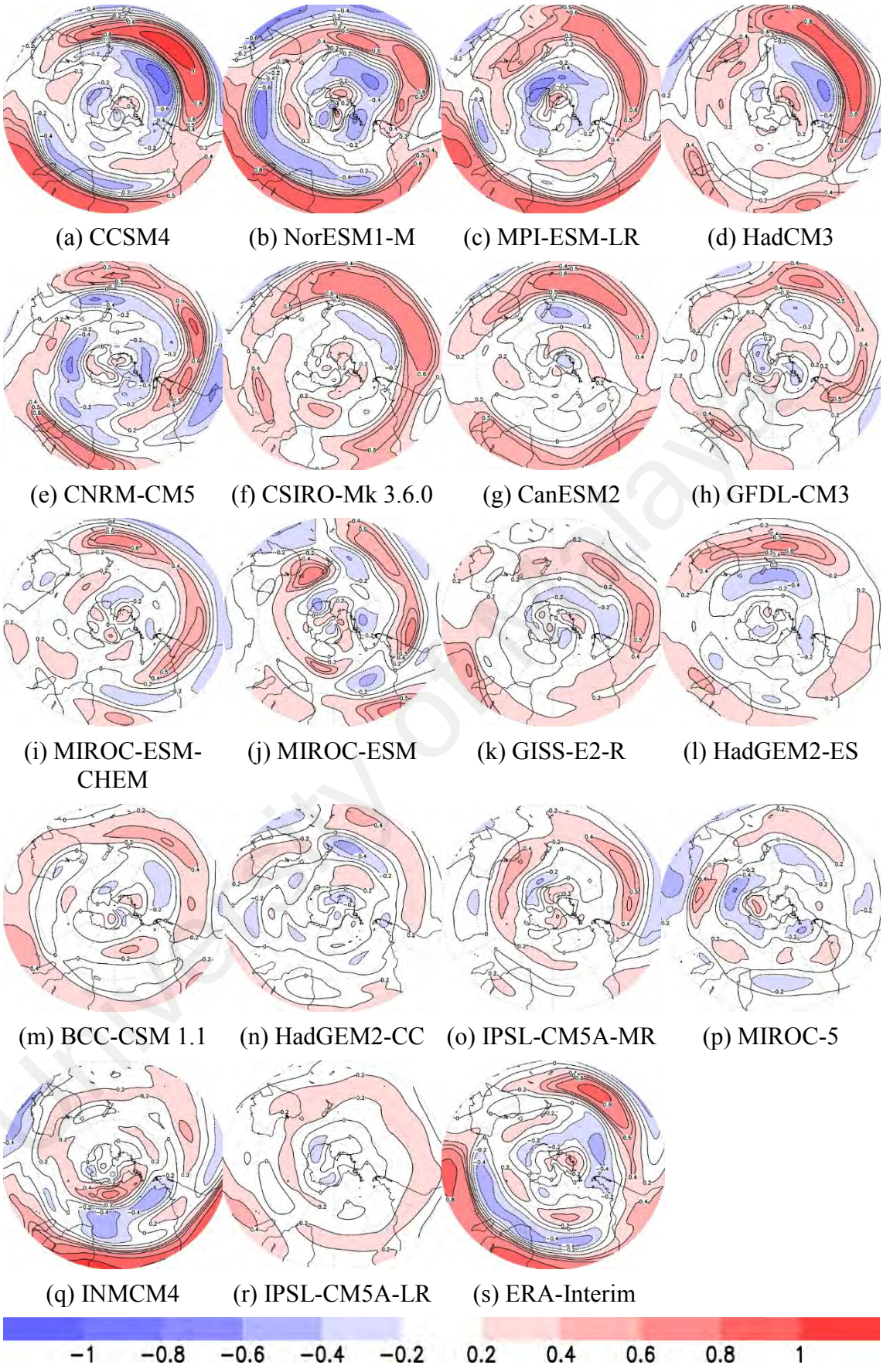

Figure 4.7 Standardised anomalies of zonal wind averaged between 300 – 100 hPa for all the El Niño events from 1979 to 2012 from CMIP5 models. Also shown is (s) standardised anomalies of zonal wind for ERA-Interim for comparison

University of Reading

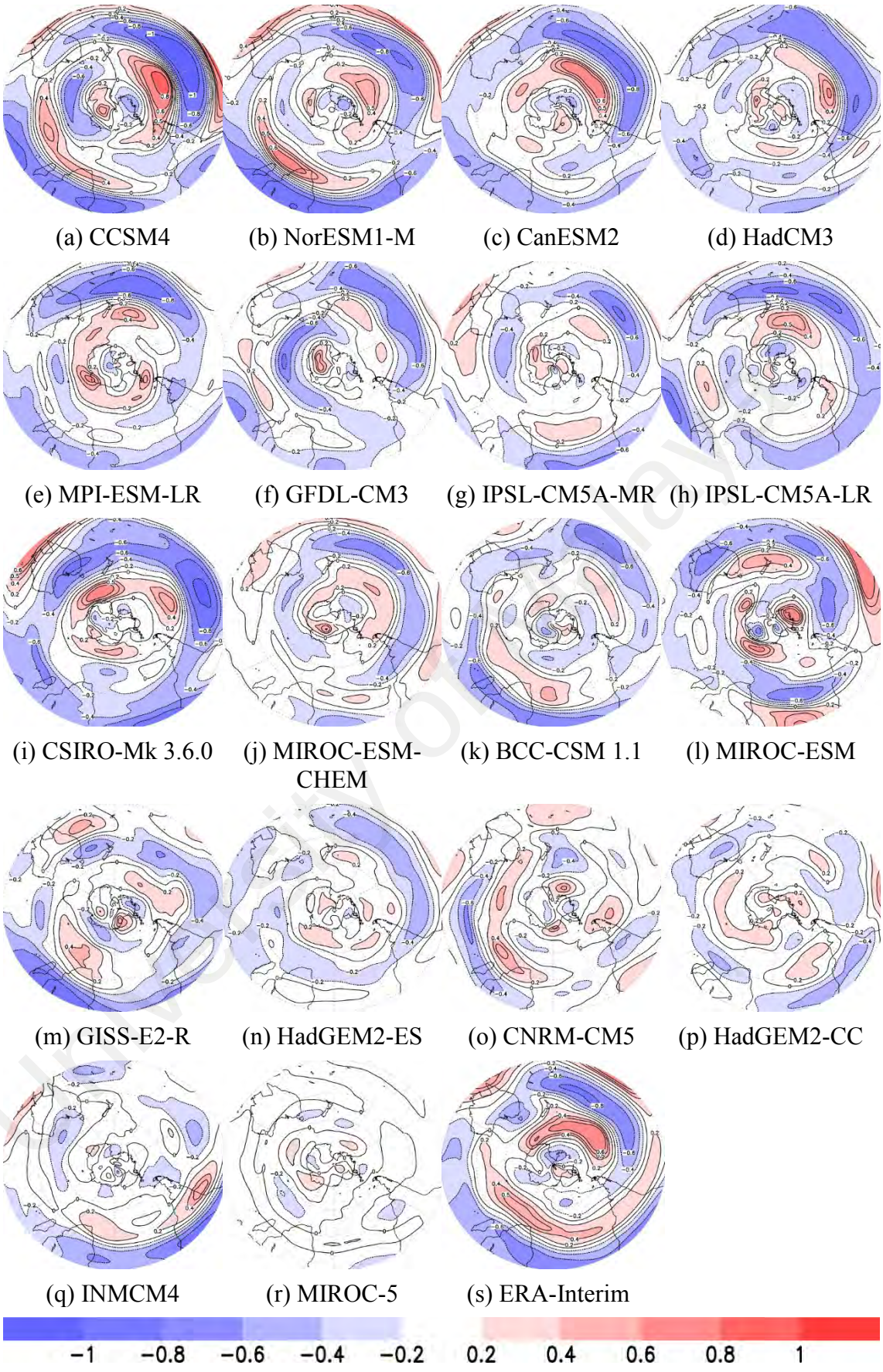

Figure 4.8 Standardised anomalies of zonal wind averaged between 300 – 100 hPa for all the La Niña events from 1979 to 2012 from CMIP5 models. Also shown is (s) standardised anomalies of zonal wind for ERA-Interim for comparison

University of Hawai'i at Manoa Library

Figure 4.7 shows the standardised anomaly of zonal wind averaged between 300 – 100 hPa for all El Niño events from 1979 to 2012 for each individual CMIP5 models. For El Niño phase, four models CCSM4, NorESM1-M, MPI-ESM-LR, and HadCM3 (Figure 4.7 a – d) were able to capture the features of El Niño impacts on the STJ close to the observed patterns both in terms of the locations as well as the changes in the strength. Other models, namely CNRM-CM5, CSIRO-MK 3.6.0, CanESM2, and GFDL-CM3 (Figure 4.7 e – h) show slight deviations from the observed El Niño pattern. MIROC-ESM-CHEM, MIROC-ESM, GISS-E2-R and HadGEM2-ES (Figure 4.7 i–l) shows major deviations of the observed El Niño pattern. BCC-CSM1-1, HadGEM2-CC, IPSL-CM5A-MR, MIROC5, INMCM4, and IPSL-CM5A-LR (Figure 4.7 m – h) fail to reproduce the observed pattern of El Niño impacts on STJ.

Figure 4.8 shows the standardised anomaly of zonal wind averaged between 300 – 100 hPa for all La Niña events from 1979 to 2012 for each individual CMIP5 models. For La Niña phase, four models, CCSM4, NorESM1-M, CanESM2, and HadCM3 (Figure 4.8 a–d) were able to capture the features of the La Niña impacts on the STJ close to the observed patterns both in terms of the locations as well as the changes in the strength. The models MPI-ESM-LR, GFDL-CM3, IPSL-CM5A-MR, and IPSL-CM5A-LR (Figure 4.8 e – h) were able to reproduce the spatial pattern of average zonal wind anomaly with slight variations. Model CSIRO-Mk 3.6.0, MIROC-ESM-CHEM, BCC-CSM1.1 and MIROC-ESM (Figure 4.8 i – l) shows major deviation of the observed El Niño pattern. Model GISS-E2-R, HadGEM2-ES, CNRM-CM5, HadGEM2-CC, INMCM4 and MIROC5 (Figure 4.8 m – r) fail to reproduce the observed pattern of La Niña impacts on STJ. As noted by Bellenger et al. (2014), the CNRM-CM5 and CCSM4 models are some of the CMIP5 models that have best ENSO characteristics and these models are more reliable to study ENSO dynamics and its sensitivity to external forcing.

University of Malaya

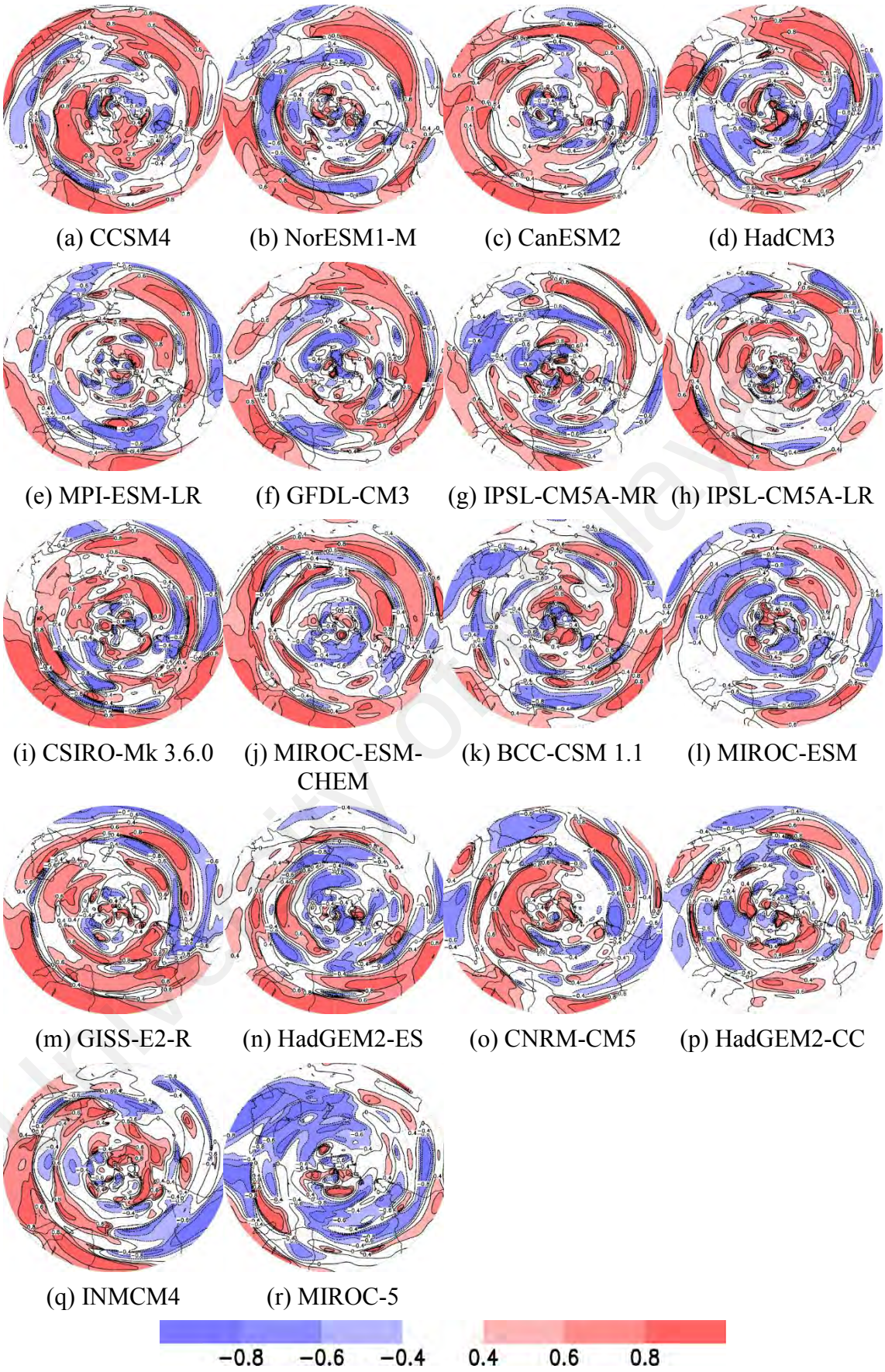

Figure 4.9 Anomaly correlation coefficient of zonal wind averaged between 300 – 100 hPa for all the El Niño events during JJA from 1979 to 2012 from CMIP5 models with ERA Interim

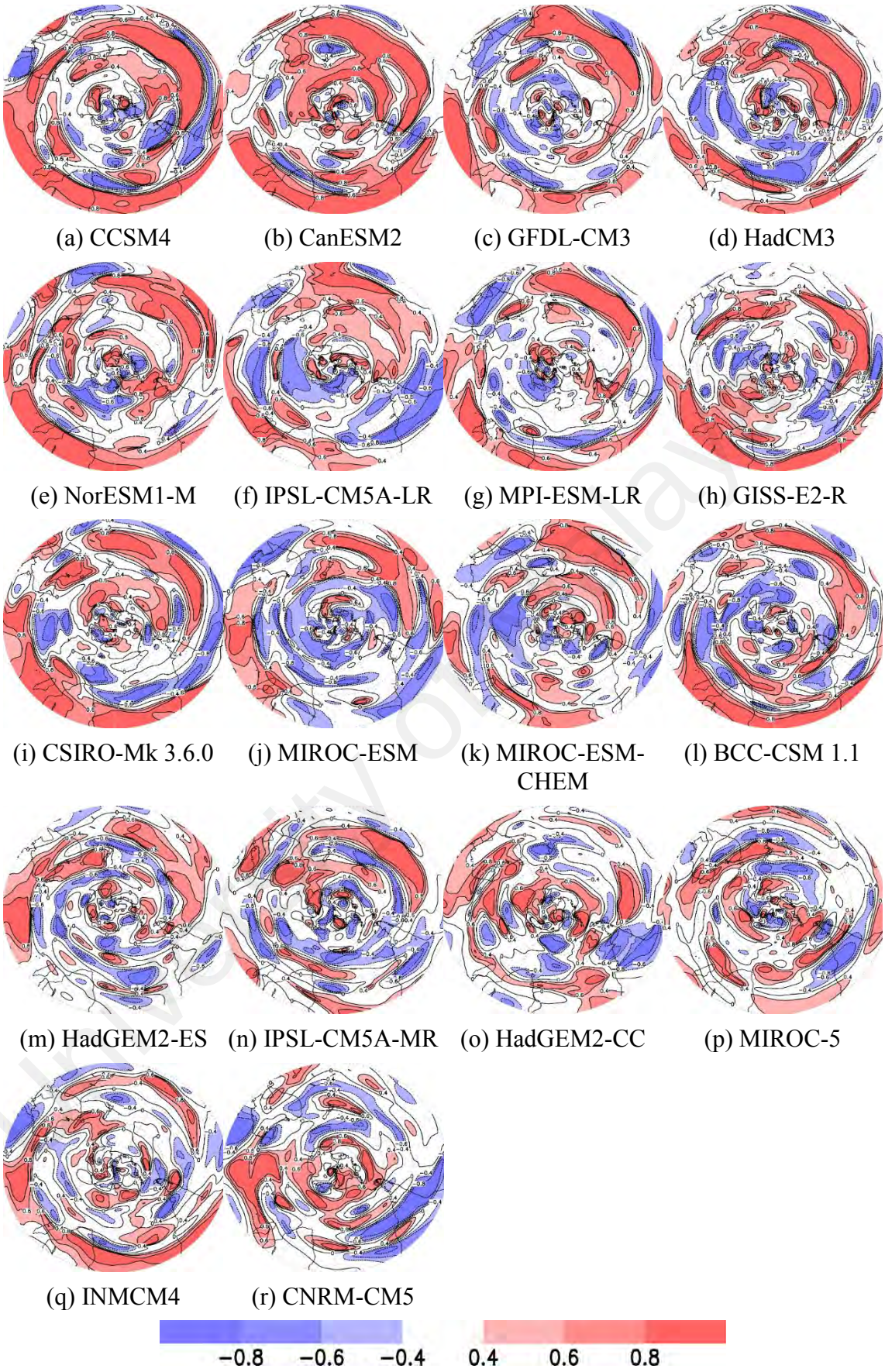

Figure 4.10 Anomaly correlation coefficient of zonal wind averaged between 300 – 100 hPa for all the La Niña events during JJA from 1979 to 2012 from CMIP5 models with ERA Interim

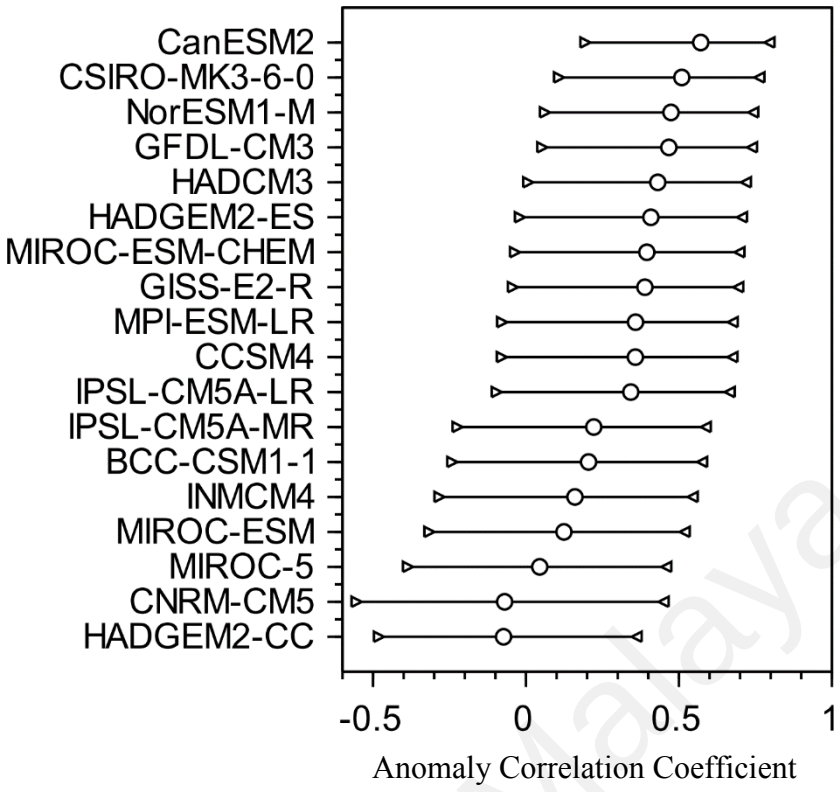

(a)

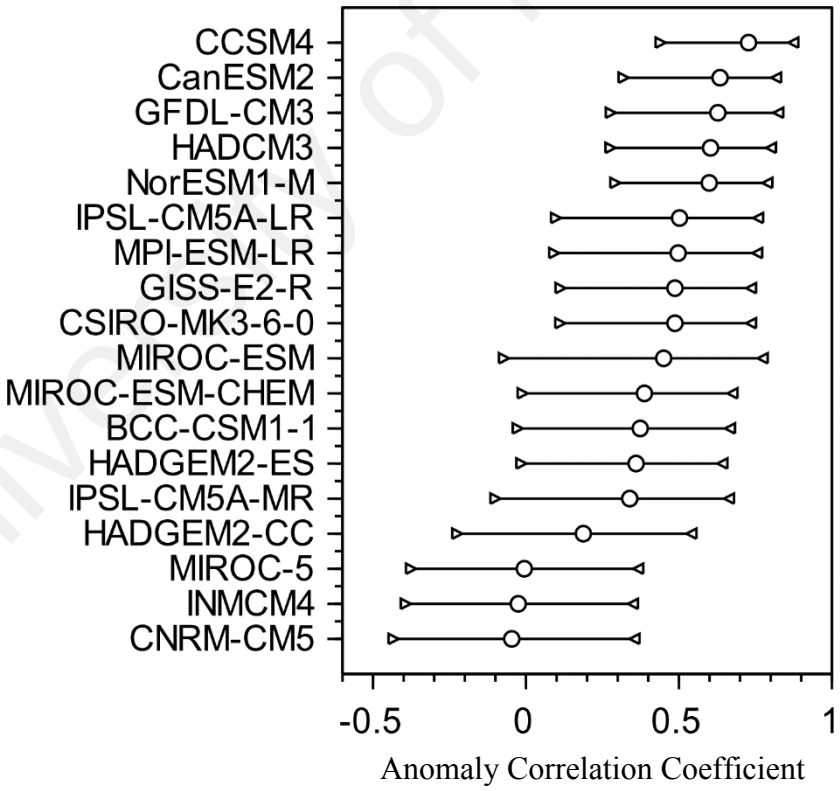

(b)

Figure 4.11 Mean of anomaly correlation coefficient of zonal wind averaged between 300 – 100 hPa between the CMIP5 models and ERA-Interim a) during El Niño events and b) during La Niña events in the area of study. The whiskers in the graph show 95% confidence interval for the respective models

University of Malaya

In order to quantify the model ability in simulating the impacts of ENSO on STJ, anomaly correlation coefficient (ACC) is used. Here, the correlation of the anomaly of zonal wind in ERA-Interim with the anomaly of zonal wind in each CMIP5 models are calculated. Figure 4.9 shows anomaly correlation coefficient of zonal wind averaged between 300 – 100 hPa for all the El Niño events during JJA from 1979 to 2012 from CMIP5 models with ERA Interim. The same is for Figure 4.10 except for La Niña.

To further characterise the representation of the magnitude of the impact of ENSO on the jet stream in CMIP5 models , the ACC average in the study area (refer Figure 3.1) are calculated and shown in Figure 4.11 (a) and Figure 4.11 (b) for El Niño and La Niña phase respectively. The whiskers in the figures indicate ($p \leq 0.05$) confidence interval. The models CanESM2, CSIRO-MK3-6-0, NorESM1-M, GFDL-CM3, HADCM3 and HADGEM2-ES reveal a moderate correlation (0.40 – 0.60) of El Niño impact on the jet stream between CMIP5 models and ERA-Interim in the study area. For impacts during La Niña, 55% of the CMIP5 models shows a higher ACC (0.45 – 0.75). In general, moderate to higher ACC averages from CanESM2, CSIRO-MK3-6-0, NorESM1-M, GFDLCM3, HADCM3 indicate that they display relatively good El Niño and La Niña characteristics in terms of magnitude and location.

A recent paper by Molteni, Stockdale, & Vitart (2015) provides a critical insight into the understanding of modelling extratropical teleconnection such as ENSO impacts with the Indo-Pacific region. They stated that ECMWF coupled model reproduces the broad features of tropical and extra-tropical teleconnections with a good degree of fidelity. However, the traditional method of linearly relating circulation anomalies to SST anomalies is only appropriate for signals originated in central and east Pacific as it fails to identify the response to anomalous heating over the west Pacific and most of the Indian Ocean. They concluded that accurate simulation of inter-decadal variability of SST is

University of Malaya

crucial in reproducing the teleconnection relationship. Also, particular care must be taken in interpreting the results of the AGCM simulation that just based on the SST because of the absence of feedback between convection and SST over the warm pool region.

4.4 Simulation of Historical Trends of STJ by CMIP5 Models

Historical trend (1979 – 2012) in the strength of STJ as well the locations were analysed based on ERA-Interim as well as CMIP5 models. The dotted vertical line and the dotted-dash lines in the Figure 4.12 represent the trend in the jet strength in ERA-Interim and position of zero trend respectively. The blue coloured data points show models that have statistically significant trends in the strength at significant level ($p \leq 0.05$) using two-tailed student test with reduced degree of freedom (Bretherton et al., 1999).

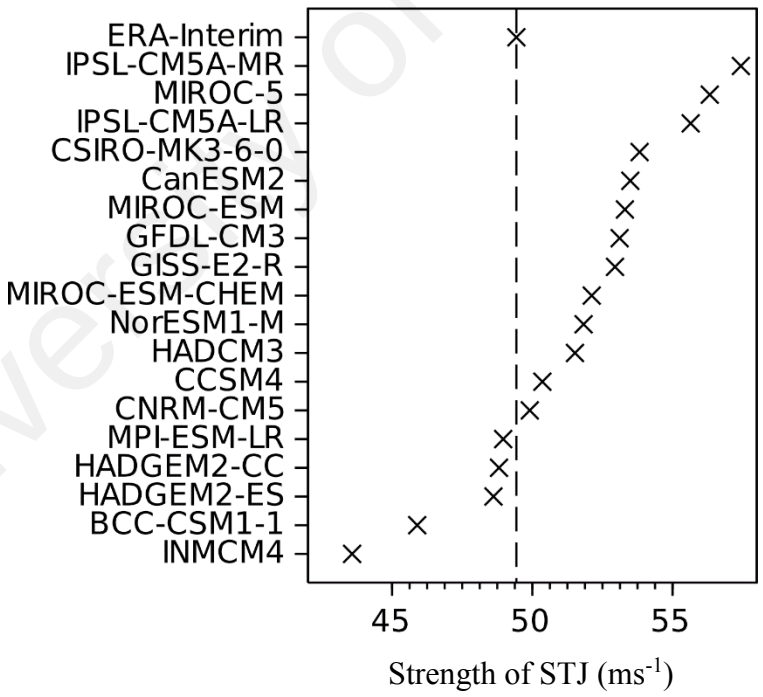

(a)

Figure 4.12 (a) Mean strength of STJ and (b) decadal trend in the strength of STJ in the historical CMIP5 simulations and ERA-Interim in the study area. The blue coloured cross marks indicates models with trends that are statistically significant ($p \leq 0.05$) using two-tailed student test. The dash vertical line and the dot-dash vertical lines in the figure represent ERA-Interim and position of zero trend line respectively

University of Malaya

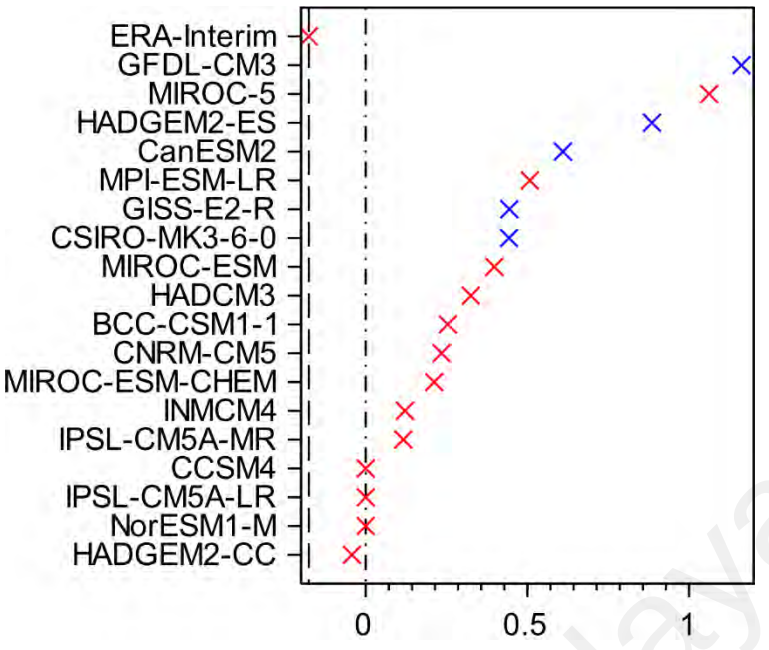

(b)

Figure 4.12 Continued

Figure 4.12 (a) shows the mean strength of STJ and Figure 4.12 (b) shows the trend in the strength of STJ in ERA-Interim and all the CMIP5 models for the period 1979 – 2012. The trend values and long term average values are given in Appendix A. The CMIP5 models shows a wide range of long-term average value, ranging from 48 – 53 ms^{-1}. Trend in the strength of STJ shows a wide range from 0.1 – 1.2 ms^{-1} $decade^{-1}$. ERA-Interim and HADGEM2-CC show negative trend in the strength of STJ, but the trends are not significant. Only five models (28%), GFDL-CM3, HadGEM2-ES, CanESM2, GISS-E2-R and CSIRO-MK3.6.0 show a significant positive trend in the strength of STJ.

University of Malaya

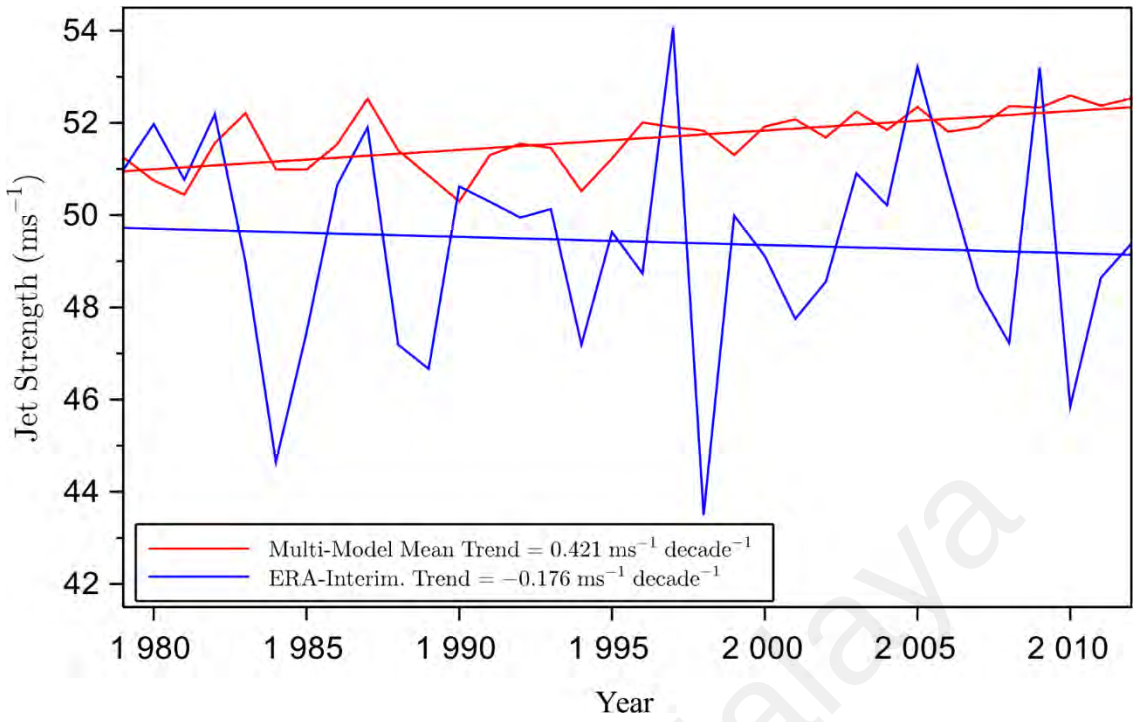

Figure 4.13 Strength of STJ during austral winter for CMIP5 multi-model mean (red line) and ERA-Interim (blue line) for the period 1979 – 2012

Figure 4.13 shows strength of STJ from ERA-Interim at -0.176 ms^{-1} $decade^{-1}$ and CMIP5 multi-model mean at 0.421 ms^{-1} $decade^{-1}$. It also shows that ERA-Interim displays a strong interannual variability in the STJ strength compared to the multi-model mean. In comparison, all the models have large differences in their interannual variability. The models CCSM4, CNRM-CM5, CSIRO-MK3-6-0, GFDL-CM3, GISS-E2-R, HadCM3 and HadGEM2-CC show standard deviations of 1.88 ms^{-1} to 2.42 ms^{-1} comparable to ERA-Interim (2.38 ms^{-1}) whereas HadGEM2-ES, INMCM4, IPSL-CM5A-LR, IPSL-CM5A-MR, MICROC-5, MICROC-ESM, MICROC-ESM-CHEM, MPI-ESM-LR and NorESM1-M show lower standard deviation in the strength of STJ compared to ERA-Interim. The values can be referred in Appendix D.

University of Malaya

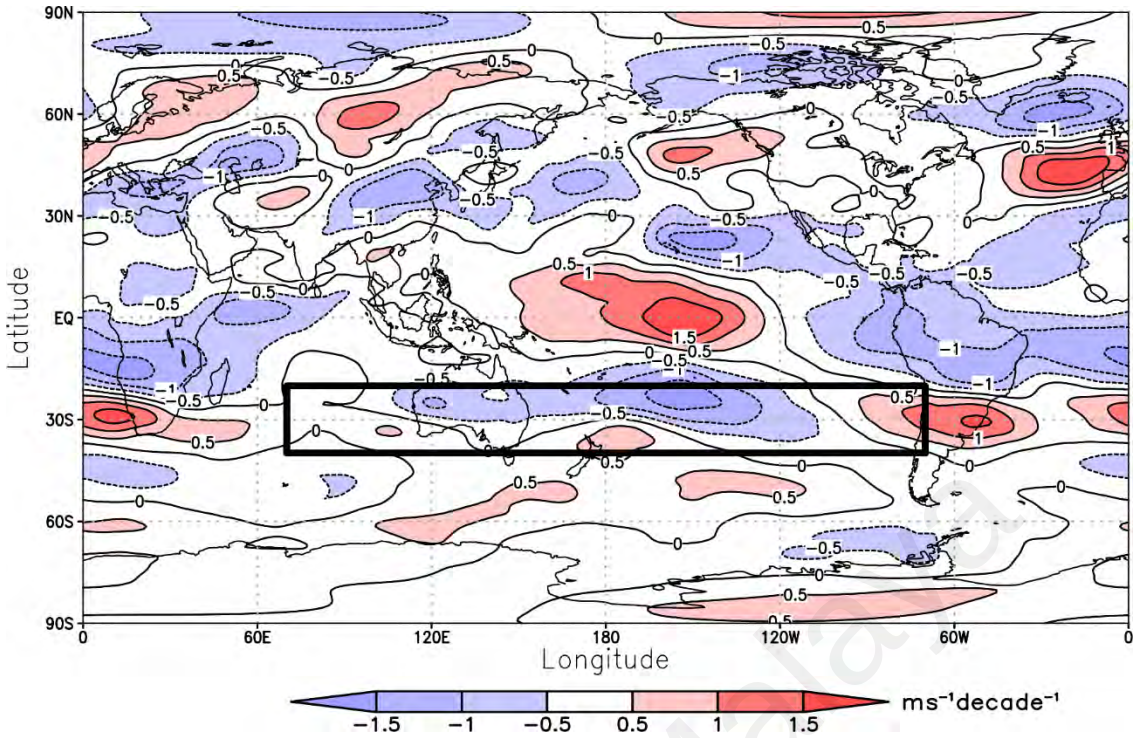

Figure 4.14 Trend in zonal wind averaged between 300 – 100 hPa during austral winter for the period 1979 – 2012 for ERA-Interim. Box highlights the study area

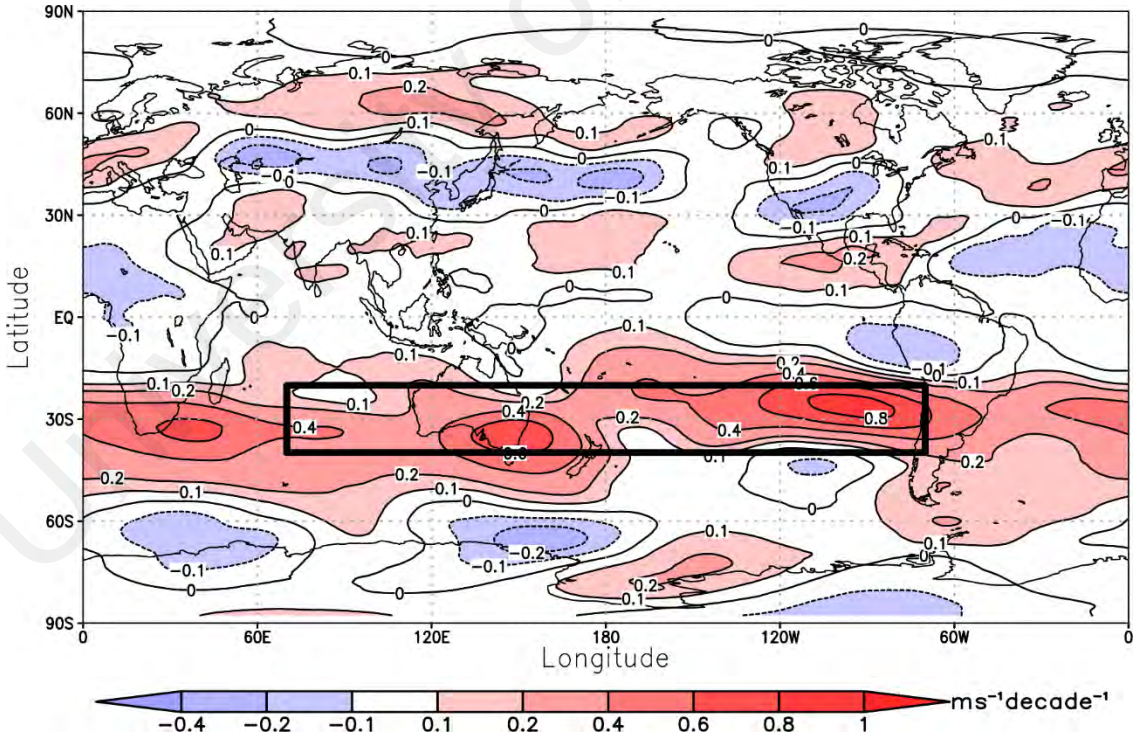

Figure 4.15 Trend in zonal wind averaged between 300 – 100 hPa for austral winter for the period 1979 – 2012 for multi-model mean. Box highlights the study area.

University of Malaya

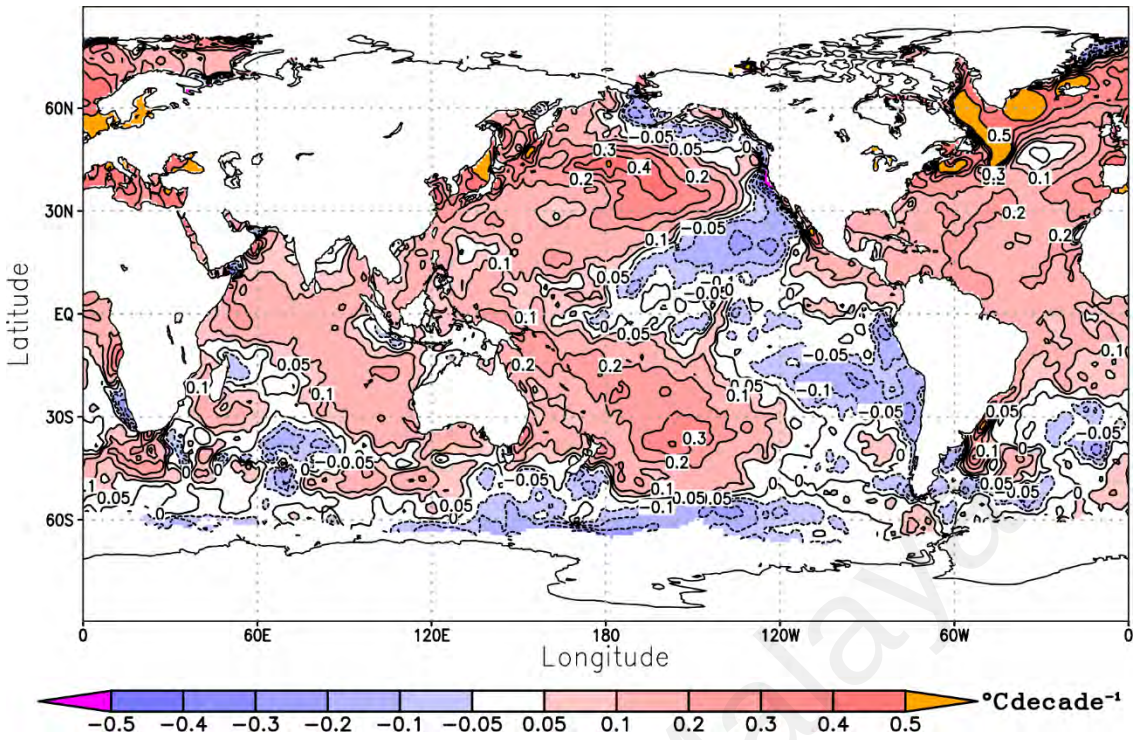

Figure 4.16 Trend of SST in HadISST for the period 1979 – 2012

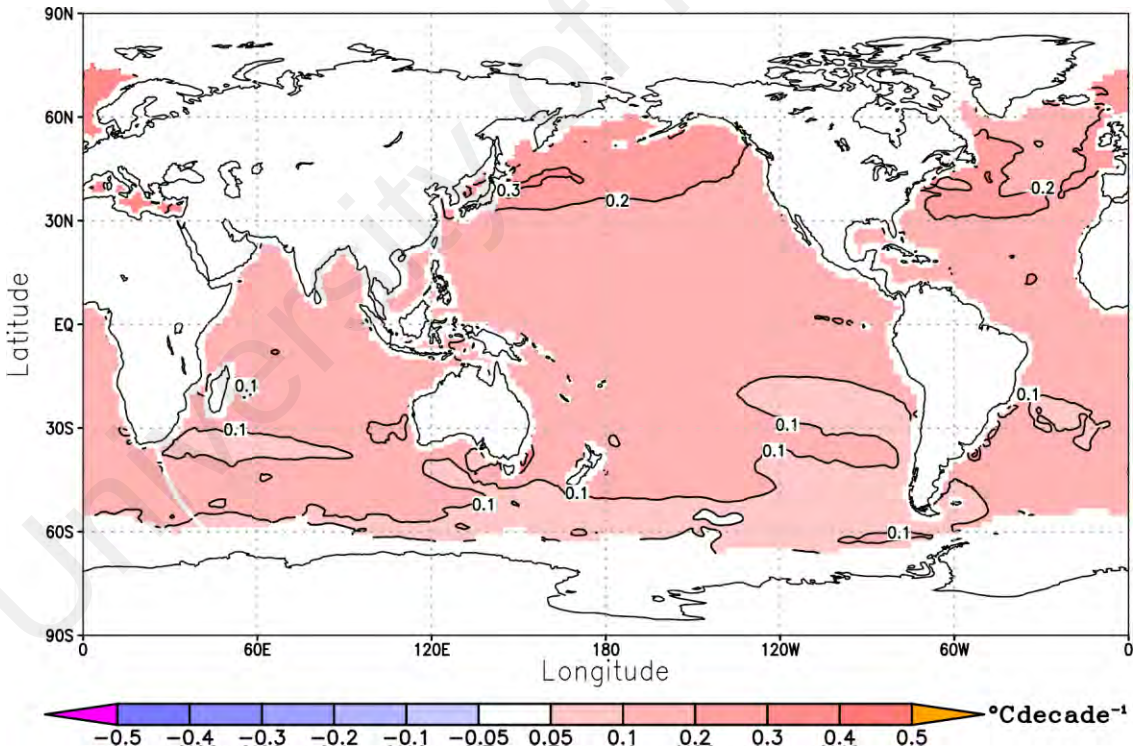

Figure 4.17 Trend of SST for CMIP5 multi-model mean for the period 1979 – 2012

Figure 4.14 and Figure 4.15 show the spatial trend of zonal wind averaged between 300 – 100 hPa during winter for the period 1979 – 2012 for ERA-Interim and CMIP5

University of Malaya

multi-model mean respectively. The zonal wind averaged between 300 – 100 hPa during austral winter from ERA-Interim has a negative trend over (highlighted by black box in Figure 4.14) the study area which indicates weakening of STJ. In contrast, the zonal wind averaged between 300 – 100 hPa from CMIP5 multi-model mean shows a positive trend over the study area and strengthening of STJ. From ERA-Interim, the strength of STJ weakens, whereas in CMIP5 multi-model mean, it strengthen.

Figure 4.16 and Figure 4.17 show the trend in SST over the tropical Pacific from during winter for the period 1979 – 2012 from HadISST and CMIP5 multi-model mean respectively. Examination of the trend in SST over the tropical Pacific from HadISST shows a slight negative trend. This is in agreement with the recent La Niña-like trend revealed in the tropical SST (L. Zhang, Wu, & Yu, 2011) and even in the SST pattern in the sub-surface ocean from different reanalysis data sets (Carton & Giese, 2008; Ishii, Kimoto, Sakamoto, & Iwasaki, 2006). The negative trends in the SST can be related to the negative trend in the strength of STJ in ERA-Interim. On the other hand, the SST trend in the CMIP5 multi-model mean demonstrates an El Niño like pattern in the tropical SSTs is consistent with the strengthening of the jet calculated in CMIP5 multi-model mean.

University of Malaya

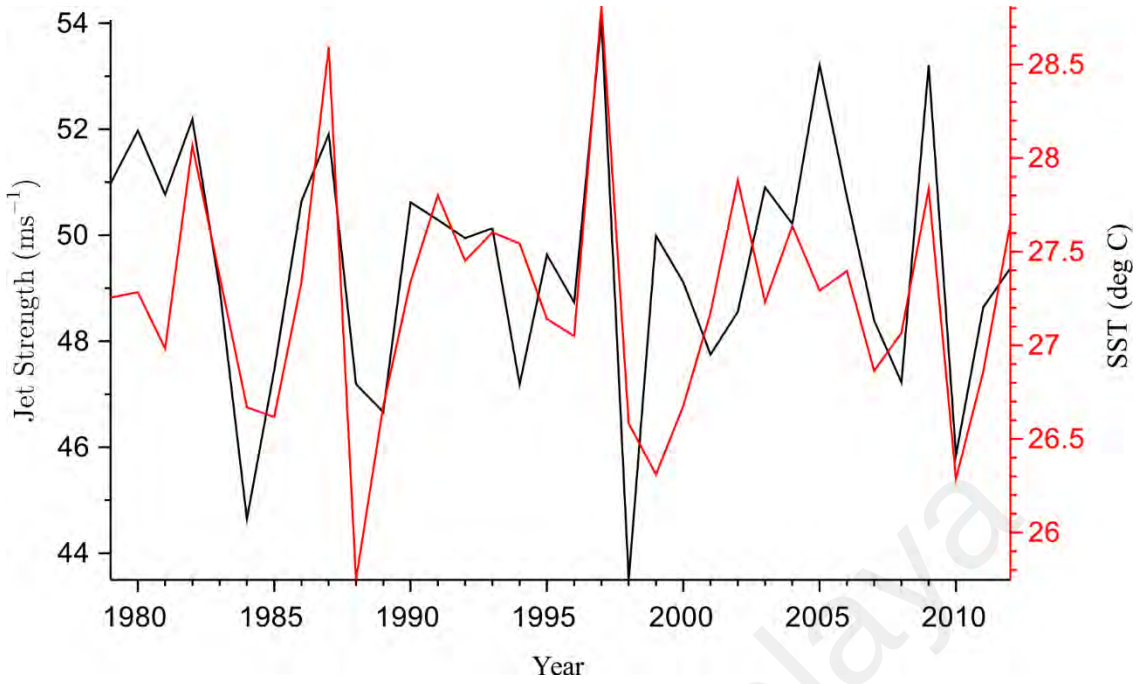

Figure 4.18 Strength of STJ (black line) from ERA-Interim and SST in Niño 3.4 area from HadISST (red line) during austral winter for the period 1979 – 2012.

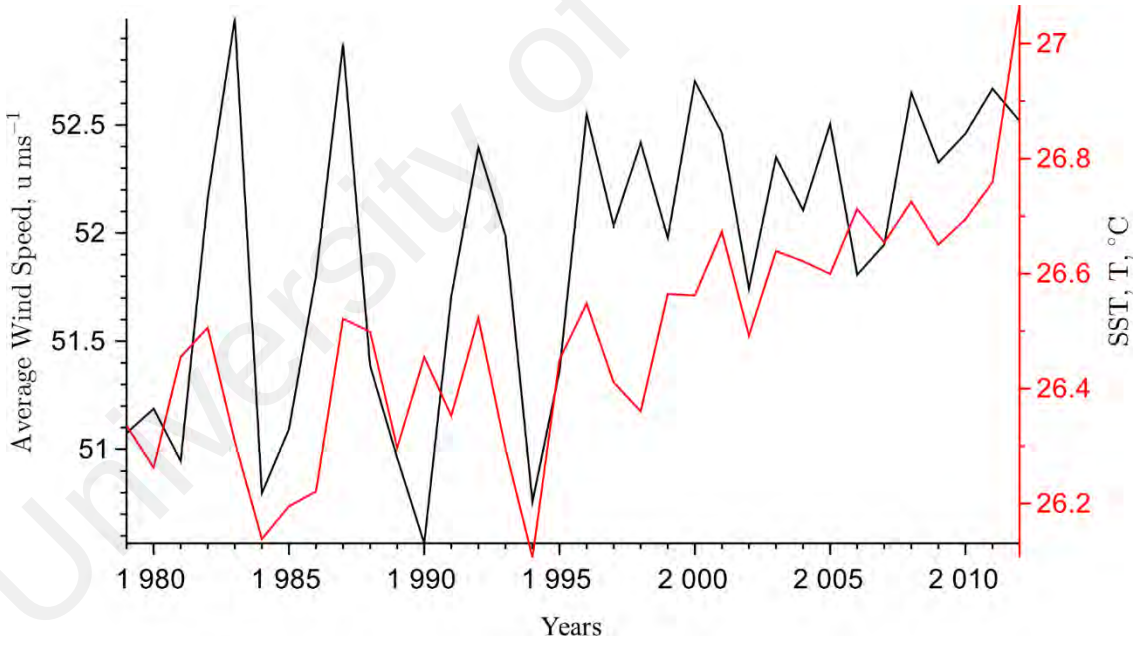

Figure 4.19 Strength of STJ (black line) and SST in Niño 3.4 area (red line) from CMIP5 multi-model mean during austral winter for the period 1979 – 2012.

In order to establish the link between the trend in the strength of the STJ and tropical SSTs we relate the trend in the strength of the STJ with the trend in SSTs in the Niño 3.4 region for the austral winter period from 1979 to 2012. Figure 4.18 shows the tropical SSTs in the Niño 3.4 region and the strength of the STJ. There is a significant

University of Malaya

($p < 0.05$) correlation coefficient 0.66 between the two. Furthermore, the sharp increase in the strength of STJ during the year 1982/83, 1986/87, and 1997/98 corresponds to strong El Niño event recorded in observation. Similarly for the CMIP5 multi-model mean, (Figure 4.19) shows a significant ($p < 0.05$) correlation of 0.58 with the multimodal mean of SST from the Niño 3.4 region.

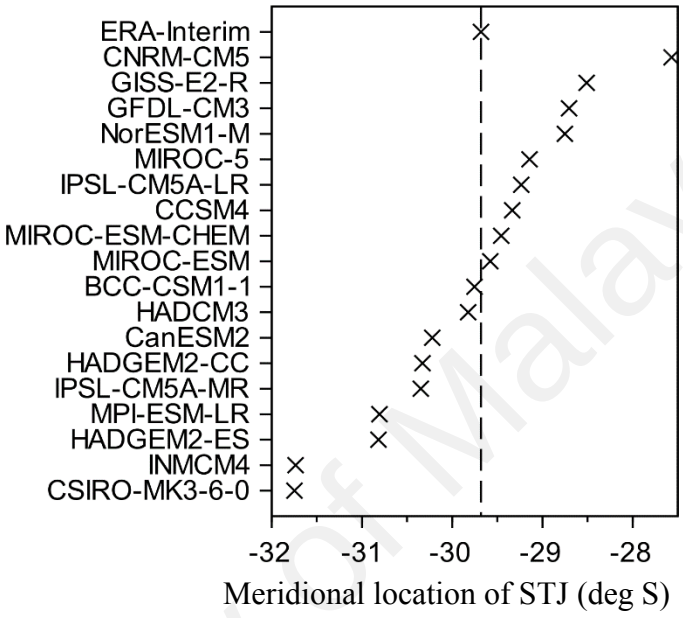

(a)

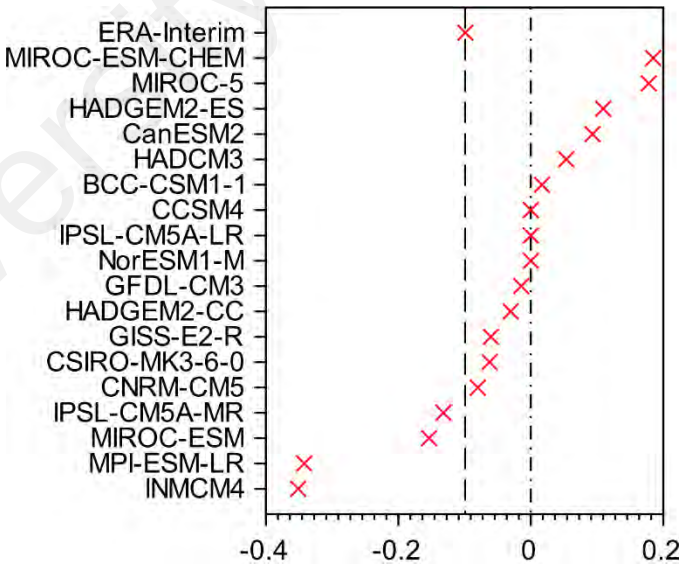

(b)

Figure 4.20 (a) Mean meridional location of the STJ and (b) trend in the meridional location of STJ in the historical CMIP5 simulations and ERA-Interim in the study area. The dash vertical line and the dot-dash lines in the figure represent ERA-Interim and position of zero trend line respectively

University of Malaya

Figure 4.20 (a) shows the mean meridional location of STJ while Figure 4.20 (b) shows the decadal trend in the meridional location of STJ in ERA-Interim and all the CMIP5 models for the period 1979 – 2012. The trend values and long-term average values can be referred in Appendix A. The mean meridional location of STJ based on ERA-Interim is 29.7°S. There is a wide range of long-term average value between 32 °S – 28 °S in CMIP5 models. Trend in the meridional location of STJ show a wide range of value from -0.36 – 0.2 °decade^{-1}. All of the CMIP5 models and ERA-Interim trends are not significant ($p < 0.05$).

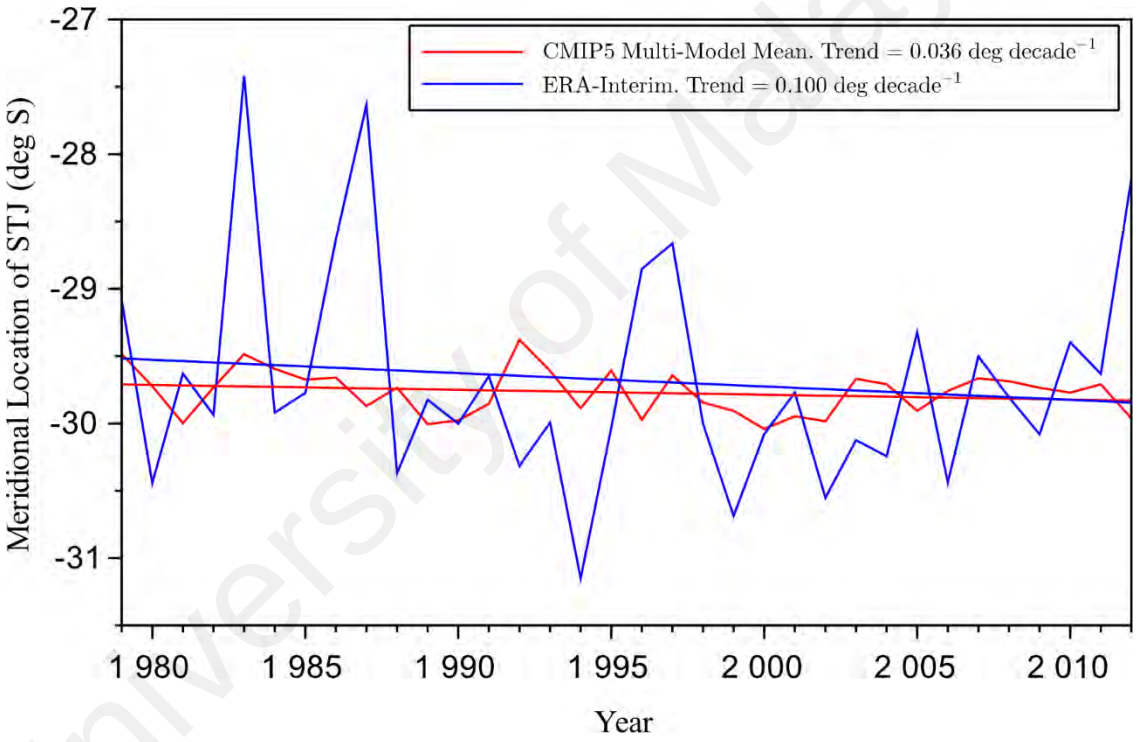

Figure 4.21 Meridional location of STJ during austral winter for CMIP5 multi-model mean (red line) and ERA-Interim (blue line) for the period 1979 – 2012

Figure 4.21 shows the trend in the meridional location of STJ from ERA-Interim and CMIP5 multi-model for the period 1979 – 2012. There has been a poleward shift in the meridional location of STJ at the rate of 0.100 ° decade^{-1} in ERA-Interim, while CMIP5 multi-model mean show poleward shift in the meridional location of STJ at the rate of 0.036 ° decade^{-1}. From Figure 4.21, it can be also noted ERA-Interim show three

University of Malaya

equatorward peak in the meridional location of STJ (refer the blue line) corresponds to three strong El Niño events in 1982/83, 1986/87, and 1997/98. During the El Niño events, contraction of the Hadley cell leads to the equatorward shift of the STJ (Lu, Chen, Frierson, & Al, 2008). However, such peaks were not observed in the multi-model mean. The reason is that ENSO events simulated by CMIP5 models occur in different times compared to observation. Investigating the time series of jet locations from individual models (not shown here) shows that the 50% of models used for the study fail to reproduce these equatorial shift during strong El Niño events in the individual models defined on the basis of model SST.

4.5 Conclusions

Several recent studies (Lee & Feldstein, 2013; Polvani, Previdi, & Deser, 2011) associated the recent poleward shift of the STJ with a cooling of the lower stratospheric polar cap caused by stratospheric ozone depletion. They suggested that high latitude cooling due to ozone depletion increases the meridional temperature gradient between the polar region and the extratropics, leading to the poleward shift of the westerly winds. The poleward jet shift shows large seasonal variations, with a comparatively large shift during summer and autumn seasons and insignificant shifts during winter and spring (Lee & Feldstein, 2013). It can also be related to the trend in the Southern Annular Mode (SAM) index during different seasons. A recent paper by Simmonds (2015) shows that there is a significant positive trend in SAM index during southern hemispheric summer and autumn and no significant trends are detected in either JJA or spring (SON) during the period 1979 – 2013.

University of Malaya

CHAPTER 5: FUTURE PROJECTION OF STJ BASED ON RCP 4.5 AND RCP 8.5

5.1 Introduction

In this chapter, the effects of climate change on STJ are analysed using climate change scenarios on both meridional location and strength of STJ. Two scenarios used in this study for future projection of STJ are RCP 4.5 and RCP 8.5.

5.2 Future Projection Scenarios

As mentioned in the Introduction, understanding how the jet streams will change in the future is of significant implications since jet stream position and intensity are tightly linked to the regional climates, especially the storm tracks in the middle latitudes. In addition, the shift in the location of STJ affects regional precipitation which lies along the boundary between the subtropical dry zone and extratropical precipitation maximum.

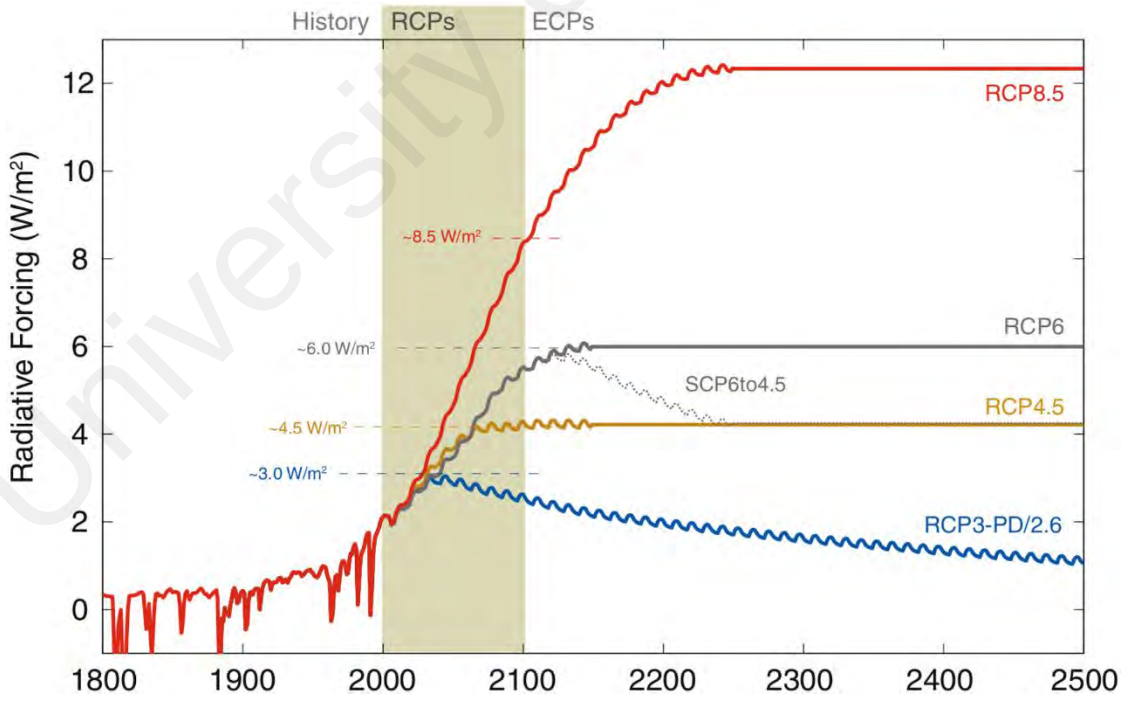

Figure 5.1 Total radiative forcing (anthrogephenic plus natural) for RCPs. Source (Meinshausen et al., 2011)

University of Malaya

In view of these, the historical simulations are to be extended by going through the four available realisations of future Representative Concentration Pathways (RCP) which cover the period between 2006 and 2100. RCPs are defined by their approximate total radiative forcing in 2100 relative to 1750 (van Vuuren et al., 2011). Thus RCPs 2.6, 4.5, 6.0 and 8.5 have relative radiative forcing of 2.6 W m^{-2} (Van Vuuren et al., 2007), 4.5 W m^{-2} (Clarke et al., 2007; Smith & Wigley, 2006; Wise et al., 2009); 6.0 W m^{-2} (Fujino, Nair, Kainuma, Masui, & Matsuoka, 2006)(Hijioka, Matsuoka, Nishimoto, Masui, & Kainuma, 2008) and 8.5 W m^{-2} (Riahi, Grübler, & Nakicenovic, 2007) respectively. The actual increment in the radiative forcing can be referred in Figure 5.1.

For future projection, two scenarios were selected for this study, namely RCP 4.5 and RCP 8.5. RCP 4.5 is an intermediate energy usage scenario, taking into account the intervention of government and international bodies in reducing the pollution and greenhouse gases in the atmosphere. RCP 8.5 is a high energy-intensive scenario which is the result of high population growth and lower rate of technology development (van Vuuren et al., 2011). In both of these scenarios, the differences in timings and magnitudes of ozone recovery changes are negligible. Therefore, the two RCPs has very little impacts in the analysis in terms of ozone recovery period.

5.3 Projected Changes in STJ

For the future projection, this study considered trend in meridional location of STJ as well its strength for the two selected RCP scenarios.

University of Malaya

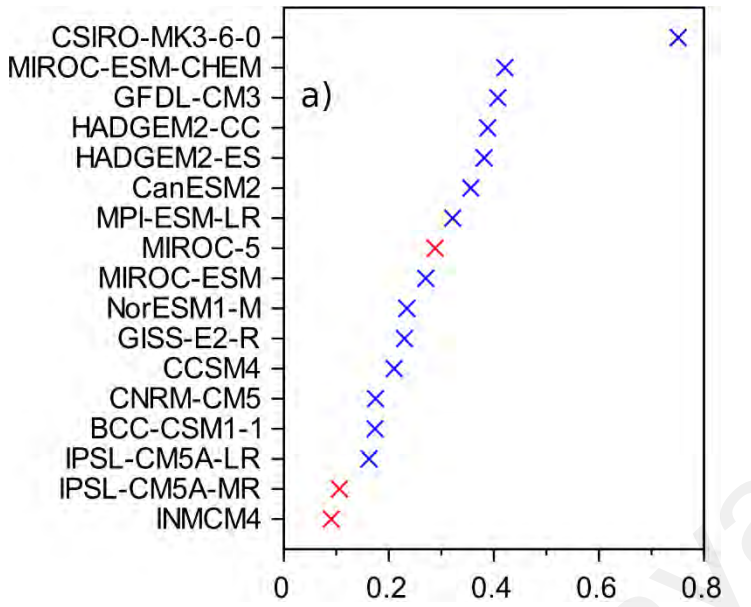

(a)

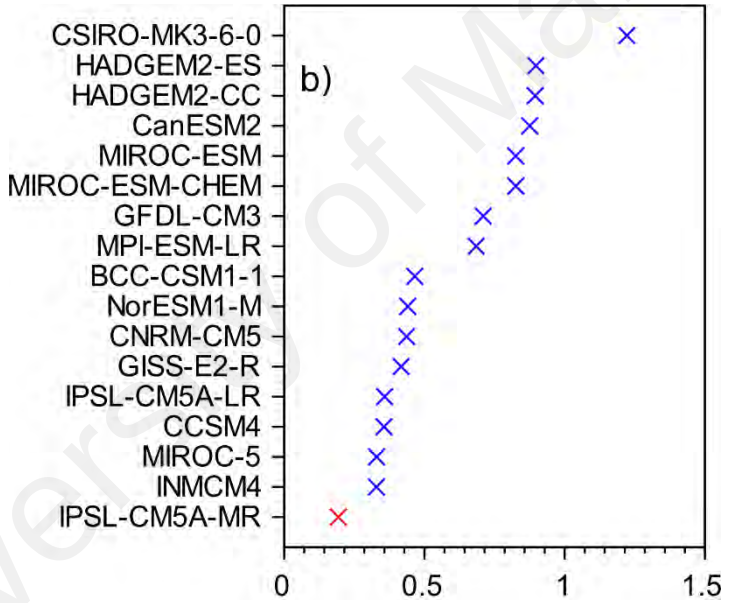

(b)

Figure 5.2 The trends in the strength of STJ for (a) RCP 4.5 and (b) RCP 8.5 scenarios from the CMIP5 models during austral winter for the period 2011 – 2099. Projection are sorted by magnitude. The blue coloured cross marks indicates models with trends that are statistically significant ($p \leq 0.05$) using two-tailed student test

Figure 5.2 (a) and (b) show the trend in the strength of STJ for RCP 4.5 and RCP 8.5 scenarios by each CMIP5 models during austral winter for the period 2011 – 2099 projection respectively. The trend values can be referred in Appendix B and Appendix C.

University of Malaya

Trend in the strength of STJ shows a wide range from 0.1 – 0.8 ms^{-1} $decade^{-1}$ and 0.2 – 1.2 ms^{-1} $decade^{-1}$ for RCP 4.5 and RCP 8.5 respectively. STJ is predicted to be strengthened significantly under both RCP 4.5 and RCP 8.5 scenarios. Under RCP 4.5 and RCP 8.5 scenarios, 82 % and 94 % of the CMIP5 models show statistically significant ($p \leq 0.05$) trend in the strengthening of STJ.

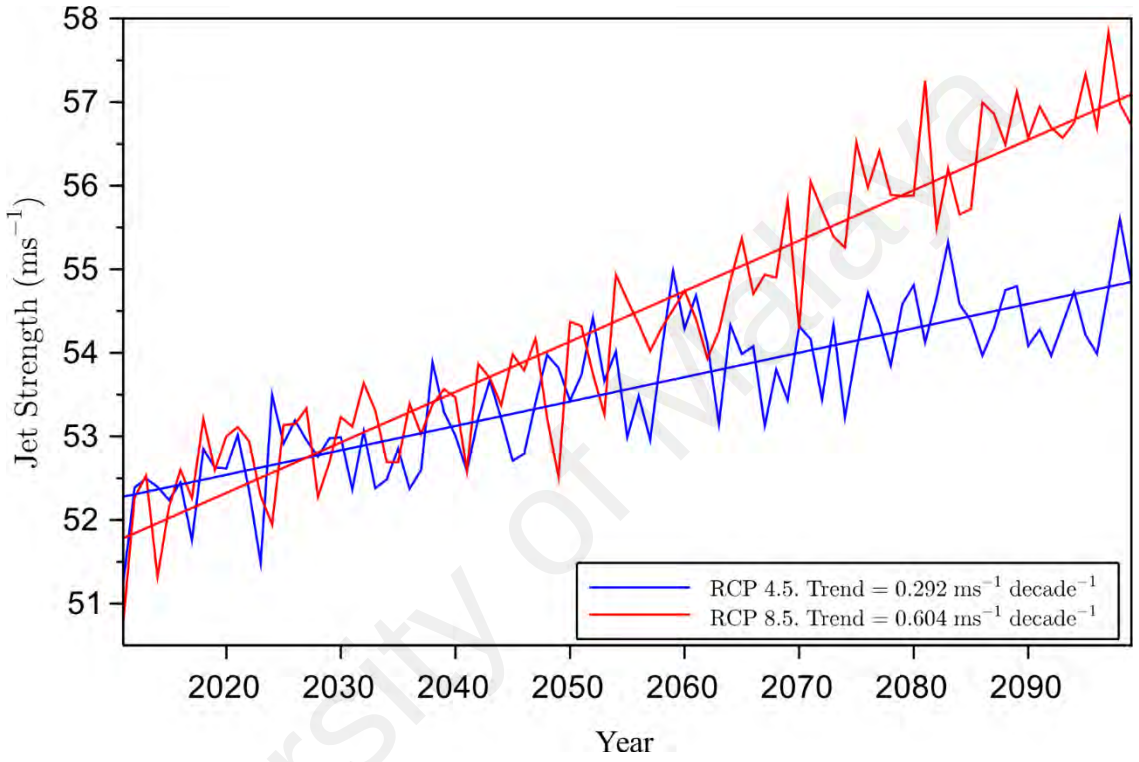

Figure 5.3 Strength of STJ for CMIP5 multi-model mean for RCP 4.5 (blue line) and RCP 8.5 (red line) scenarios during austral winter for the period 2011 – 2099

Figure 5.3 illustrates the multi-model means of the strength of STJ under RCP 4.5 and RCP 8.5. The multi-model mean suggests a significant increase in the strength of STJ by up to 0.292 ms^{-1} $decade^{-1}$ for RCP 4.5 and 0.604 ms^{-1} $decade^{-1}$ for RCP 8.5. The trend in the jet strength from the multi-model mean for RCP 8.5 is approximately double that for the RCP 4.5. Also, the strength of STJ after the year 2050 shows an increasing divergence between the two scenarios. The large difference in the strengthening of STJ in RCP 4.5 and RCP 8.5 is due to the fact that the RCP 4.5 scenario shows little change during the period of stratospheric ozone recovery (2050), whereas there is a significant change in

University of Malaya

the speed of the STJ in RCP 8.5 scenario due to the continual exponential increase in greenhouse gas concentrations. Gerber & Son (2014) suggested that differences in ozone-related polar stratospheric temperatures would be able to explain the divergence of future jet trends better as compared to the temperature differences due to global warming adopted in the CMIP5 models.

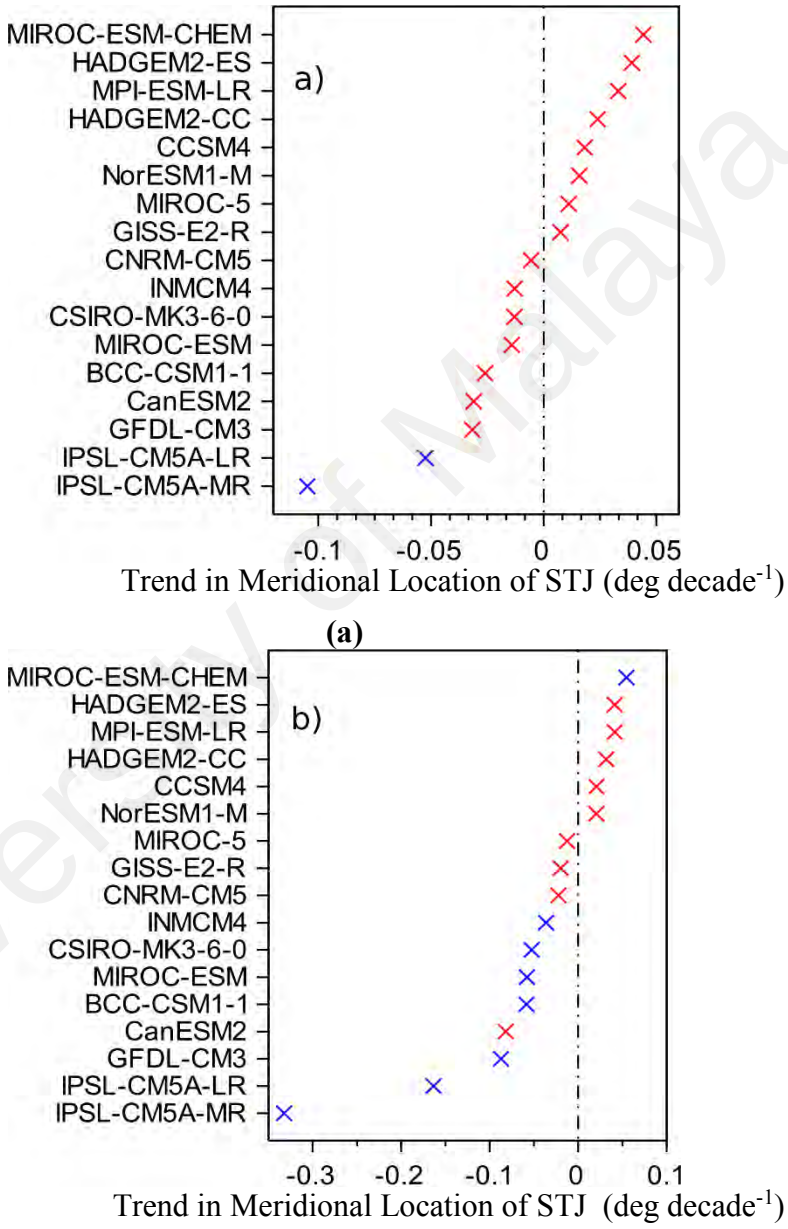

Figure 5.4 The trends in the strength of STJ for (a) RCP 4.5 and (b) RCP 8.5 scenarios from the CMIP5 models during austral winter for the period 2011 – 2099. Projection are sorted by magnitude. The blue coloured cross marks indicates models with trends that are statistically significant ($p \leq 0.05$) using two-tailed student test. The dot-dash vertical lines in the figure represent position of zero trend line

University of Malaya

The trends in meridional location of STJ for RCP 4.5 and RCP 8.5 scenarios by each CMIP5 models during austral winter for the period 2011-2099 projection are shown in the Figure 5.4. The trend values can be referred in Appendix B and Appendix C. All models show a poleward shift under these two scenarios with trend values ranging from -0.1 – 0.05 °decade^{-1} and -0.34 – 0.05 °decade^{-1} for RCP 4.5 and RCP 8.5 respectively. However, in most of the models within RCP 4.5, the changes are small and insignificant, while in RCP 8.5, 47% of the models show a significant ($p \leq 0.05$) poleward shift.

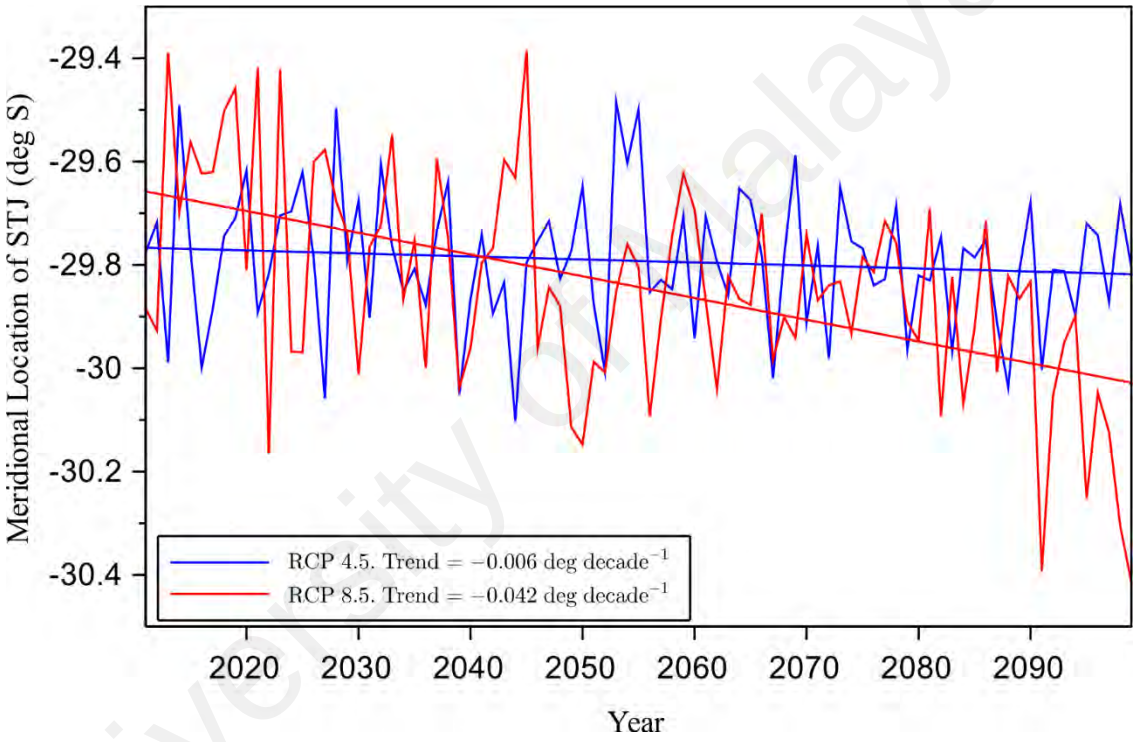

Figure 5.5 Meridional location of STJ for CMIP5 multi-model mean for RCP 4.5 (blue line) and RCP 8.5 (red line) scenarios during austral winter for the period 2011 – 2099

The multi-model mean shift of the trend in the jet latitude is shown in Figure 5.5. Scenario RCP 4.5 results in little change in the mean meridional location of STJ, whereas scenario RCP 8.5 shows a clear poleward shift. Trend in the shift by the end of the century is 0.006 ° decade^{-1} and 0.042 ° decade^{-1} towards the pole in RCP 4.5 and RCP 8.5 respectively. This is due to the fact that STJ shows a maximum shift during austral summer and insignificant shift during austral winter. Poleward jet shift is largely caused

University of Malaya

by the changes in the ozone concentration and the contribution due to the increase in the greenhouse gases is comparatively smaller. Though the ozone depletion occurs in September to November the tropospheric response is strongest during summer (Charlton-perez et al., 2013; Thompson & Solomon, 2002).

5.4 Intermodel Variability

The previous sections show that 18 selected CMIP5 models exhibit a large intermodel variability in predicting the trend in location as well as the strength. Information on factors underlying the intermodel variability contributes to a better understanding of changes in the jet stream structure. To investigate the causes of the large spread in the projected jet strength, the possible role of SSTs in the CMIP5 models was assessed.

Figure 5.6 (a) and (b) shows the spatial correlation between the multi-model mean of projected strength of STJ with the multi-model mean projected SST for RCP 4.5 and RCP 8.5 scenarios respectively. For both the scenarios, there is a strong correlation between SST and strength of STJ, in particular near the equatorial Pacific with the values, 0.88 and 0.96 for RCP 4.5 and RCP 8.5 respectively. This manifests that the strength of STJ is highly affected by SST in the equatorial Pacific.

Figure 5.7 (a), (b), (c) and (d) show the projection of SST trend from the models IPSL-CM5A-MR, INM-CM4, CSIRO-MK3-6.0, and MIROC-ESM-CHEM respectively in the scenario RCP 4.5. It is clear that the models with low trend in the strength of STJ have the lowest SST trend in the equatorial Pacific. This suggests that the inter-model variability in the magnitude of trends of the strength of STJ is linked to the SSTs predicted by the individual models.

University of Malaya

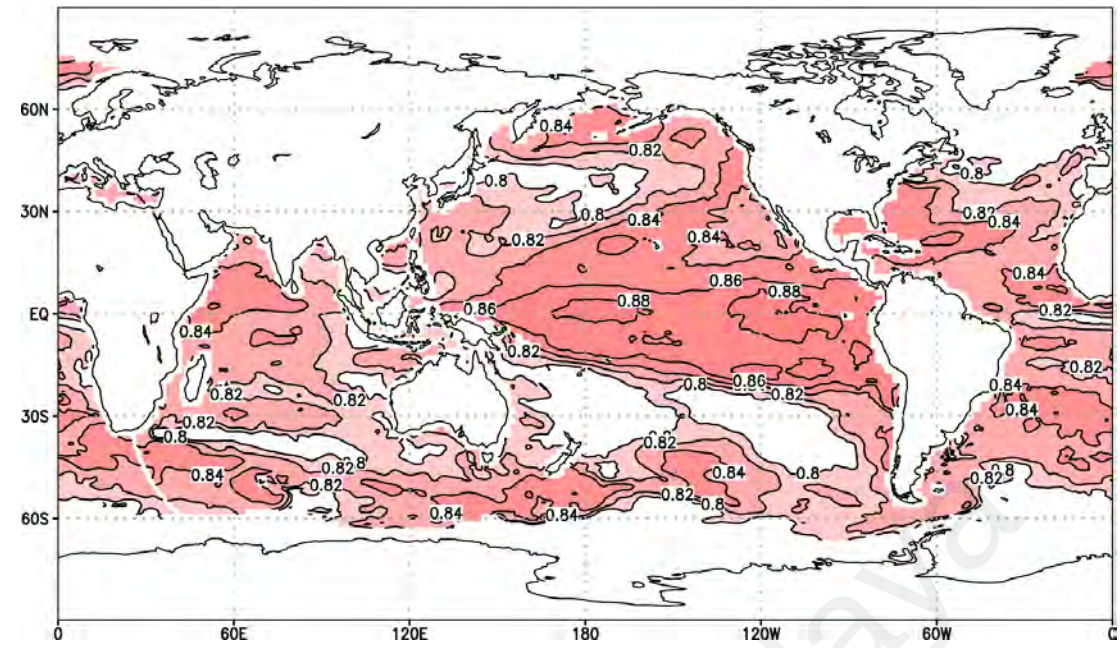

(a) RCP 4.5

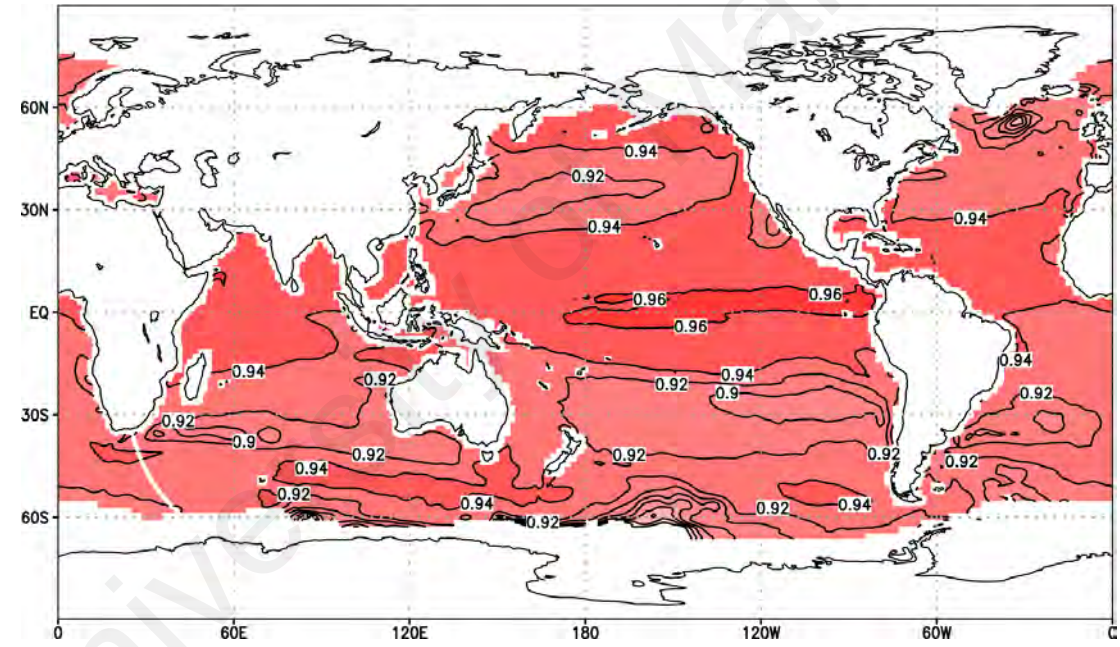

(b) RCP 8.5

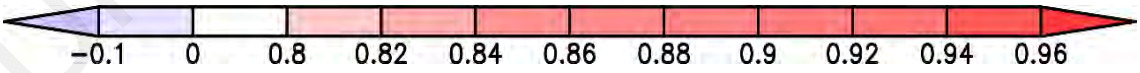

Figure 5.6 Spatial correlations between the multi-model mean projected trend in strength of STJ (2011-2099) and the multi-model mean projected trend in SST from (a) RCP 4.5 and (b) RCP 8.5 scenarios

University of Malawi

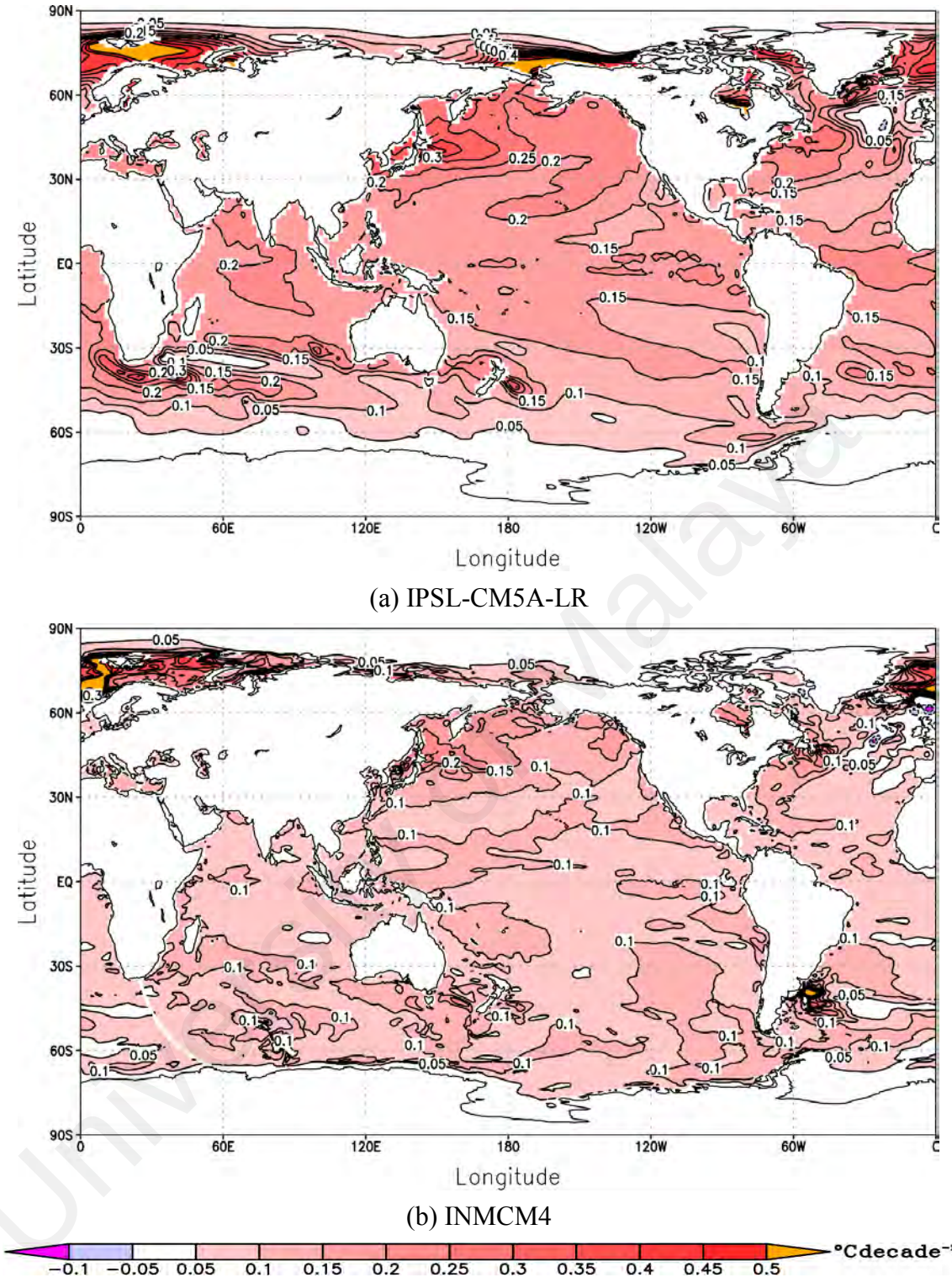

(a) IPSL-CM5A-LR

(b) INMCM4

Figure 5.7 Projected SST trends from RCP 4.5 for (a) IPSL-CM5A-LR (b) INMCM4 (c) CISRO-Mk3.6.0 (d) MIROC-ESM-CHEM for the period 2011 – 2099

University of Malawi

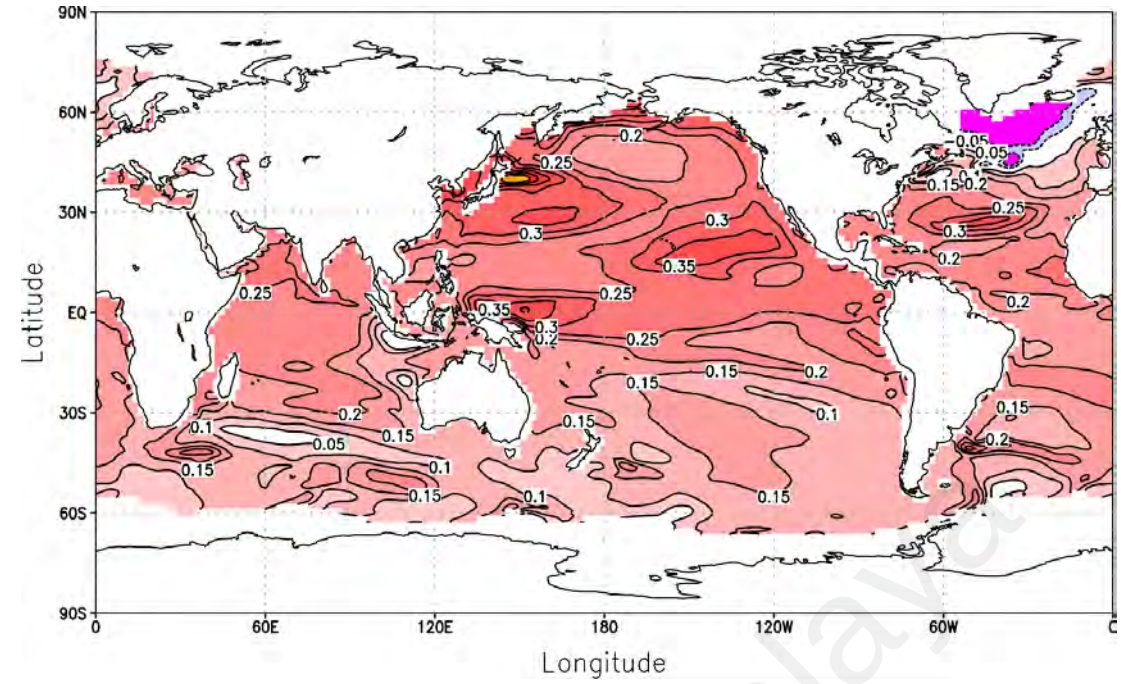

(c) CSIRO-Mk 3.6.0

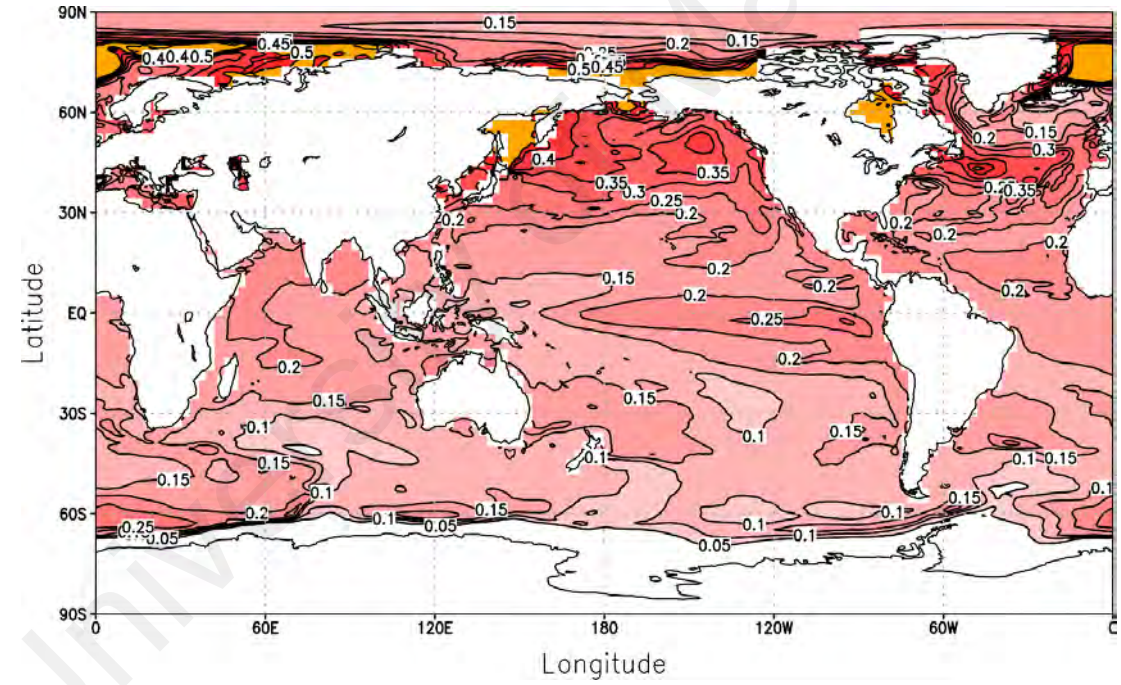

(d) MIROC-ESM-CHEM

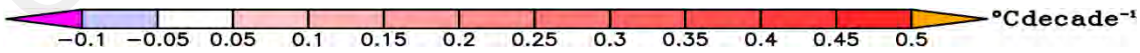

Figure 5.7 continued

5.5 Conclusions

The projected changes in the strength and meridional location from this study show a wide range of responses among the different models, though all the models agree with the poleward shift and strengthening of STJ. The RCP 4.5 (RCP 8.5) projection suggests

an increase in the strength of STJ up to 2.5 ms^{-1} (5.5 ms^{-1}) by the end of the century for 82 % (94 %) of the models. The meridional location of STJ under RCP 4.5 (RCP 8.5) is projected to move poleward by 0.06° (0.42°) with 11.8 % (47.1 %) of the models showing significant poleward shift. There are large differences in the projected magnitude of the trend in the STJ strength in individual CMIP5 models. The study also shows that intermodal variability in the projection of the strength of STJ is well correlated with biases in the equatorial SSTs in the individual CMIP5 models. Evaluation of CMIP5 model simulations by comparing with the observed data increases the confidence in the model also in future projections. Knowledge of the factors that lead to the intermodal variability will contribute to the understanding as well as improvement of CMIP5 models.

University of Malaya

CHAPTER 6: SUMMARY AND CONLUSION

6.1 Introduction

This chapter describes the summary and the conclusions of this study. In addition future work that can supplement to this study is also presented.

6.2 Summary

This study assesses the performance of CMIP5 models in simulating STJ, its ability to simulate the impacts of ENSO on STJ and assess the future projection of STJ. Climatological analysis based on the ERA-Interim shows that the Southern Hemisphere subtropical jet stream is clearly defined in the region 20 °S to 40 °S, 70 °E to 290 °E and 300 hPa to 100 hPa.

STJ is strongest and most stable during JJA, and weak and not well defined in DJF. South Atlantic Ocean was excluded from the study area because STJ often merges with PFJ over this area, thus making it hard to distinguish between the two jet stream. Three dimensional analysis was performed to identify the jet stream and the study area was defined based on climatological analysis.

The strength of STJ is defined as the longitudinal average of identified maximum of zonal winds at each longitudinal grid point for a given time. The meridional location of STJ is defined as the longitudinal average of location of the identified maxima. Steps were taken to ensure that the maxima selected are part of STJ.

STJ is strongly affected by the state of SST across the tropical ocean in response to the changes in the phases of ENSO. The ENSO influence is noticeable more in the Pacific sector than in the other parts of the SH. Using an expanded method based on conventional method, ENSO events were identified in ERA-Interim and CMPI5 models. CMIP5

University of Malaya

models simulated more El Niño events than those obtained from the ERA-Interims but less La Niña event than those from ERA-Interim.

From the ERA-Interim analysis, it is found that, during El Niño phase, the strength of the STJ over the Pacific area is greater than that during normal years. In contrast, during La Niña phase, the strength of the STJ over the Pacific area is weaker than that during the normal year. 50% of the CMIP5 models were able to simulate the increase and decrease in the strength of STJ during ENSO events.

CMIP5 models show a wide variation of trends both in the strength and meridional location of STJ. From the historical simulation, trend in the strength of STJ in ERA-Interim is -0.176 ms^{-1} $decade^{-1}$. This coincide with the negative trend of SST in the tropical Pacific Ocean. The trend in meridional location of STJ is 0.10 ° $decade^{-1}$ (poleward trend). In contrast to ERA-Interim, 94% of the models shows a strengthening of STJ, with range of 0.1 – 1.2 ms^{-1} $decade^{-1}$ and multi-model mean of 0.42 ms^{-1} $decade^{-1}$. CMIP5 models show a wide range of trend in meridional location of STJ, at 0.36 – 0.2 ° $decade^{-1}$, and multi-model mean of 0.04° $decade^{-1}$ (equatorward). The multi-model mean of SST inside the models shows an increasing/warming trend globally compared to ERA.

The trend in strength of STJ is highly correlated to the trend in SST over Niño 3.4 region, with significant correlation coefficient value of 0.67. Furthermore, there is a sharp increase in strength of STJ and poleward shift of meridional location of STJ during the years 1982/83, 1986/87, and 1997/98 which correspond to strong El Niño events observed. CMIP5 multi-model mean also shows a significant correlation of 0.58 with SST over Niño 3.4 region.

University of Malaya

For future projections, RCP 4.5 scenario which represents a midrange mitigation emission scenario and RCP 8.5 which is a high emission scenario were used. The projected changes in the strength and meridional location documented in this study show a wide range of responses among the different models. The RCP 4.5 (RCP 8.5) projection suggests an increase in the strength of STJ up to 2.5 ms^{-1} (5.5 ms^{-1}) by the end of the century for 64.7% (82.2%) of the models. The meridional location of STJ under RCP 4.5 (RCP 8.5) is projected to move polewards by 0.06 ° (0.42 °) with 11.8% (52.9%) of the models showing significant poleward shift. There are large differences in the projected magnitude of the trend in the STJ strength in individual CMIP5 models.

By comparing both the trends of SST and the strength of STJ, it revealed that models with low trend in strength of STJ have the lowest SST trend in the equatorial Pacific and vice versa. This suggests that the inter-model variability in the magnitude of the jet strength is linked and well correlated to the SSTs as predicted by the individual models.

6.3 Major Conclusions

1. Based on the observation (ERA-Interim), STJ weakens at the rate of -0.176 ms^{-1} $decade^{-1}$ and shifts polewards at the rate of 0.10 ° $decade^{-1}$. CMIP5 models simulates strengthening of STJ, with range of trends from 0.1 – 1.2 ms^{-1} $decade^{-1}$ and its multi-model mean is found to be 0.42 ms^{-1} $decade^{-1}$. The models show a wide range of trend in meridional location of STJ, at -0.36 – 0.2 ° $decade^{-1}$, with a multi-model mean of equatorward shift 0.04 ° $decade^{-1}$.
2. The trend in strength of STJ is highly correlated to the trend in SST over Niño 3.4 region, with significant correlation coefficient value of 0.67. CMIP5 models show a significant correlation of 0.58. From observation, sharp increase in strength of

University of Malaya

STJ and poleward shift of meridional location of STJ during the years 1982/83, 1986/87, and 1997/98 correspond to strong El Niño events recorded.

3. RCP 4.5 projection suggests an increase in the strength of STJ up to 2.5 ms^{-1} by the end of the century for 64.7% of the models used in this study. The meridional location of STJ under RCP 4.5 is projected to move polewards by 0.06° with 11.8% of the models showing significant poleward shift.
4. RCP 8.5 projection suggests an increase in the strength of STJ up to 5.5 ms^{-1} by the end of the century for 82.2% of the models. The meridional location of STJ under RCP 8.5 is projected to move polewards by 0.4 ° with 52.9% of the models showing significant poleward shift.
5. Analysis also shows that intermodal variability in the future projections of the strength of STJ is strongly correlated to the global SST.

6.4 Suggestion for future work

The present study has shown that there is a significant influence of ENSO on the meridional location and strength of the STJ. It is also possible to look at how ENSO Modoki is simulated by CMIP5 models as well as to assess the impact of ENSO Modoki on the variability of STJ strength and the meridional location.

Another persistent feature shown by STJ is the presence of a split jet across the South Pacific east of Australia during the austral winter. The split jet is composed of the subtropical jet (STJ) on its equatorward branch and the polar front jet (PFJ) on its poleward branch. It would be extremely useful to investigate how the structure and evolution of the winter season SH split jet is simulated in CMIP5 models. The split jets are important as they affect the weather and climate of New Zealand.

University of Malaya

REFERENCES

Achuta Rao, K., & Sperber, K. R. (2006). ENSO simulation in coupled ocean-atmosphere models: Are the current models better? *Climate Dynamics*, *27*(1), 1–15. http://doi.org/10.1007/s00382-006-0119-7

Arblaster, J. M., Meehl, G. a., & Karoly, D. J. (2011). Future climate change in the Southern Hemisphere: Competing effects of ozone and greenhouse gases. *Geophysical Research Letters*, *38*(2), n/a-n/a. http://doi.org/10.1029/2010GL045384

Archer, C. L., & Caldeira, K. (2008). Historical trends in the jet streams. *Geophysical Research Letters*, *35*(8), 1–6. http://doi.org/10.1029/2008GL033614

Athanasiadis, P., Wallace, J. M., & Wettstein, J. J. (2010). Patterns of Wintertime Jet Stream Variability and Their Relation to the Storm Tracks*. *Journal of the Atmospheric Sciences*, *67*(1981), 1361–1382. http://doi.org/10.1175/2009JAS3270.1

Bals-Elsholz, T. M., Atallah, E. H., Bosart, L. F., Wasula, T. a., Cempa, M. J., & Lupo, a. R. (2001). The wintertime southern hemisphere split jet: Structure, variability, and evolution. *Journal of Climate*, *14*(21), 4191–4215. http://doi.org/10.1175/1520-0442(2001)014<4191:TWSHSJ>2.0.CO;2

Barnes, E. A., & Hartmann, D. L. (2011). Rossby Wave Scales, Propagation, and the Variability of Eddy-Driven Jets. *Journal of the Atmospheric Sciences*, *68*(12), 2893–2908. http://doi.org/10.1175/JAS-D-11-039.1

Barnes, E. A., & Polvani, L. (2013). Response of the Midlatitude Jets, and of Their Variability, to Increased Greenhouse Gases in the CMIP5 Models. *Journal of Climate*, *26*(18), 7117–7135. JOUR. http://doi.org/10.1175/JCLI-D-12-00536.1

Bellenger, H., Guilyardi, E., Leloup, J., Lengaigne, M., & Vialard, J. (2014). ENSO representation in climate models: From CMIP3 to CMIP5. *Climate Dynamics*, *42*(7–8), 1999–2018. http://doi.org/10.1007/s00382-013-1783-z

Blackmon, M. L., Wallace, J. M., Lau, N.-C., & Mullen, S. L. (1977). An Observational Study of the Northern Hemisphere Wintertime Circulation. *Journal of the Atmospheric Sciences*. http://doi.org/http://dx.doi.org/10.1175/1520-0469(1977)034<1040:AOSOTN>2.0.CO;2

Bordi, I., Fraedrich, K., Lunkeit, F., & Sutera, A. (2007). Tropospheric Double Jets, Meridional Cells, and Eddies: A Case Study and Idealized Simulations. *Monthly Weather Review*, *135*, 3118–3133. http://doi.org/10.1175/MWR3464.1

Bracegirdle, T. J., & Marshall, G. J. (2012). The reliability of antarctic tropospheric pressure and temperature in the latest global reanalyses. *Journal of Climate*, *25*(20), 7138–7146. http://doi.org/10.1175/JCLI-D-11-00685.1

Bretherton, C. S., Widmann, M., Dymnikov, V. P., Wallace, J. M., & Bladé, I. (1999).

University of Malaya

The effective number of spatial degrees of freedom of a time-varying field. *Journal of Climate*, *12*(7), 1990–2009. http://doi.org/10.1175/1520-0442(1999)012<1990:TENOSD>2.0.CO;2

Bromwich, D. H., Nicolas, J. P., & Monaghan, A. J. (2011). An Assessment of precipitation changes over antarctica and the southern ocean since 1989 in contemporary global reanalyses. *Journal of Climate*, *24*(16), 4189–4209. http://doi.org/10.1175/2011JCLI4074.1

Carton, J. a., & Giese, B. S. (2008). A Reanalysis of Ocean Climate Using Simple Ocean Data Assimilation (SODA). *Monthly Weather Review*, *136*(8), 2999–3017. http://doi.org/10.1175/2007MWR1978.1

Ceppi, P., Zelinka, M. D., & Hartmann, D. L. (2014). The response of the Southern Hemispheric eddy-driven jet to future changes in shortwave radiation in CMIP5. *Geophys. Res. Lett*, *5*, 3244–3250. http://doi.org/10.1002/2014GL060043.1.

Charlton-perez, A. J., Baldwin, M. P., Birner, T., Black, R. X., Butler, A. H., Calvo, N., … Wilcox, L. J. (2013). On the lack of stratospheric dynamical variability in low-top versions of the CMIP5 models. *Journal of Geophysical Research*, *118*, 1–12. http://doi.org/10.1002/jgrd.50125

Chen, B., Smith, S. R., & Bromwich, D. H. (1996). Evolution of the Tropospheric Split Jet over the South Pacific Ocean during the 1986–89 ENSO Cycle. *Monthly Weather Review*. http://doi.org/10.1175/1520-0493(1996)124<1711:EOTTSJ>2.0.CO;2

Chen, G., & Held, I. M. (2007). Phase speed spectra and the recent poleward shift of Southern Hemisphere surface westerlies. *Geophysical Research Letters*, *34*(21), 1–5. JOUR. http://doi.org/10.1029/2007GL031200

Clarke, L., Edmonds, J., Jacoby, H., Pitcher, H., Reilly, J., & Richels, R. (2007). *Scenarios of greenhouse gas emissions and atmospheric concentrations*. *US Department of Energy Publications*. Washington.

Dee, D. P., Uppala, S. M., Simmons, a. J., Berrisford, P., Poli, P., Kobayashi, S., … Vitart, F. (2011). The ERA-Interim reanalysis: configuration and performance of the data assimilation system. *Quarterly Journal of the Royal Meteorological Society*, *137*(656), 553–597. http://doi.org/10.1002/qj.828

Delcambre, S. C., Lorenz, D. J., Vimont, D. J., & Martin, J. E. (2013). Diagnosing Northern Hemisphere Jet Portrayal in 17 CMIP3 Global Climate Models: Twenty-First-Century Projections. *Journal of Climate*, *26*(14), 4930–4946. http://doi.org/10.1175/JCLI-D-12-00359.1

Diaz, H. F., & Bradley, R. S. (2004). The Hadley Circulation: Present, Past, and Future BT - The Hadley Circulation: Present, Past and Future. In H. F. Diaz & R. S. Bradley (Eds.), (pp. 1–5). CHAP, Dordrecht: Springer Netherlands. http://doi.org/10.1007/978-1-4020-2944-8_1

Dore, M. H. I. (2005). Climate change and changes in global precipitation patterns: what do we know? *Environment International*, *31*(8), 1167–81. http://doi.org/10.1016/j.envint.2005.03.004

University of Malaya

Edwards, P. N. (2010). *A Vast Machine: Computer Models, Climate Data, and the Politics of Global Warming*. Cambridge: MIT Press.

Fu, Q., Johanson, C. M., Wallace, J. M., & Reichler, T. (2006). Enhanced Midlatitude Tropospheric Warming in Satellite Measurements. *Science*, *312*, 1179. http://doi.org/10.1126/science.1125566

Fujino, J., Nair, R., Kainuma, M., Masui, T., & Matsuoka, Y. (2006). Multi-gas Mitigation Analysis on Stabilization Scenarios Using Aim Global Model. *The Energy Journal*, *27*(2006), 343–353. http://doi.org/10.5547/ISSN0195-6574-EJ-VolSI2006-NoSI3-17

Gallego, D., Ribera, P., Garcia-Herrera, R., Hernandez, E., Gimeno, L., Hernandez, G. Æ. E., & Gimeno, Æ. L. (2005). A New look for the Southern Hemisphere jet stream. *Climate Dynamics*, *24*(6), 607–621. http://doi.org/10.1007/s00382-005-0006-7

Gerber, E. P., & Son, S. W. (2014). Quantifying the summertime response of the Austral jet stream and hadley cell to stratospheric ozone and greenhouse gases. *Journal of Climate*, *27*(14), 5538–5559. JOUR. http://doi.org/10.1175/JCLI-D-13-00539.1

Guemas, V., & Codron, F. (2011). Differing Impacts of Resolution Changes in Latitude and Longitude on the Midlatitudes in the LMDZ Atmospheric GCM. *Journal of Climate*, *24*(22), 5831–5849. JOUR. http://doi.org/10.1175/2011JCLI4093.1

Guilyardi, E. (2006). El Niño-mean state - Seasonal cycle interactions in a multi-model ensemble. *Climate Dynamics*, *26*, 329–348. http://doi.org/10.1007/s00382-005-0084-6

Harvey, B. J., Shaffrey, L. C., & Woollings, T. J. (2014). Equator-to-pole temperature differences and the extra-tropical storm track responses of the CMIP5 climate models. *Climate Dynamics*, *43*(5–6), 1171–1182. http://doi.org/10.1007/s00382-013-1883-9

Held, I. M., & Hou, A. Y. (1980). Non axially Symmetric Circulations in a Nearly Inviscid Atmosphere. *Journal of the Atmospheric Sciences*, *37*, 515–533.

Hijioka, Y., Matsuoka, Y., Nishimoto, H., Masui, T., & Kainuma, M. (2008). Global GHG Emission Scenarios under GHG Concentration Stabilization Targets. *J. Glob. Environ. Eng.*, *13*, 97–108.

Holton, J. R. (1992). *An Introduction to Dynamic Meteorology* (Third Edit, Vol. 88). San Diego: Academic Press.

Hourdin, F., Foujols, M.-A., Codron, F., Guemas, V., Dufresne, J.-L., Bony, S., … Bopp, L. (2013). Impact of the LMDZ atmospheric grid configuration on the climate and sensitivity of the IPSL-CM5A coupled model. *Climate Dynamics*, *40*(9), 2167–2192. JOUR. http://doi.org/10.1007/s00382-012-1411-3

Hu, Y., & Fu, Q. (2007). Observed poleward expansion of the Hadley circulation since 1979. *Atmospheric Chemistry and Physics Discussions*, *7*, 5229–5236. http://doi.org/10.5194/acpd-7-9367-2007

University of Malaya

IPCC. (2007). *Climate Change 2007: The Physical Science Basis. Contribution of Working Group I to the Fourth Assessment Report of the Intergovernmental Panel on Climate Change*. (S. Solomon, D. Qin, M. Manning, Z. Chen, M. Marquis, K. B. Averyt, … H. L. Miller, Eds.). Cambridge, United Kingdom: Cambridge University Press.

Ishii, M., Kimoto, M., Sakamoto, K., & Iwasaki, S. I. (2006). Steric sea level changes estimated from historical ocean subsurface temperature and salinity analyses. *Journal of Oceanography*, *62*(2), 155–170. http://doi.org/10.1007/s10872-006-0041-y

James, I. N. (2006). On the forcing of planetary-scale Rossby waves by Antarctica. *Quarterly Journal of the Royal Meteorological Society*, *114*(481), 619–637. http://doi.org/10.1002/qj.49711448105

Karpechko, A. Y., Gillett, N. P., Marshall, G. J., & Scaife, A. A. (2008). Stratospheric influence on circulation changes in the Southern Hemisphere troposphere in coupled climate models. *Geophysical Research Letters*, *35*(20), L20806. JOUR. http://doi.org/10.1029/2008GL035354

Kidson, J. W. (1999). Principal modes of Southern Hemisphere low-frequency variability obtained from NCEP-NCAR reanalyses. *Journal of Climate*, *12*(9), 2808–2830. http://doi.org/10.1175/1520-0442(1999)012<2808:PMOSHL>2.0.CO;2

Kidston, J., & Gerber, E. P. (2010). Intermodel variability of the poleward shift of the austral jet stream in the CMIP3 integrations linked to biases in 20th century climatology. *Geophysical Research Letters*, *37*(9), n/a-n/a. JOUR. http://doi.org/10.1029/2010GL042873

Kidston, J., & Vallis, G. (2011). Can the increase in the eddy length scale under global warming cause the poleward shift of the jet streams? *Journal of Climate*, 3764–3781. http://doi.org/10.1175/2010JCLI3738.1

Koch, P., Wernli, H., & Davies, H. C. (2006). An event-based jet-stream climatology and typology. *International Journal of Climatology*, *26*(3), 283–301. http://doi.org/10.1002/joc.1255

Lee, S., & Feldstein, S. B. (2013). Detecting ozone- and greenhouse gas-driven wind trends with observational data. *Science (New York, N.Y.)*, *339*(6119), 563–7. http://doi.org/10.1126/science.1225154

Lee, S., & Kim, H. (2003). The dynamical relationship between subtropical and eddy-driven jets. *Journal of the Atmospheric Sciences*, *60*(12), 1490–1503. JOUR. http://doi.org/10.1175/1520-0469(2003)060<1490:TDRBSA>2.0.CO;2

Leloup, J., Lengaigne, M., & Boulanger, J. P. (2008). Twentieth century ENSO characteristics in the IPCC database. *Climate Dynamics*, *30*(2–3), 277–291. http://doi.org/10.1007/s00382-007-0284-3

Limbach, S., Schömer, E., & Wernli, H. (2012). Detection, tracking and event localization of jet stream features in 4-D atmospheric data. *Geoscientific Model Development*, *5*(2), 457–470. http://doi.org/10.5194/gmd-5-457-2012

University of Malaya

Lindzen, R., & Hou, A. (1988). Hadley circulations for zonally averaged heating centered off the equator. *Journal of the Atmospheric Sciences*, *45*(17), 2416–2427. http://doi.org/http://dx.doi.org/10.1175/1520-0469(1988)045%3C2416:HCFZAH%3E2.0.CO;2

Liu, J., Yuan, X., Rind, D., Martinson, D. G., & Nin, E. (2002). Mechanism study of the ENSO and southern high latitude climate teleconnections. *Geophysical Research Letters*, *29*(14), 8–11.

Lorenz, D. J., & Deweaver, E. T. (2007). Tropopause height and zonal wind response to global warming in the IPCC scenario integrations. *Journal of Geophysical Research*, *112*(D10), D10119. http://doi.org/10.1029/2006JD008087

Lu, J., Chen, G., Frierson, D. M. W., & Al, L. U. E. T. (2008). Response of the Zonal Mean Atmospheric Circulation to El Niño versus Global Warming. *Journal of Climate*, *21*(22), 5835–5851. http://doi.org/10.1175/2008JCLI2200.1

Lu, J., Vecchi, G. a., & Reichler, T. (2007). Expansion of the Hadley cell under global warming. *Geophysical Research Letters*, *34*(6), 2–6. http://doi.org/10.1029/2006GL028443

Maloney, E. D., & Chelton, D. B. (2006). An Assessment of the Sea Surface Temperature Influence on Surface Wind Stress in Numerical Weather Prediction and Climate Models. *Journal of Climate*, *19*(12), 2743–2762. JOUR. http://doi.org/10.1175/JCLI3728.1

Manney, G. L., Hegglin, M. I., Daffer, W. H., Santee, M. L., Ray, E. a., Pawson, S., … Walker, K. a. (2011). Jet characterization in the upper troposphere/lower stratosphere (UTLS): applications to climatology and transport studies. *Atmospheric Chemistry and Physics*, *11*(12), 6115–6137. http://doi.org/10.5194/acp-11-6115-2011

Meehl, G. A., Goddard, L., Murphy, J., Stouffer, R. J., Boer, G., Danabasoglu, G., … Stockdale, T. (2009). Decadal Prediction. *Bulletin of the American Meteorological Society*, *90*(10), 1467–1485. JOUR. http://doi.org/10.1175/2009BAMS2778.1

Meinshausen, M., Smith, S. J., Calvin, K., Daniel, J. S., Kainuma, M. L. T., Lamarque, J.-F., … Vuuren, D. P. P. (2011). The RCP greenhouse gas concentrations and their extensions from 1765 to 2300. *Climatic Change*, *109*(1–2), 213–241. http://doi.org/10.1007/s10584-011-0156-z

Mignone, B. K., Gnanadesikan, A., Sarmiento, J. L., & Slater, R. D. (2006). Central role of Southern Hemisphere winds and eddies in modulating the oceanic uptake of anthropogenic carbon. *Geophysical Research Letters*, *33*(1), 1–5. http://doi.org/10.1029/2005GL024464

Miller, R. L., Schmidt, G. A., & Shindell, D. T. (2006). Forced annular variations in the 20th century Intergovernmental Panel on Climate Change Fourth Assessment Report models. *Journal of Geophysical Research: Atmospheres*, *111*(D18), n/a-n/a. JOUR. http://doi.org/10.1029/2005JD006323

Molteni, F., Stockdale, T. N., & Vitart, F. (2015). Understanding and modelling extra-

University of Malaya

tropical teleconnections with the Indo-Pacific region during the northern winter. *Climate Dynamics*, (1998), in press. http://doi.org/10.1007/s00382-015-2528-y

Nakamura, H., Sampe, T., Tanimoto, Y., & Shimpo, A. (2004). Observed associations among storm tracks, jet streams and midlatitude oceanic fronts. *Geophysical Monograph*, *147*, 329–345. CHAP. http://doi.org/10.1029/147GM18

Nakamura, H., & Shimpo, A. (2004). Seasonal variations in the Southern Hemisphere storm tracks and jet streams as revealed in a reanalysis dataset. *Journal of Climate*, 1828–1844. http://doi.org/10.1175/1520-0442(2004)017<1828:SVITSH>2.0.CO;2

Pena-ortiz, C., Gallego, D., Ribera, P., Ordonez, P., & Alvarez-castro, M. D. C. (2013). Observed trends in the global jet stream characteristics during the second half of the 20th century. *Journal of Geophysical Research: Atmospheres*, *118*, 2702–2713. http://doi.org/10.1002/jgrd.50305

Polvani, L. M., Previdi, M., & Deser, C. (2011). Large cancellation, due to ozone recovery, of future Southern Hemisphere atmospheric circulation trends. *Geophysical Research Letters*, *38*(4), 1–6. http://doi.org/10.1029/2011GL046712

Polvani, L. M., Waugh, D. W., Correa, G. J. P., & Son, S. W. (2011). Stratospheric Ozone Depletion: The Main Driver of Twentieth-Century Atmospheric Circulation Changes in the Southern Hemisphere. *Journal of Climate*, *24*(3), 795–812. http://doi.org/10.1175/2010JCLI3772.1

Rayner, N. a. A., Parker, D. E. E., Horton, E. B. B., Folland, C. K. K., Alexander, L. V. V, Rowell, D. P. P., … Kaplan, A. (2003). Global analyses of sea surface temperature, sea ice, and night marine air temperature since the late nineteenth century. *Journal of Geophysical Research: Atmospheres*, *108*(D14), 4407. JOUR. http://doi.org/10.1029/2002JD002670

Riahi, K., Grübler, A., & Nakicenovic, N. (2007). Scenarios of long-term socio-economic and environmental development under climate stabilization. *Technological Forecasting and Social Change*, *74*(7), 887–935. http://doi.org/10.1016/j.techfore.2006.05.026

Rind, D., Chandler, M., Lerner, J., Martinson, D. G., & Yuan, X. (2001). Climate response to basin-specific changes in latitudinal temperature gradients and implications for sea ice variability. *Journal of Geophysical Research*, *106*(D17), 20161. http://doi.org/10.1029/2000JD900643

Russell, J., Dixon, K., Gnanadesikan, A., Stouffer, R. J., & Toggweiler, J. R. (2006). The Southern Hemisphere Westerlies in a warming world: Propping open the door to the deep ocean. *Journal of Climate*, *19*(24), 6382–6390. http://doi.org/10.1175/JCLI3984.1

Sampe, T., Nakamura, H., Goto, A., & Ohfuchi, W. (2010). Significance of a midlatitude SST frontal zone in the formation of a storm track and an eddy-driven westerly jet. *Journal of Climate*, *23*(7), 1793–1814. http://doi.org/10.1175/2009JCLI3163.1

Seager, R., Harnik, N., Kushnir, Y., Robinson, W., & Miller, J. (2003). Mechanisms of Hemispherically Symmetric Climate Variability*. *Journal of Climate*, *16*, 2960–

University of Malaya

2978. http://doi.org/10.1175/1520-0442(2003)016<2960:MOHSCV>2.0.CO;2

Simmonds, I. (2015). Comparing and contrasting the behaviour of Arctic and Antarctic sea ice over the 35 year period 1979–2013. *Annals of Glaciology*, *56*(69), 18–28. http://doi.org/10.3189/2015AoG69A909

Simmons, A. J., Poli, P., Dee, D. P., Berrisford, P., Hersbach, H., Kobayashi, S., & Peubey, C. (2014). Estimating low-frequency variability and trends in atmospheric temperature using ERA-Interim. *Quarterly Journal of the Royal Meteorological Society*, *140*(679), 329–353. JOUR. http://doi.org/10.1002/qj.2317

Sinclair, M. R. (1996). A Climatology of Anticyclones and Blocking for the Southern Hemisphere. *Monthly Weather Review*. http://doi.org/10.1175/1520-0493(1996)124<0245:ACOAAB>2.0.CO;2

Smith, S. J., & Wigley, T. M. L. (2006). Multi-gas forcing stabilization with minicam. *Energy Journal*, *27*(SPEC. ISS. NOV.), 373–391. http://doi.org/10.5547/ISSN0195-6574-EJ-VolSI2006-NoSI3-19

Son, S. W., Gerber, E. P., Perlwitz, J., Polvani, L. M., Gillett, N. P., Seo, K.-H. H., … Yamashita, Y. (2010). Impact of stratospheric ozone on Southern Hemisphere circulation change: A multimodel assessment. *Journal of Geophysical Research*, *115*, 1–18. http://doi.org/10.1029/2010JD014271

Son, S. W., Polvani, L. M., Waugh, D. W., Akiyoshi, H., Garcia, R., Kinnison, D., … Shibata, K. (2008). The impact of stratospheric ozone recovery on the Southern Hemisphere westerly jet. *Science*, *320*(5882), 1486–9. http://doi.org/10.1126/science.1155939

Strong, C., & Davis, R. E. (2008). Variability in the Position and Strength of Winter Jet Stream Cores Related to Northern Hemisphere Teleconnections. *Journal of Climate*, *21*(3), 584–592. http://doi.org/10.1175/2007JCLI1723.1

Taylor, K. E., Stouffer, R. J., & Meehl, G. A. (2012). An Overview of CMIP5 and the Experiment Design. *Bulletin of the American Meteorological Society*, *93*(4), 485–498. http://doi.org/10.1175/BAMS-D-11-00094.1

Thompson, D. W. J., & Solomon, S. (2002). Interpretation of recent Southern Hemisphere climate change. *Science*, *296*(5569), 895–9. http://doi.org/10.1126/science.1069270

Trenberth, K. E. (1997). The Definition of El Niño. *Bulletin of the American Meteorological Society*, *78*(August), 2771–2777. JOUR. http://doi.org/10.1175/1520-0477(1997)078<2771:TDOENO>2.0.CO;2

Turner, J. (2004). The El Niño–southern oscillation and Antarctica. *International Journal of Climatology*, *24*(1), 1–31. http://doi.org/10.1002/joc.965

Van Vuuren, D. P., Den Elzen, M. G. J., Lucas, P. L., Eickhout, B., Strengers, B. J., Van Ruijven, B., … Van Houdt, R. (2007). Stabilizing greenhouse gas concentrations at low levels: An assessment of reduction strategies and costs. *Climatic Change*, *81*(2), 119–159. http://doi.org/10.1007/s10584-006-9172-9

University of Malaya

van Vuuren, D. P., Edmonds, J., Kainuma, M., Riahi, K., Thomson, A., Hibbard, K., … Rose, S. K. (2011). The representative concentration pathways: an overview. *Climatic Change*, *109*(1–2), 5–31. http://doi.org/10.1007/s10584-011-0148-z

Wang, B., Wu, R., Fu, X., & Al, W. E. T. (2000). Pacific – East Asian Teleconnection : How Does ENSO Affect East Asian Climate ?*. *Journal of Climate*, *13*, 1517–1536.

Watterson, I. G. (2015). Improved Simulation of Regional Climate by Global Models with Higher Resolution: Skill Scores Correlated with Grid Length*. *Journal of Climate*, *28*(15), 5985–6000. http://doi.org/10.1175/JCLI-D-14-00702.1

Wilcox, L. J., Gray, L. J. file:///home/yunus/Downloads/Test1/J. pd., & Charlton-Perez, J. (2012). Trends in Austral jet position in ensembles of high- and low-top CMIP5 models. *Journal of Geophysical Research*, *117*(D13), 1–10. http://doi.org/10.1029/2012JD017597

Wise, M., Calvin, K., Thomson, A., Clarke, L., Bond-Lamberty, B., Sands, R., … Edmonds, J. (2009). Implications of Limiting CO2 Concentrations for Land Use and Energy. *Science*, *324*(5931), 1183–1186. JOUR. http://doi.org/10.1038/ncb2099

Yeh, S.-W., Ham, Y.-G., & Lee, J.-Y. (2012). Changes in the Tropical Pacific SST Trend from CMIP3 to CMIP5 and Its Implication of ENSO*. *Journal of Climate*, *25*(21), 7764–7771. http://doi.org/10.1175/JCLI-D-12-00304.1

Yin, J. J. H. (2005). A consistent poleward shift of the storm tracks in simulations of 21st century climate. *Geophys. Res. Lett*, *32*(18), L18701. http://doi.org/10.1029/2005GL023684

Yuan, X. (2004). ENSO-related impacts on Antarctic sea ice: a synthesis of phenomenon and mechanisms. *Antarctic Science*, *16*(4), 415–425. http://doi.org/10.1017/S0954102004002238

Zhang, L., Wu, L., & Yu, L. (2011). Oceanic origin of a recent La Niña-like trend in the tropical Pacific. *Advances in Atmospheric Sciences*, *28*(5), 1109–1117. JOUR. http://doi.org/10.1007/s00376-010-0129-6

Zhang, Y., Wallace, J., & Battisti, D. (1997). ENSO-like interdecadal variability: 1900-93. *Journal of Climate*, *10*, 1004–1020.

University of Malaya

LIST OF PUBLICATIONS AND PAPERS PRESENTED

PAPERS

Rahmat, R., Archevarahuprok, B., Kang, C. P., Xiang, C. J., Hein, D., Gunawan, D., … **Ahmad Mazuki, Y. M.**, … Soe, W. (2014). A Regional Climate Modelling Experiment for Southeast Asia Using PRECIS Regional Climate Model and selected CMIP3 Global Climate Models. *Centre for Climate Research Singapore of the Meteorological Service Singapore.* Singapore.

Chenoli, S. N., **Ahmad Mazuki, Y. M.**, Turner, J., & Samah, A. A. (2016). Historical and projected changes in the Southern Hemisphere Sub-tropical Jet during winter from the CMIP5 models. *Climate Dynamics*, 1–21. http://doi.org/10.1007/s00382-016-3102-y

PRESENTATIONS

Chenoli, S. N., **Ahmad Mazuki, M. Y**., & Turner, J. (2013). Assessment of Trends in The Southern Hemispheric Subtropical Jet Stream Based on CMIP5 Models. In *6th Malaysian International Seminar on Antartica*. Penang.

Ahmad Mazuki, M. Y., Chenoli, S. N., Turner, J., & Samah, A. A. (2015). AS13-A024: Assessment of Southern Hemisphere Subtropical Jet Stream Historical Changes and Projected Changes in CMIP5 Model Output. In *AOGS2015*. Singapore.

University of Malaya